

AD 713656

LAMONT-DOHERTY GEOLOGICAL OBSERVATORY  
OF COLUMBIA UNIVERSITY  
Palisades, New York 10964

ARCTIC OCEAN GEOPHYSICAL STUDIES:  
THE ALPHA CORDILLERA AND MENDELEYEV RIDGE.

by

John K. Hall

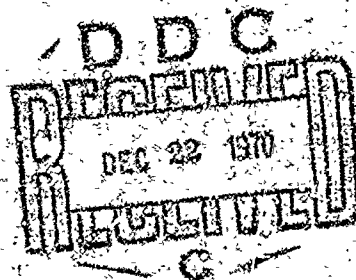
November 1970

CU-2-70

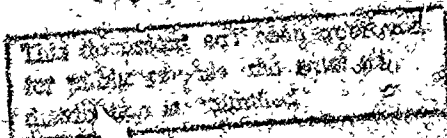
Technical Report No. 2

Contract N-00014-67-A-0108-0016 with the  
Office of Naval Research

Task Number NR 507-320/1-6-69 (413)



Reproduction of this document in whole or in part is permitted  
for any purpose of the U.S. Government.



**Best  
Available  
Copy**

## ABSTRACT

### ARCTIC OCEAN GEOPHYSICAL STUDIES: THE ALPHA CORDILLERA AND MENDELEYEV RIDGE

John Kendrick Hall

The geophysical findings from Fletcher's Ice Island (T-3) for the period mid-1962 to mid-1970 are presented. During this time the ice station traversed the Chukchi Rise, portions of the Alpha Cordillera and Mendelejev Ridge, and the Chukchi, Mendelejev, and Canada Plains. The findings, together with pertinent observations from older investigations, support the suggestion of earlier investigators that the Alpha Cordillera is an inactive center of seafloor spreading. Several fractures were observed to cut the Mendelejev Ridge and Alpha Cordillera, and many other closely spaced fractures are suggested by topographic, magnetic, and gravity trends. These fractures appear to parallel the 142° West meridian. Seismic reflection profiles show a buried topography similar to that of the Mid-Atlantic Ridge. Offsets in the apparent axial rift suggest that the fractures are the traces of transform faults. The angular relationship between the Mendelejev Ridge and the Alpha Cordillera appears to result from a southerly displacement of the cordillera crest along numerous en echelon transform faults. Magnetic anomalies are consistent with the seafloor spreading hypothesis. A crustal gravity model based upon a continuous 600 km long gravity and bathymetric profile and one reversed refraction measurement from Station Alpha shows the observed gravity to be consistent with a section of East Pacific Rise type with a 5 km thick oceanic layer overlying 27 km of anomalous ( $\rho = 3.15$ ) mantle.

The relation of the Alpha Cordillera to the surrounding continental geology is explored. A history for the Amerasia Basin since Late Precambrian time is proposed, in which the basin experienced spreading at least once in the Paleozoic, and again in the Late Mesozoic and early Tertiary. The Early Paleozoic episode is related to the opening

and closing of a proto-Atlantic Ocean and the development of the Appalachian/Caledonian orogen. Arguments are presented which lead to the conclusion that the oceanic crust beneath the Beaufort Sea is Permo-Carboniferous or older.

Seismic reflection profiles show more than 2 kilometers of sediment beneath the Mendelejev and Canada Plains, with no basement reflections recorded. Prominent reflectors may represent major climatic or depositional changes. Sediment cover on the ridges varies from several hundred meters to more than one kilometer. Sedimentary ridges up to 55 meters high blanket the crestal plateau of the Alpha Cordillera, and appear to be the result of currents which transport sediment across the ridge from northwest to southeast. This process is presently inactive, and may have terminated with the initiation of continental glaciation, perhaps as early as Upper Miocene time. Similar sedimentary structures 700 meters beneath the Mendelejev Plain suggest a strong bottom circulation in the past. A zone of bottom erosion along the Mendelejev Ridge flank may reflect a circulation of water through the Cooperation Gap, a trough which appears to cross the ridge. Two buried channels extending to subbottom depths of 700 meters were observed between the Mendelejev Fracture Zone and the Mendelejev Plain.

Three general-purpose computer programs are included. They compute 1) geographic position from celestial observations, 2) probable drift between known positions using wind data, and 3) gravity meter calibrations at a base station with correction for earth tides based upon a calculation by means of an abbreviated lunar and solar ephemeris.

## TABLE OF CONTENTS

INTRODUCTION	1
Geographical Setting	1
Previous Work	4
Present Work	10
DATA REDUCTION	14
Navigation	14
Depth Soundings	18
Gravity Measurements	18
Magnetic Measurements	20
Seismic Reflection Measurements	22
Data Storage and Presentation	24
INTERPRETATION	26
PART I: TECTONIC FEATURES	26
Bathymetry	26
Seismic Reflection Measurements	34
Gravity Measurements	42
Magnetic Measurements	51
Inferred Fracture Zone Pattern	56
Speculations concerning the Alpha Cordillera as an Inactive Center of Seafloor Spreading	62
Proposed Model	62
Alternative Proposals	67
Geological Evidence	69
Precambrian to Carboniferous	69
Carboniferous to Upper Mesozoic	74
Upper Mesozoic to Present	75
Age of the Canada Basin	78
A Final Note	80
PART II: SEDIMENTARY FEATURES	31
Hyperbolic Echoes observed on the Precision Depth Recorder	81
Data bearing on the Origin of the Hyperbolization	83
Seismic Reflection Measurements	83
Sediment Cores	85
Camera Stations	86
Bottom Current Measurements	87
Nepheloid Measurements	88
Discussion	91
The Mendelejev Plain and Buried Hyperbolization	92
The Mendelejev Fracture Zone	96
Bottom Erosion Zone along the Mendelejev Ridge	98
Buried Channels through the Flank of the Mendelejev Fracture Zone	101

BIBLIOGRAPHY	104
APPENDIX	111
Celestial Navigation Programs: EDOC, LUNE, and CELPS	111
Wind Drift Program: WDF	114
Gravity Tie Program: GRVT	115

## LIST OF FIGURES

<u>Figure</u>		<u>Page</u>
1	Physiographic Diagram of the Arctic Ocean	2
2	Seismicity of the Arctic	7
3	Magnetic Anomaly Pattern over the Eurasian Basin	9
4	T-3 Drift Track 1962-70	12
5	Area I Drift Track	15
6	Area II Drift Track	16
7	Area III Drift Track	17
8	G-27 Gravity Meter Drift Curve	19
9	Area I Bathymetry	27
10	Area II Bathymetry	29
11	Area III Bathymetry	31
12	Geophysical Profile across the Alpha Cordillera	33
13	Geophysical Profiles across the Mendelejev Fracture Zone	35
14	Area I Bathymetric and Reflection Profiles	36
15	Area II Bathymetric and Reflection Profiles	38
16	Selected Reflection and Magnetic Profiles, 1962-63	39
17	Area III Reflection Profiles, Western Part	40
18	Area III Bathymetric and Reflection Profiles, Eastern Part	41
19	Comparison of the Alpha Cordillera Basement with the Mid-Atlantic Ridge	43
20	Area I Free-Air Anomalies	44
21	Area II Free-Air Anomalies	45
22	Area III Free-Air Anomalies	46
23	Gravity Derived Crustal Section through the Alpha Cordillera	49
24	Plot of Free-Air Gravity versus Latitude	50
25	Area I Magnetics	52
26	Area II Magnetics	53
27	Area III Magnetics	54

28A	Inferred Fracture Zone Pattern - Bathymetric Base	59
28B	Inferred Fracture Zone Pattern - Gravity Base	60
28C	Inferred Fracture Zone Pattern - Magnetics Base	61
29	Relation of the Alpha Cordillera and Mendelejev Ridge to the Continental Geology around the Arctic Ocean	63
30	Sedimentary Features on the Crest of the Alpha Cordillera	82
31	Area III Microphysiography and Observed Bottom Currents	84
32	Area III Camera Station and Nepheloid Layer Characteristics	90
33	Seismic Reflection Record from the Mendelejev Plain	93
34	Comparison of Seismic Reflection Records from Four Arctic Plains	95
35	Seismic Reflection Record from the Mendelejev Fracture Zone	97
36	Mendelejev Ridge Erosion Zone; Bottom Photos and Seismic Reflection Record	99
37	Buried Channels on the Flank of the Mendelejev Fracture Zone	102
38	Sample Fix with Celestial Navigation Program	121

## ACKNOWLEDGEMENTS

This investigation was conducted under contracts NONR 266(82) and N00014-67-A-0108-0016 with the Office of Naval Research. The data used in this study were obtained by some forty scientists of the Lamont-Doherty Geological Observatory over a period of more than eight years. Their contribution is greatly acknowledged. The Naval Arctic Research Laboratory in Barrow Alaska, maintained the camp on T-3 and provided the support so necessary to this work. Allan Gill provided the magnetic measurements from the winter drift of the British Trans-Arctic Expedition. Ralph Shaver prepared the explosion seismic reflection profiles and carried out many of the measurements. The magnetic model for Harris and Wilkins Seamounts was prepared in 1966 by Jeffrey Friedberg. Dr. Ned A. Ostenso kindly supplied preprints describing the results of University of Wisconsin work within the Arctic Basin. This study was accomplished under the supervision of Dr. Kenneth L. Hunkins and Professor John E. Nafe. Discussions with Professor Bruce C. Heezen, Professor M. Talwani, Dr. H. Kutschale, Dr. W. Pitman, Dr. X. LePichon, Mr. J. I. Ewing, and Prof. R. W. Fairbridge were extremely helpful.

## INTRODUCTION

### Geographical Setting

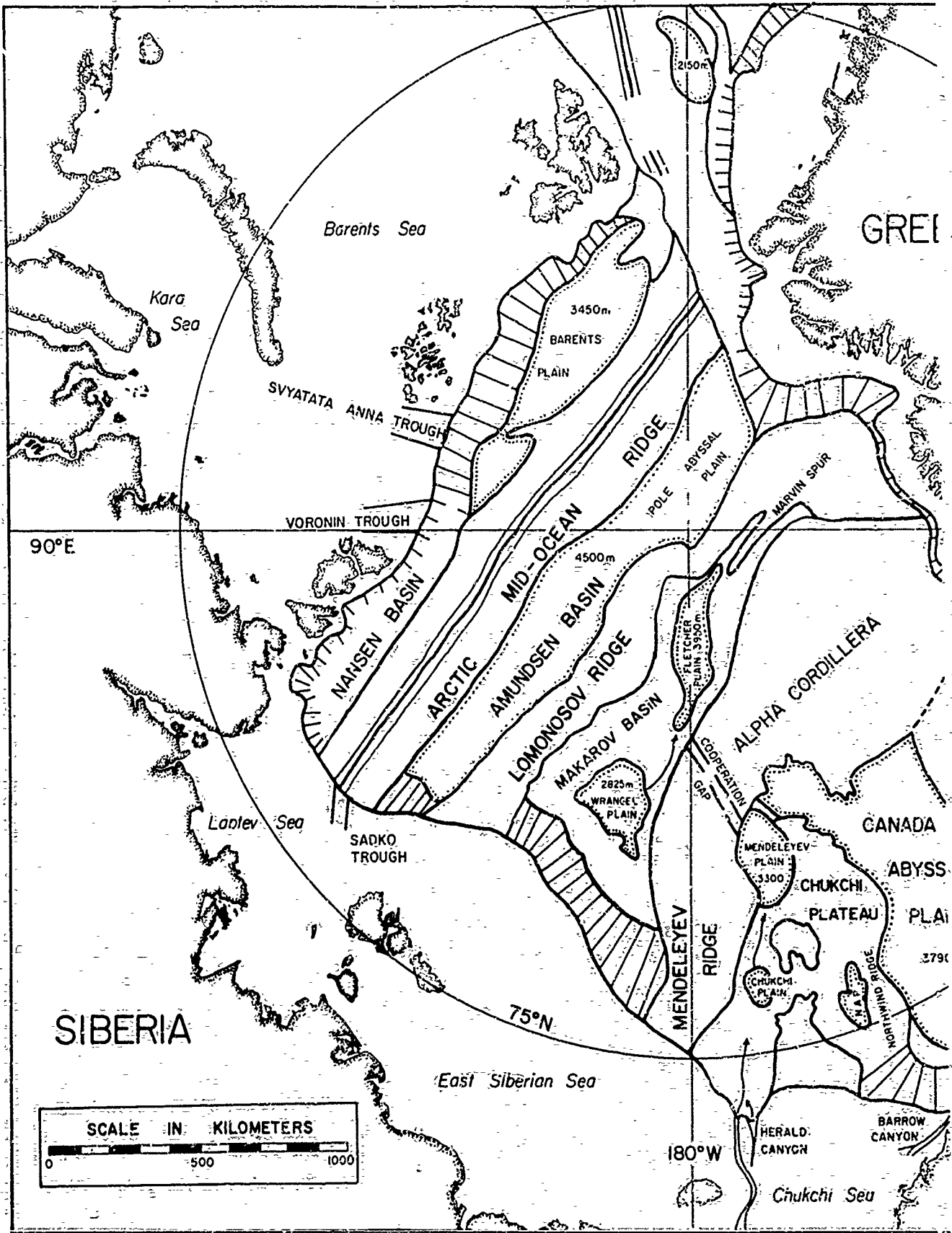
The Arctic Ocean, with an area of about 14 million square kilometers, is the smallest of the world oceans. This ocean is unique in several significant respects. It is almost land-locked, it has a perennial cover of pack ice, continental shelves occupy one third of its area, and it is divided by three subparallel submarine ridges. Figure 1 is a physiographic diagram of the Arctic Ocean showing the major features. This diagram is based upon a diagram given by Hunkins (1968).

The deep portions of the ocean form an almost rectangular basin, approximately 1800 kilometers wide and 2500 kilometers long. The three subparallel ridges cross this basin along its minor axis. The Lomonosov Ridge lies in the center, dividing the basin into the Amerasia Basin north of Alaska, and the smaller and deeper Eurasia Basin north of Europe. This ridge has steep slopes that are convex upward, and has minimum depths of 1100-1200 meters on the North American side, and about 1700 meters where sounded on the Siberian side. The width of this ridge varies between 40 and 75 kilometers.

The deeper Eurasia Basin is divided into two smaller basins by the Arctic Mid-Ocean Ridge, a seismically active belt of high ridges and deep rifts. This feature is considered to be the Arctic extension of the Mid-Atlantic Ridge, a center of seafloor spreading. The Amundsen Basin lies between the Mid-Ocean Ridge and the Lomonosov Ridge and encloses the Pole Abyssal Plain. This plain is the deepest and second largest plain in the ocean basin; its depth increases from about 3900 meters near the Lomonosov Ridge to more than 4200 meters along the Arctic Mid-Ocean Ridge. South of the Mid-Ocean Ridge lies the Nansen Basin, which encloses the small Barents Plain at depths between 3750 and 3900 meters.

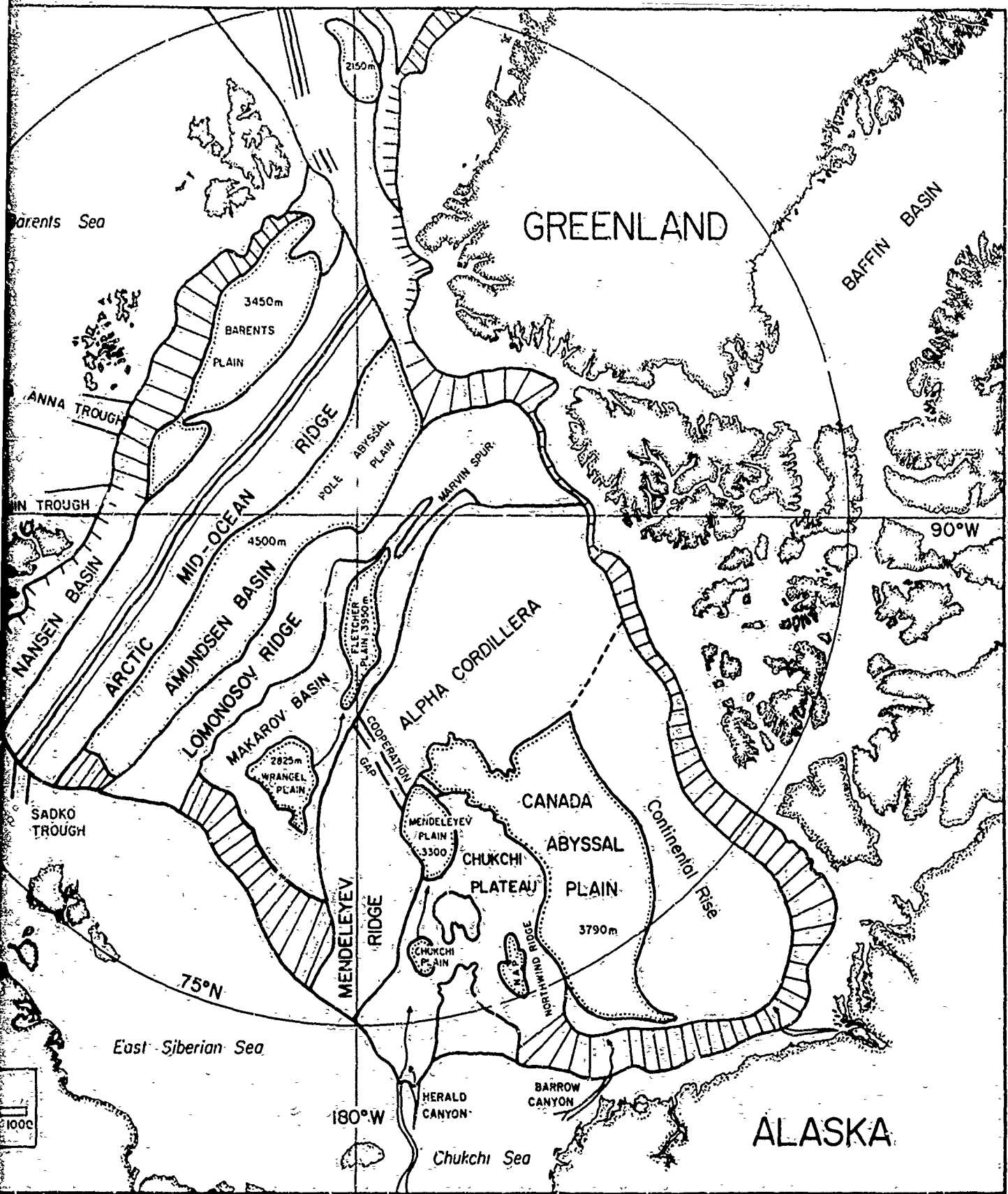
South of the Lomonosov Ridge, the Alpha Cordillera divides the Amerasia Basin into two smaller basins, the Makarov Basin on the

A



ARCTIC OCEAN PHYSIOGRAPHIC DIA

B



ARCTIC OCEAN PHYSIOGRAPHIC DIAGRAM

Figure 1

north, and the Canada Basin on the south. Two plains form the deep floor of the Makarov Basin. The Wrangel Plain at 2825 meters lies below the East Siberian Shelf, and connects with the deeper Fletcher Plain at 3900 meters via the Arlis Gap. The Marvin Spur projects into this basin from the Lomonosov Ridge north of Ellesmere Island.

The Alpha Cordillera is the largest single submarine feature in the Arctic Ocean. Like most of the features in this ocean, the Alpha Cordillera has not been extensively sounded, but its outline is generally known. It crosses the basin from the vicinity of Ellesmere Island to the East Siberian Shelf, forming broad triangular plateaus where it abuts the shelves. The width of the Alpha Cordillera varies considerably, reaching a maximum on the Canadian side, and a minimum of about 300 kilometers near the center, where the crestal regions reach their maximum depth of more than 2000 meters. Soviet workers (Belov and Lapina, 1958) report this crestal low to consist of a long deep trough with topographically complex, convex-upward slopes, and a maximum depth of 2700 meters. At this point, called the Sotrudnichestva (Cooperation) Gap by Treshnikov et al. (1967), the cordillera axis changes direction toward the south, heading away from the Laptev Shelf and toward the East Siberian Shelf, and the feature becomes the Mendeleev Ridge.

Between the Alpha Cordillera and the Chukchi Shelf lies the Canada Basin, the largest of the four Arctic basins. In the center lies the Canada Plain, the largest plain, with depths of about 3850 meters along the flank of the Northwind Ridge. The Chukchi Rise, including the Northwind Ridge, projects about 600 kilometers north from the edge of the Chukchi Shelf. Two small plains are located between the Chukchi Rise and the Mendeleev Ridge. The Chukchi Plain, located near the East Siberian Shelf at a depth of 2200 meters, connects with a deeper plain to the north via the Charlie Gap (Figure 9). This plain, at a depth of about 3300 meters, is described here for the first time, and has been called the Mendeleev Plain. It

presumably connects with the Canada Plain north of the Chukchi Rise via another gap.

#### Previous Work

The perennial surface ice cover on the Arctic Ocean makes navigation by conventional vessels impossible. This single fact accounts for the slow growth of knowledge about the Arctic Ocean. What knowledge there is has been acquired through a wide variety of means. Chief among these are the drift of vessels imprisoned in the pack, spot landings of aircraft and airlifted temporary camps on ice floes, limited penetrations by icebreakers along the fringes of the pack, underwater probings and transits by conventional and nuclear submarines, and in the case of the present investigation, the meanderings of ice islands within the pack. In addition, long range aircraft are measuring the magnetic field, and together with artificial earth satellites, are acquiring data about ice conditions. Beal (1968) and Ostenso (1962) have presented interesting discussions of the history of scientific research in the north polar regions.

Drifting ice stations have contributed much to our knowledge of the Alpha Cordillera. The broad outline of this feature was first shown in a diagrammatic chart of volcanism in the Arctic Ocean by Hakkel' (1958), and was based primarily upon soundings made from the drifting Soviet ice station NP-4 in November 1955. In 1957 and 1958 Drifting Station Alpha crossed the cordillera, permitting Hunkins (1961; also JGY, 1959, and 1961) to carry out investigations which showed this feature to be a major morphological province. Over 600 explosive soundings revealed water depth, bottom dip and strike, and subbottom information. Three unreversed refraction profiles indicated an average of 0.38 km of unconsolidated sediment overlying, in one case, a 2.80 km thick layer with 4.70 km/sec compressional wave velocity. Below this lay a 6.44 km/sec "oceanic" layer of undetermined thickness. The central portions of the Alpha Cordillera were sounded from Soviet drift station

NP-7 at about the same time.

Ice Station T-3 drifted over the Canadian terminus of the Alpha Cordillera in 1952 and 1953. Data taken along the track outlined the Marvin Spur (Crary, 1954). Crary and Goldstein (1957) reported three unreversed refraction profiles which showed a shallow velocity structure more continental than oceanic. Kutschale (1966) gave the results of geophysical investigations from Drifting Station Arlis II within the Makarov Basin. He reported the existence of a steeply dipping basement ridge beneath the Wrangel Plain. This ridge separates that plain from the deeper Fletcher Plain, and appears to connect with the Alpha Cordillera. Seismic reflection profiles showed at least 3.5 km of stratified sediment beneath the Wrangel Plain.

Dietz and Shumway (1961) published the first continuous sounding lines across the Arctic Ocean, taken by the submarine U. S. S. Nautilus in 1958, and by the U. S. S. Skate in 1958 and 1959. They observed steep flanks and a relatively smooth upper surface lacking in jagged topography, and concluded that the cordillera was non-volcanic and bounded by major faults. Gravity measurements made from Station Alpha showed a regional free-air gravity anomaly of +60 milligals over the cordillera, which Ostenso (1963) interpreted as being further evidence of a horst structure, as suggested by the submarine profiles.

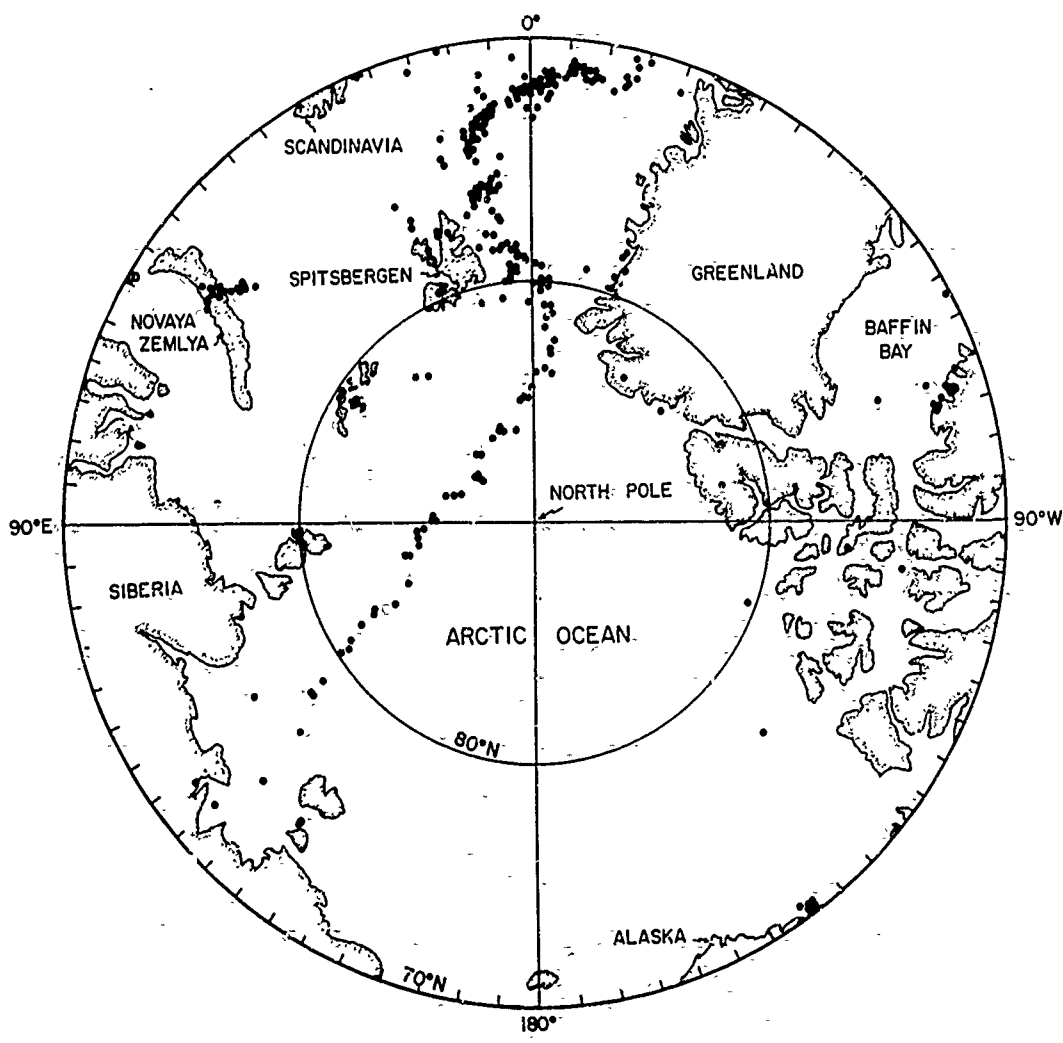
A low level aeromagnetic survey was made over part of the Arctic in 1961, and was reported by Ostenso (1962). Depth to source computations were made from the anomalies. These revealed that the high amplitude anomalies associated with the cordillera were of shallow origin, suggesting an uplifted basement. These same high amplitude anomalies, observed in a high altitude survey flown in 1950 and 1951, led King et al. (1966) to designate a "central magnetic zone" whose anomalies parallel and extend beyond the flanks of the Alpha Cordillera. They noted the presence of broad long wavelength "block shaped" positive and negative anomalies along the flanks, which they considered

to be related to the "block-faulted mountain range" origin suggested by Hunkins (1961) to explain the rugged relief observed from Station Alpha.

King et al. (1964, 1966) also noted the resemblance between the high amplitude anomalies on the cordillera and adjacent plains, and those over the Canadian Shield. They concluded that the Amerasia Basin consists of a large sunken block of highly magnetic continental rock, presumably Precambrian like the rocks in the Canadian Shield Complex. A process of crustal thinning was evoked to explain the thin (hence oceanic) character of the basin crust as suggested by a) the surface wave studies of Oliver et al. (1955) and Hunkins (1963), and b) the gravity observations of Ostenso (1963). The downdropped-block hypothesis, commonly called upon in early speculations on the origin of the Arctic Basin to provide a connection between similar tectonic features observed on opposing sides of the basin, seems to make its last appearance in the paper of King et al. (1966).

Lachenbruch and Marshall (1966) measured the heat flow at twenty stations over the cordillera flank and on the adjacent plain from T-3 in 1963, and found the flux over the cordillera to be about one half that of the normal and uniform ( $1.41 \pm 4\%$  microcalories./cm<sup>2</sup>sec) flux measured on the plain. Using models they concluded that their measurements were best explained by a zone of low conductivity rock extending below the cordillera to a depth of at least 15 kilometers, and projecting out at this depth for some distance beneath the adjacent plain. This model is similar to the anomalous mantle models for the mid-oceanic ridges given by Talwani et al. (1965).

Sykes (1965) relocated all well-recorded Arctic earthquakes for the period January 1955 to March 1964. In the vicinity of the Alpha Cordillera only one earthquake was recorded. This was a small event, of magnitude 4.9, which occurred on June 3, 1956 on the Canadian Shelf at 79.91° North, 117.70° West. Barazangi and Dorman (1970) prepared



SEISMICITY OF THE ARCTIC, 1961-SEPT. 1969, ESSA, CGS EPICENTERS

Figure 2

an updated Arctic seismicity map (Figure 2) based upon the ESSA and USC&GS epicenters for 1961 through September 1969. Again only one epicenter was observed along the trend of the Alpha Cordillera, on the continental shelf north of Canada. From these data one can conclude that the Amerasia Basin is essentially aseismic.

Beal (1968) reported on the bathymetry and structure of the Arctic Ocean, based primarily on the bathymetric data collected during United States nuclear submarine cruises between 1958 and 1962. Nine profiles across the Alpha Cordillera assisted greatly in defining the physiography of this feature. Beal (1968) describes the Alpha Cordillera as a broad arch, marked with volcanoes and regions of "high fractured plateau" similar to those observed on the Mid-Atlantic Ridge, and by scarps 500 to 1000 meters high. On the basis of the physiography, the magnetic lineations, and the relatively small quantity of geophysical data pertaining to the crustal structure, Beal (1968) interpreted the cordillera as an inactive mid-oceanic ridge which has undergone some subsidence. The Alpha Cordillera was considered to be an Arctic extension of the buried ridge discovered beneath the Labrador Sea by Drake et al. (1963), and probably responsible for the opening of the Amerasia Basin.

In the meantime, Soviet investigators mapped the magnetic patterns in the Eurasia Basin. Rassokho et al. (1967) and Karasik (1968) showed a linear anomaly pattern (Figure 3) paralleling the Arctic Mid-Ocean Ridge and exhibiting rough symmetry relative to the ridge axis. Karasik (1968) obtained a preliminary spreading rate of 1.1 cm/year for the past 8-10 million years by comparison with the known anomaly pattern for the other oceans. Toward the Alpha Cordillera and the Mendeleev Ridge the anomaly wavelengths were seen to increase with the pattern becoming more irregular. The magnetic anomaly amplitudes over the Arctic Mid-Ocean Ridge are considerably smaller than those on the Alpha Cordillera.

Vogt and Ostenso (1970) examined the existing geophysical and

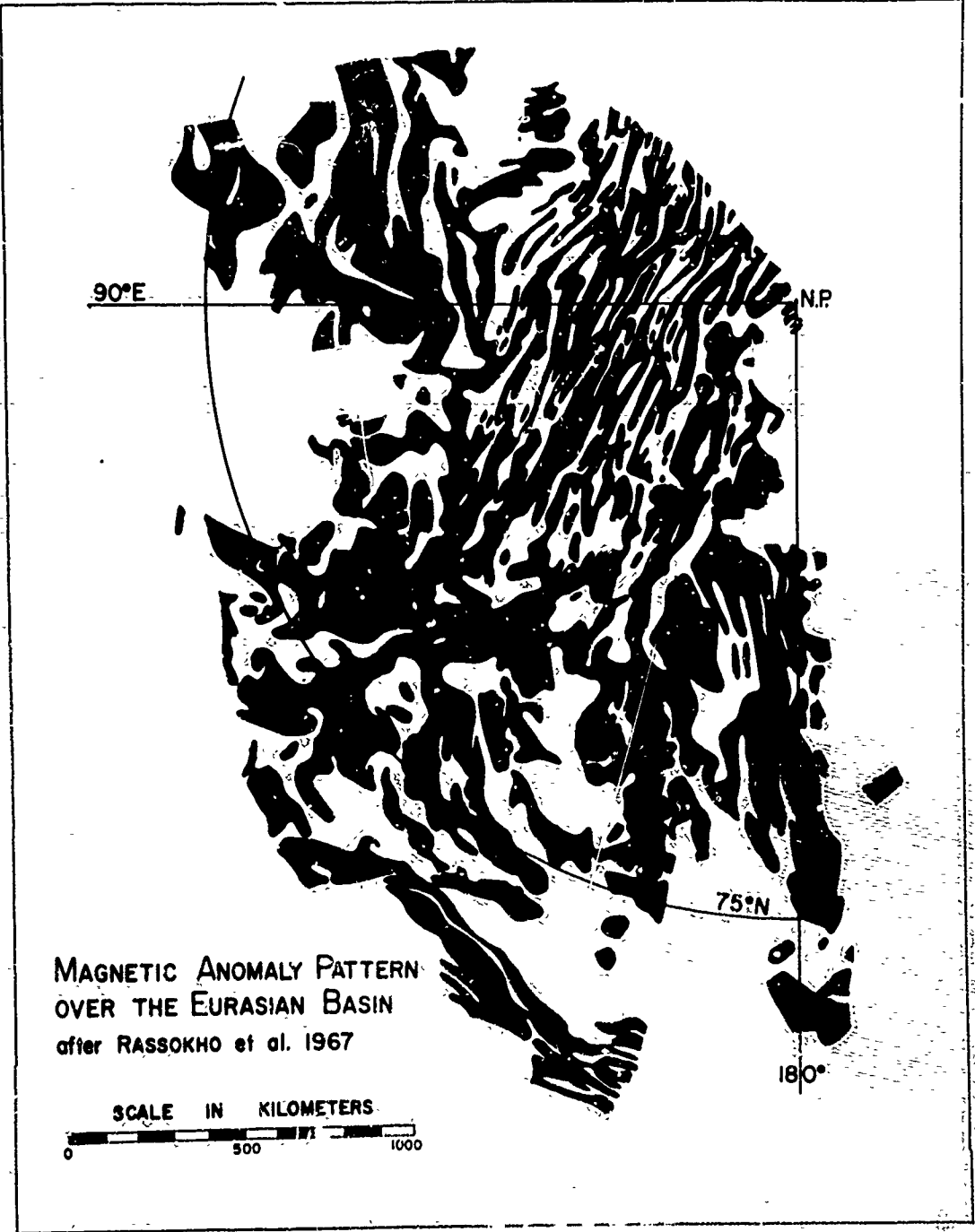


Figure 3

geological data, and found it to be consistent with the hypothesis that the Alpha Cordillera is an inactive mid-oceanic ridge. Using additional low level aeromagnetic profiles flown in 1963 and 1964, they attempted to date the anomaly pattern over the cordillera. A comparison of selected profiles projected perpendicular to the cordillera with profiles from the North Atlantic suggested a correlation with anomalies now found between 300 and 500 kilometers from the axis of the Reykjanes Ridge, indicating that the cordillera became inactive in the Tertiary, probably about 40 million years ago. A small degree of symmetry was observed in some of the profiles.

Vogt and Ostenso (1970) also used early gravity measurements from Ice Station Arlis II over the Mendeleev Ridge, and from T-3 and Alpha over the Canadian end of the Alpha Cordillera, to make three projected gravity and bathymetric profiles across the cordillera. Model calculations were made for the two end profiles, using six layers. A root of anomalous mantle extending to about 70 kilometers was required to fit the observed anomalies.

#### Present Work

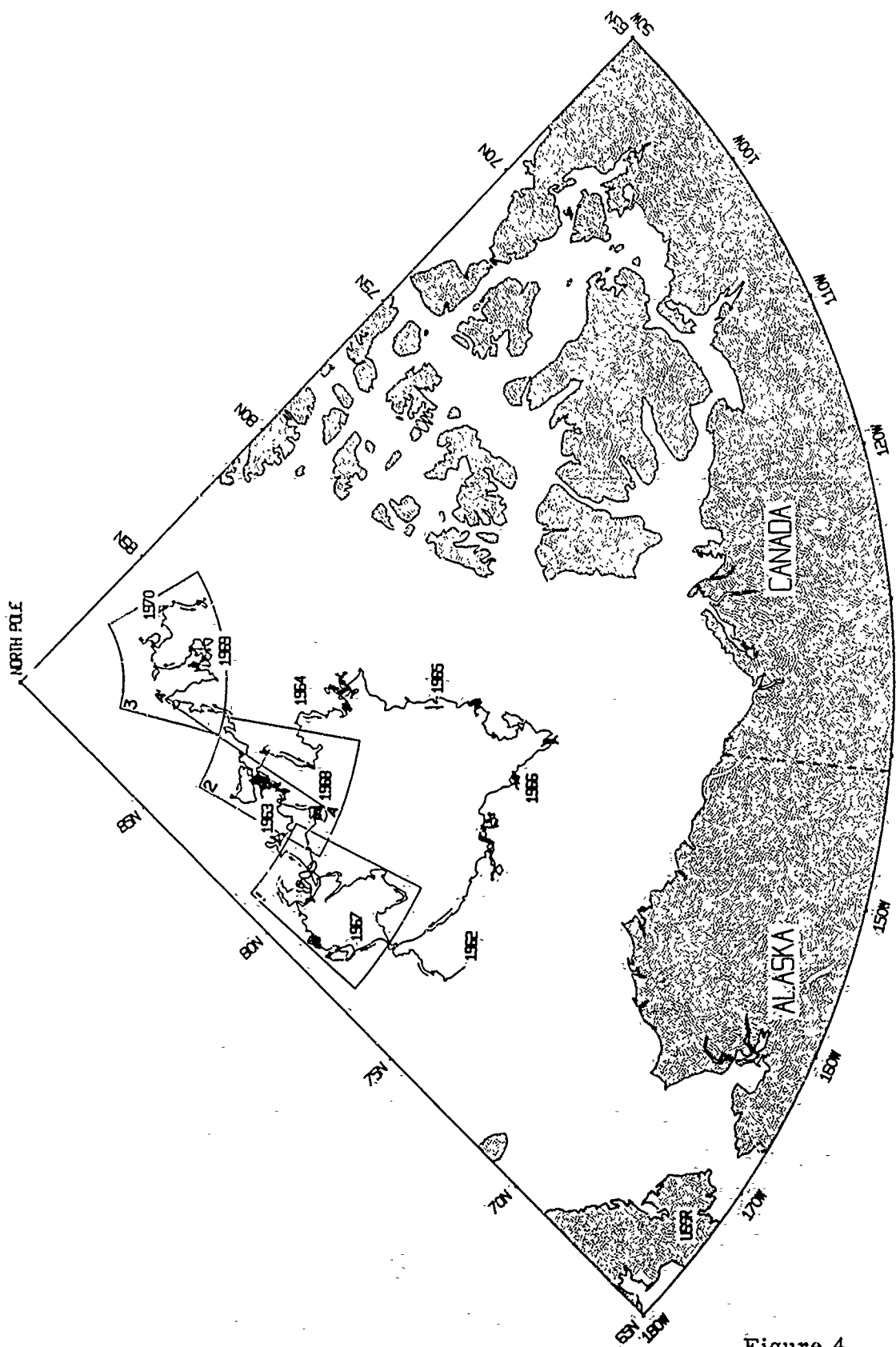
This paper presents the geophysical findings of the post-1962 drift of Fletcher's Ice Island (T-3) in the vicinity of the Alpha Cordillera. Fletcher's Ice Island began operations in March 1952 with the landing of a scientific party under the leadership of Lt. Col. Joseph O. Fletcher on a large (approximately 170 square kilometers) and thick (about 50 meters) piece of glacial ice. This tabular iceberg is believed to have broken off from the land-fast ice shelf along the northern coast of Ellesmere Island. The morphology of the ice island has been described by Smith (1960):

For the next eight years, T-3 drifted south and west from its initial position 230 km from the north pole, skirting the continental margin north of Canada, and eventually grounding, in April 1960, on a shoal 150 km northwest of Barrow, Alaska. Many investigations, some of which have been mentioned in the previous section, were carried out

from the station, and the results have been compiled by Bushnell (1959), and by Cabaniss et al. (1965). Following the grounding, the station was occupied for more than a year, but was finally abandoned in September 1961 when it was decided that T-3 was there to stay

Sometime during the next winter the island drifted free, and on February 16, 1962 it was discovered by an Arctic Research Laboratory (ARL) plane on a routine supply flight to the new ice island, Arlis II. Within a few days the station was reoccupied by ARL personnel, and its life began anew. By the middle of May a geophysical program was being conducted by scientists of the Lamont-Doherty Geological Observatory. This program, consisting of navigation, depth soundings, and gravity and magnetic observations, plus supplemental seismic reflection measurements, coring and bottom photography, continues to the present time, with numerous additions and refinements. This program is customarily carried out by two or three field personnel.

Figure 4 shows the drift of T-3 since its reoccupation. During this period the station has completed one clockwise orbit around the Canada Basin, and is now on its way through a second. Three insets show the areas to be considered. Area I and II, on the flank of the Mendeleev Ridge, and between the Chukchi Rise and Alpha Cordillera, were investigated during the 1962-63 and 1966-68 drift of T-3. Area III was investigated during 1968-70. Depth soundings were made along much of the drift track. In 1966 a seismic profiler was installed, and reflection measurements were obtained along much of the 1967 and 1968-70 track. During these periods a number of piston cores, bottom photographs, and light scattering measurements were also obtained. The T-3 data, together with pertinent observations from Stations Alpha, Charlie, and Arlis II, as well as the Russian drift station North Pole 2, have been used in the study. The recent T-3 data is available in reduced graphical form in a report by Hunkins et al. (1969). The earlier supplemental data was taken from compilations by Bushnell (1959), Black and Ostenso (1962), Cabaniss (1962), Cabaniss et al. (1965),



T-3 DRIFT TRACK 1962-1970

Figure 4

and Somov (1955).

Additional magnetic measurements were made by members of the British Trans-Arctic Expedition (BTAE) wintering on an ice floe approximately 140 kilometers to the northwest of T-3 during the period November 1968 to February 1969. These measurements filled in many details of the anomaly pattern over the ridge crest.

The present findings are wholly consistent with the suggestion of Beal (1968) and Vogt and Ostenso (1970) that the Alpha Cordillera is an inactive mid-oceanic ridge. The principal evidence for this is the identification of at least five fracture zones that cut the cordillera, and apparent offsets of the ridge axis in the crestal regions. Bathymetric data suggest the presence of other fractures, while seismic reflection studies suggest a buried basement topography similar to that found on the Mid-Atlantic Ridge. The magnetic and gravity data support this thesis, and suggest the existence of still other fractures.

Bottom currents appear to control sedimentation over a large part of the area studied. Elongate sedimentary ridges or waves appear to cover the crestal plateau, but are blanketed with a uniform cover of pelagic sediment, suggesting that they have been inactive for a considerable period of time. These waves are apparently the result of a strong paleocirculation, similar to the weak one found today, which transported sediment across the ridge from northwest to southeast. Along the eastern flank of the Mendeleev Ridge a region of submarine erosion is observed, apparently maintained by a strong flow of water through the Cooperation Gap, from the Makarov Basin to the Canada Basin. A zone of sediment waves observed beneath the present Mendeleev Plain indicates that bottom currents have apparently been an effective agent of deposition in the past.

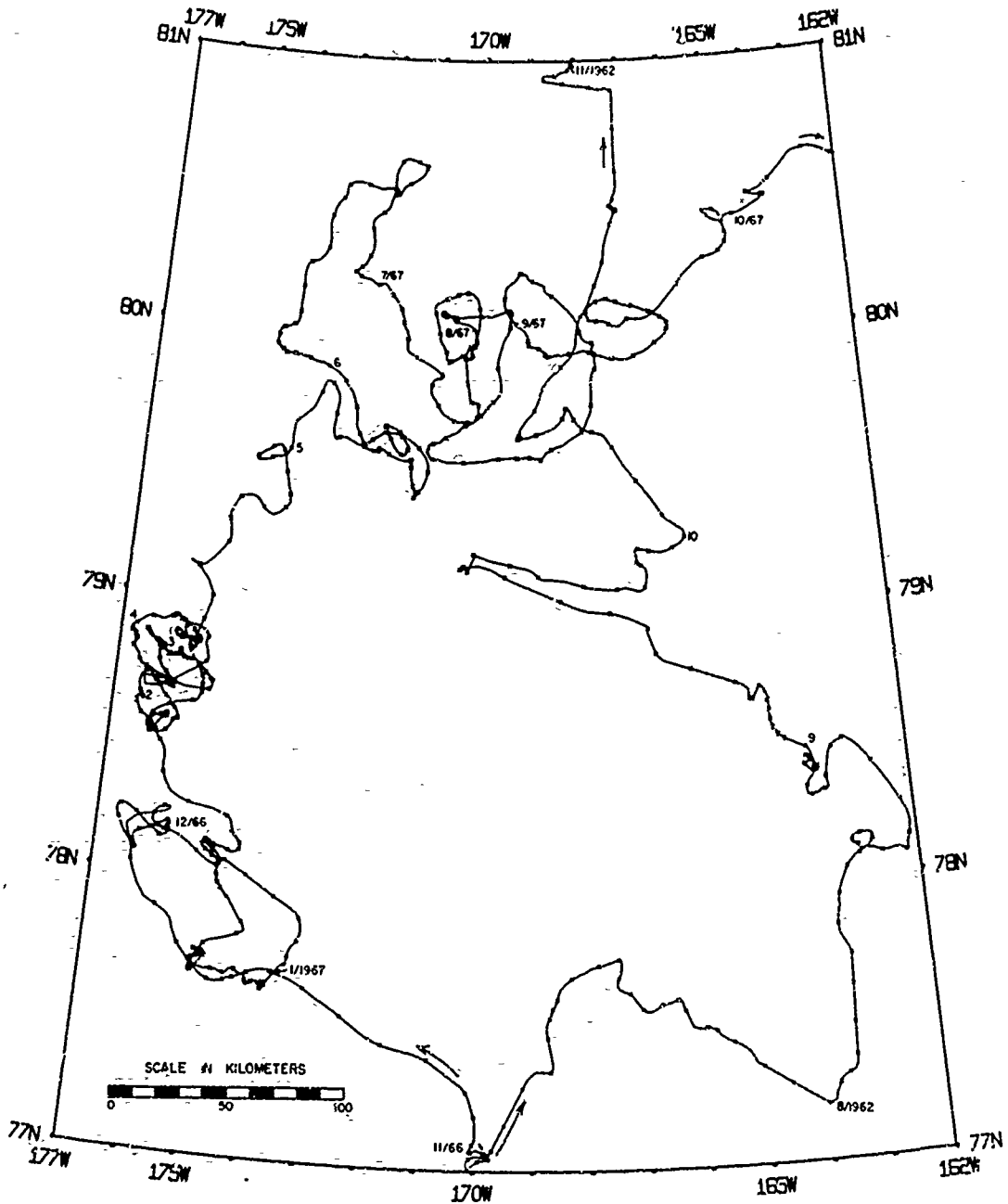
## DATA REDUCTION

All data used in this study were reduced and processed with the aid of an electronic digital computer. Several Fortran language programs developed for this investigation, but having a wider range of applicability, are described and listed in the Appendix.

### Navigation

The drift track for T-3 (Figure 4) is based upon two types of navigational fixes. Positions prior to April 15, 1967, and for the periods November 18, 1967 to February 17, 1968, March 3, 1968 to April 28, 1968, November 2, 1968 to December 4, 1968, and January 2, 1969 to February 25, 1969 were determined by celestial navigation with a theodolite, whenever visibility permitted. The fixes were reduced by computer (see Appendix). A maximum error of  $\pm 1$  km was possible when sun shots were used in daylight periods, and  $\pm \frac{1}{2}$  km when star sights were used. Positions for all other periods are from satellite fixes using the U. S. Navy Navigation Satellite System (NNSS) described by Guier (1966) and reviewed by Talwani et al. (1966). Errors in excess of  $\pm \frac{1}{4}$  km are unlikely because of the high rate of fixing with this method at polar latitudes, and because of the low rate of ice drift. Wind data were used in another program (see Appendix) to compute the most probable drift of the island between fixes by applying the "rule" observed by Nansen during the drift of the Fram. This rule, describing the effect at the surface of the Ekman spiral, states that the ice tends to drift at a small fraction of the wind speed, and at a fixed angle to the right (in the northern hemisphere) of the wind.

The detailed track for Areas I-III, shown as insets in Figure 4, is presented in Figures 5, 6, and 7. Individual fixes are not plotted on the drift track, as up to fifty per day are available with the satellite system. Approximately 11,000 kilometers of track are represented on these three maps. Daily distances varied from zero for periods of calm to a maximum of 25 kilometers. An analysis of more than 2500 days drift for T-3 showed the average daily drift to be 5.2 km/day.



AREA I TRACK CHART

Figure 5

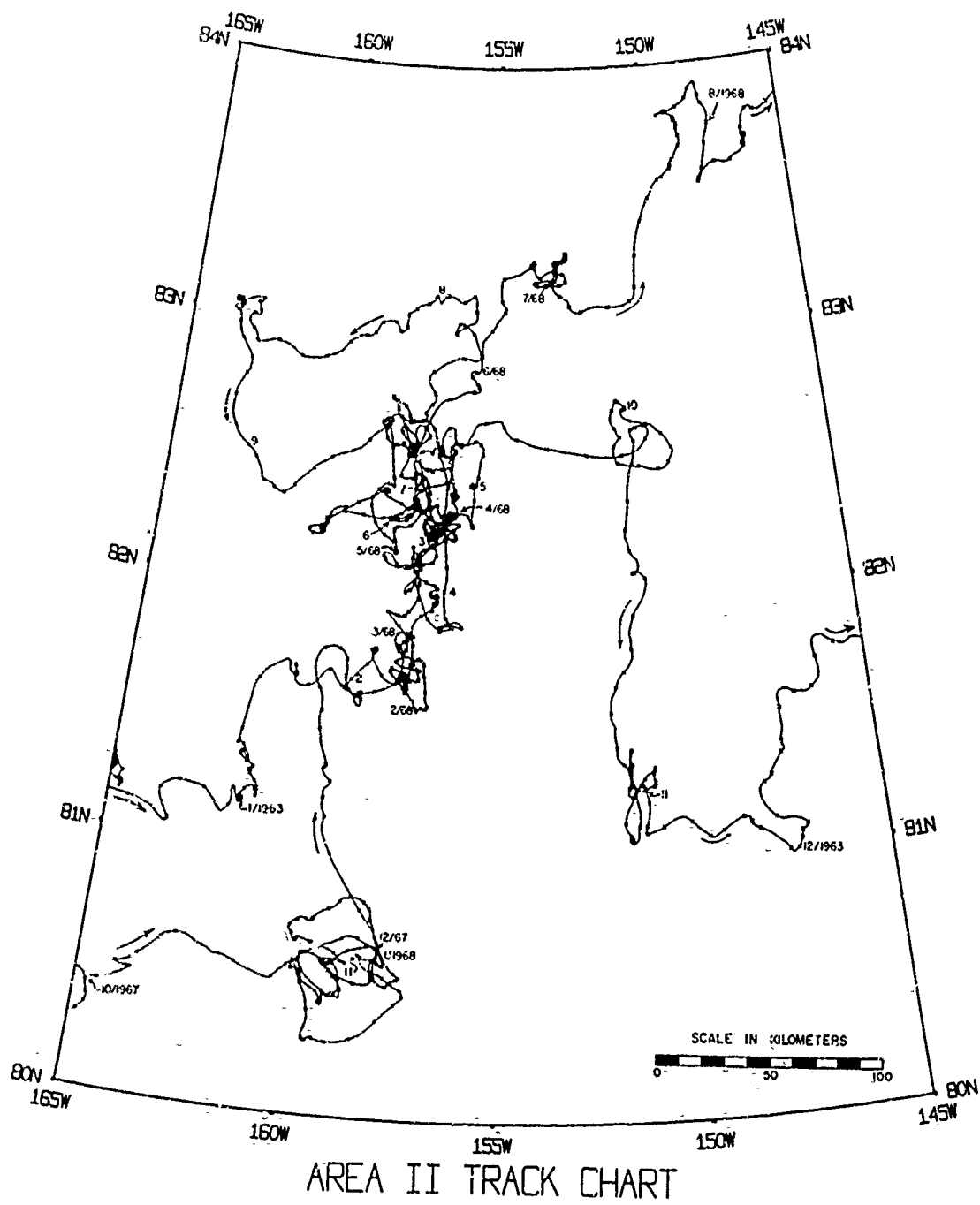
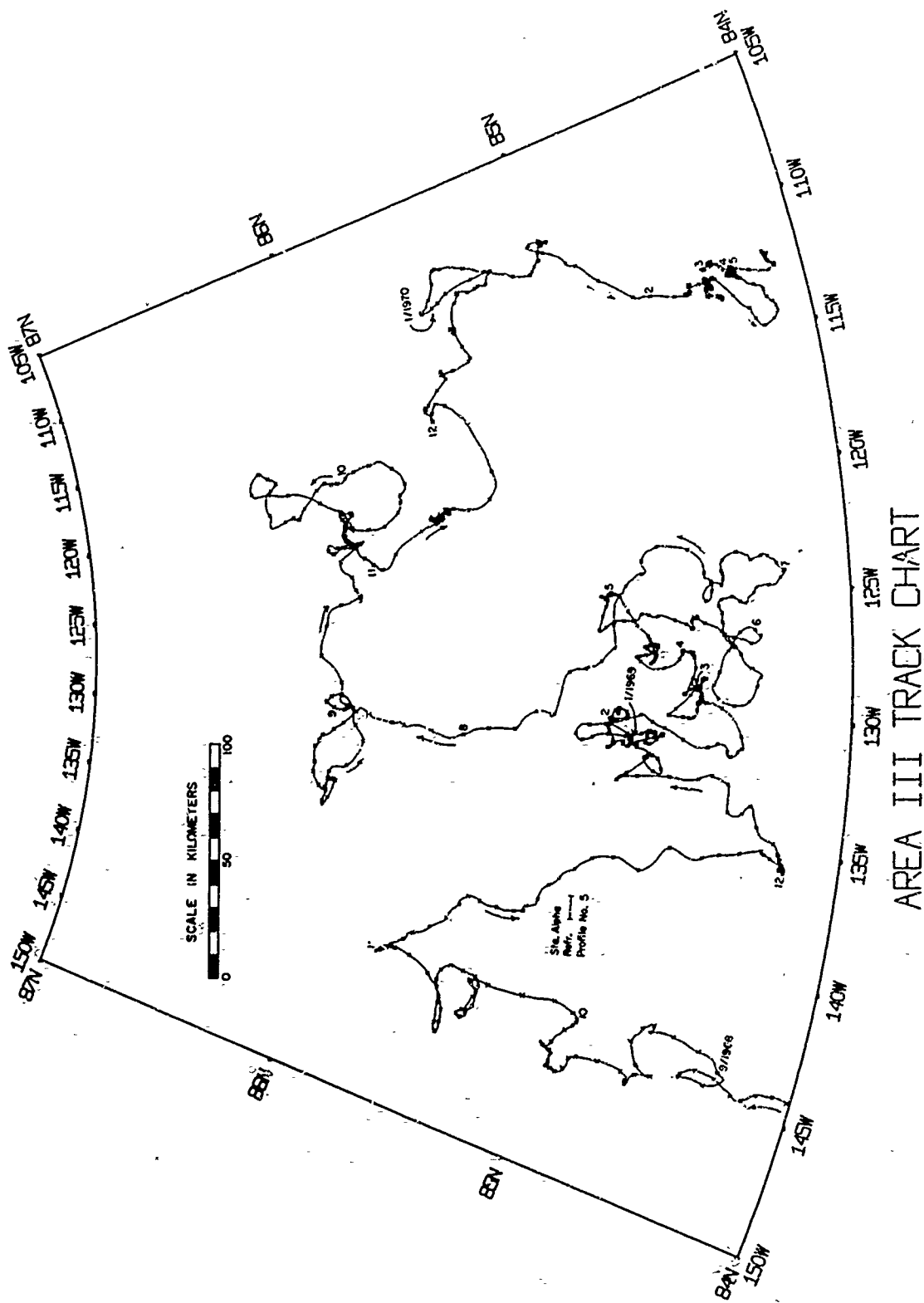


Figure 6



AREA III TRACK CHART

Figure 7

### Depth Soundings

Depth soundings were made almost continuously using a precision depth recorder (PDR) of the type described by Hubbard and Luskin (1959). A Giffit ESRTR-3 sonar transceiver was used as the sound transmitter and receiver, driving an EDO Corporation AN/UQN 12 KHz transducer at a nominal pulsed power of 1000 watts. All soundings were made on a 1 second (750 meters) recording scale, with a paper feed rate of approximately 1 cm/hour. The echo-distance error due to timing in the recorder and reading of the records was about 0.0025 seconds ( $\pm$  2 meters). The records were digitized at frequent intervals (0.1 to 0.5 km), and at all slope changes to allow accurate interpolations. These soundings were corrected for the vertical variations in the sound velocity (Matthews, 1939) as part of the computer reduction program. Corrections of the order of +60 meters were needed for water depths of 3000 meters. No slope corrections were applied.

Between May 1962 and June 1963, when the PDR was put into operation, soundings were obtained using explosive charges and a geophone detector. A total of 617 spot soundings were obtained, with measurement accuracy of  $\pm$  1 millisecond, or less than 2 meters. These soundings were corrected in the same manner as the PDR data.

### Gravity Measurements

Gravity measurements were made several times a day with a Lacoste & Romberg Model G (No. 27) geodetic gravity meter. The meter was mounted on a wooden post which projected through the laboratory floor and was securely frozen into the ice. The meter height was approximately 4 meters above sealevel. Ice vibrations generally did not interfere with the observations. In order to record its instrumental drift, this meter was used in comparison measurements at the University of Wisconsin pendulum station at Barrow, Alaska, twenty-five times between 1962 and 1970. The drift is shown in Figure 8. Abrupt changes in drift occurred in late 1964 and 1969 (not shown in diagram), but these

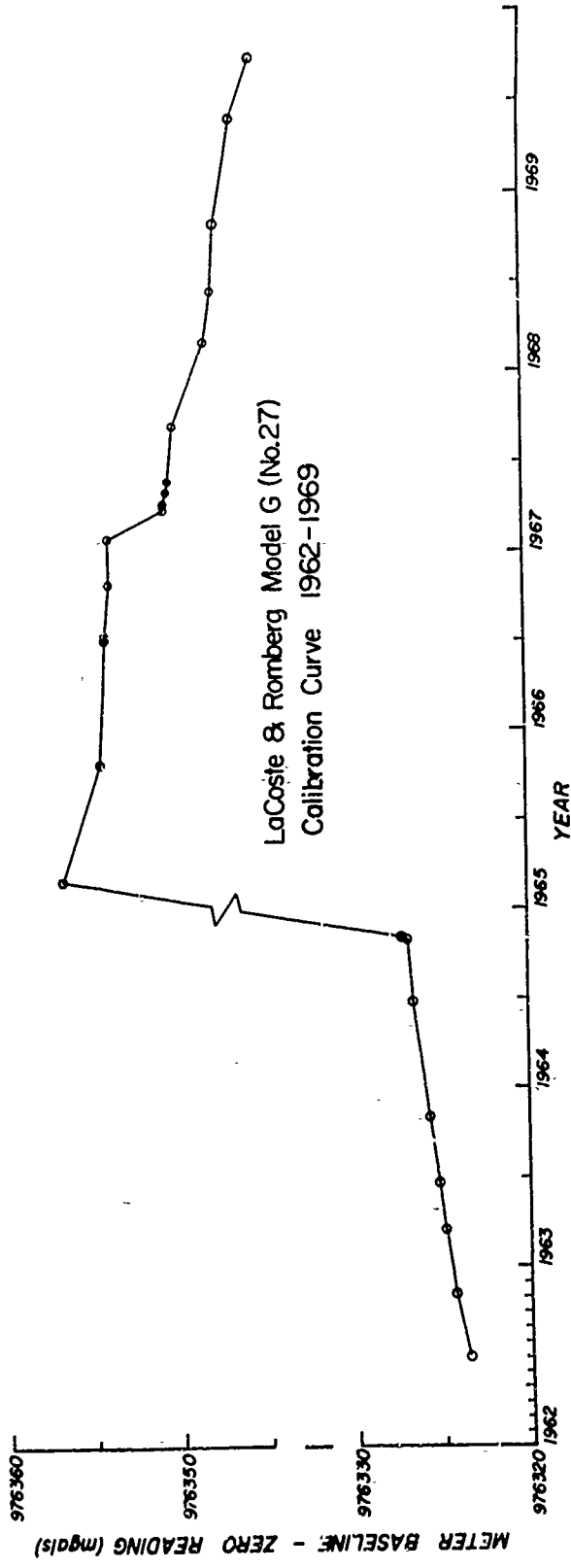


Figure 8.

have been accounted for and the data corrected. Elsewhere, a linear drift has been assumed between calibrations.

The observations were reduced to sealevel, and corrected for the acceleration due to east-west motion (the Eotvos correction) by the reduction program. This correction seldom exceeded  $\pm 1$  milligal. Maximum errors are considered to be less than 1 milligal for most observations, but possibly as much as  $\pm 5$  milligals during the severest storms.

Simple bouguer anomalies were computed for each observation by adding the attraction of a horizontally infinite plate, of density 1.64 g/cc and thickness equal to the water depth, to the free air anomaly. Approximately 8000 gravity observations were used in the present study.

An additional 150 gravity measurements, obtained from Station Alpha in 1958 with a Frost C-1-15 gravity meter, were used in Area III to assist in contouring. These observations are of limited value because the abandonment of the station, following seven months of measurements, did not permit a final calibration. Comparison of the Alpha measurements with the calibrated observations from T-3 at five Alpha/T-3 track intersections show the Alpha data to be about 15 milligals too high, and they have been adjusted accordingly.

#### Magnetic Measurements

The total intensity of the earth's magnetic field was measured almost continuously with a proton precession magnetometer (Packard and Varian, 1954) built at the Lamont-Doherty Geological Observatory. Readings were made every six seconds and recorded on a strip chart. Magnetic total intensity was calculated from precession frequency according to the relation  $H = 23.487386 f$  where  $H$  is the total field in gammas ( $10^{-5}$  gauss) and  $f$  is the proton precession frequency in hertz. The precession frequency measurements were made with a frequency counter, whose crystal oscillator time base was checked periodically

against other frequency standards. The individual measurements are accurate to better than  $\pm 10$  gammas.

Diurnal variations of the earth's magnetic field in polar regions commonly exceed one hundred gammas (Hunkins et al., 1962, and Walker, 1962). The periodic nature of these variations was used to eliminate them by averaging the observations over 24 hour periods. The records were read every hour, and the filtered field strength computed at each observation point by taking an average of the twenty-four hourly readings centered about that time.

The value of the earth's regional field was removed by the use of a Taylor series expansion of third degree, fitted by least squares to the regional field in this area by the Dominion Observatory of Canada (Haines, 1967). The area of this investigation lies near the center of their aeromagnetic survey. The magnetic total intensity anomalies presented here are defined as the difference between the observed total magnetic field and the computed regional field at the point of observation.

During the winter of 1968-69, the magnetic observations from T-3 were supplemented by measurements made by the British Trans-Arctic Expedition (BTAE) from an ice floe approximately 140 kilometers to the northwest of T-3. A Varian M-49 portable proton precession magnetometer was read every hour when possible. This instrument uses vibrating reeds to indicate the precession frequency, and gives a direct readout of field strength in gammas. These observations are accurate to better than  $\pm 20$  gammas, and were reduced in the same manner as those from T-3. This same instrument was used on T-3 in 1962.

Airborne total intensity measurements reported by Ostenso and Wold (1970) were a useful aid to interpretation. These measurements were made at an altitude of 450 meters with a proton precession magnetometer. No attempt was made to reduce these observations to sealevel, a change of less than 20 gammas. A correction for temporal variations in the magnetic field was not considered necessary as all

flights through these areas were of less than two hour's duration. Any difference will be shown as a constant factor relative to the ice island measurements. The estimated error in positioning for these measurements is less than 15 kilometers.

#### Seismic Reflection Measurements

A seismic reflection profiler was in operation between February and October 1967, November 1967 and March 1968, August 1968 and June 1969, during two weeks in August and September of 1969, and November 1969 to June 1970. Approximately 4000 kilometers of track have been profiled. The system used is a modification of that used aboard oceanographic vessels, and will be described below.

The sound source consists of a triggered capacitor bank from a 9000 joule storage capacity "boomer" (Edgerton and Hayward, 1964), discharging through an underwater spark transducer. The transducer is a flexible two-conductor cable, terminated by a tape-covered 5/8" diameter brass rod with one end open to the seawater, and by a length of exposed copper braid wrapped around the cable 30 cm back from the end. When the spark is triggered, the capacitor banks discharge into the ocean via the brass rod, causing breakdown of the seawater and producing an acoustic shock pulse. The copper braid ensures a good connection of the capacitor bank ground to the seawater. Spectral measurements of the pulse at a listening array 5 km from the transducer indicated a peak intensity at 80 hertz. Caulfield (1962) has described the various parameters affecting pulse shape and intensity.

The transducer was suspended about 8 meters below the sea ice near the edge of the ice island. The cable was passed through an oil-filled pipe frozen into the 4 meter thick ice, so that it could be pulled up periodically for inspection. Maintenance of the transducer was minimal -- a five minute check each week to assure that the electrode and tape cover eroded together, and replacement about every eight months. Details of electrode construction are discussed by Hall (1964).

The reflected signals were detected by two hydrophones, 30 meters apart, suspended on electrical cables approximately 4 meters below the sea ice adjacent to the ice island. The hydrophones were faired to reduce tow noise, and had horizontal separations of 20 meters and 30 meters from the spark source. The hydrophones are barium titanate, flexural disk transducers built by the U. S. Navy Underwater Sound Laboratory (Woollett, 1960). These highly sensitive hydrophones have a 0.1 mfd capacitance, eliminating the need for a preamplifier in the hydrophone case.

The hydrophone signals were mixed and preamplified at the ice surface, then amplified, filtered, and recorded on a modified Westrex chart recorder. This recorder uses an electrified stylus, riding on a translating steel band, to write on electro-sensitive dry recording paper passing slowly under the band. The band has three styli spaced at equal intervals, so that as one stylus finishes writing a line, the next one commences its sweep. A six second sweep was used for this work, controlled by a precision frequency derived mechanically from a synchronous clock. The paper speed was approximately 11 centimeters per day. A cam and gating arrangement was used to control the operating program of the profiler. Once every five minutes, this programmer turned off the PDR so that it would not interfere with the profiler, fired the spark source as one stylus began its sweep, allowed the reflected signals to print on the paper, then disconnected the print amplifier from the stylus so that nothing was printed until the beginning of the next five minute interval.

A two-channel drum recorder with brake-clutch mechanism, similar to that used by Kutschale (1966) on Arlis II, was used along with the chart recorder during part of 1967 and 1968. This 10 second sweep recorder generally produced better records, but required considerably more maintenance.

Individual seismic reflection measurements were obtained prior

to June 1963 by allowing the direct writing oscillograph used to record depth soundings to record also the subbottom reflections following the direct bottom arrival. The most prominent subbottom reflections were then used to prepare the seismic reflection profiles shown in Figure 16.

#### Data Storage and Presentation

The results of the reduction programs for navigation, bathymetry, gravity and magnetics were combined to form a single magnetic tape for the computer, containing blocks of data with observation time, geographic position, ice island orientation (azimuth), water depth, observed gravity, free-air and Bouguer anomalies, total magnetic field, and magnetic anomaly for every hour along the drift track. For purposes of comparison, one hour of track at usual ice island speeds is roughly equivalent in distance to that traversed in 45 seconds by a 12 knot ship. Altogether the tape contains data recorded over 70,000 hours.

The tape was used to prepare contour maps and construct profiles, using an automatic 30" plotter controlled by the computer. The contour program is arranged to print out the contour number at the location along the track at which that particular contour is crossed. Any map scale and contour interval can be used. In this fashion the computer performs the task of interpolating contour crossings, and the portion of track between contours acts as a constraint during the manual process of drawing contour lines.

Profiles were produced by specifying endpoint positions for each segment of the profile, and then specifying the beginning and end times of portions of track that should be projected onto the profile. Bathymetry, free-air and Bouguer anomalies, and magnetic anomalies were projected in this manner. Because of the contorted nature of the track, the seismic profiles were also digitized in sections, and fed into the computer for projection. The vertical scale for bathymetry and subbottom reflections on all projected profiles is in meters, not reflection time.

Water depths are all expressed as corrected meters. Sediment thicknesses are based upon an assumed sediment sound velocity of 2 kilometers per second, so that the thickness in kilometers is equal to the round-trip travel time in seconds.

## INTERPRETATION

## PART I: TECTONIC FEATURES

Bathymetry

The area of investigation has been subdivided into three areas, shown as Areas I - III in the index map (Figure 4). Contour maps with 100 meter isobaths have been prepared for each area. In those parts where no new depth information is available, generalized 500 meter isobaths from the Canadian Hydrographic Survey Chart No. 897 (DeLeeuw, 1967) have been added. All three areas have been combined into one bathymetric chart in Figure 28a. Selected profiles from these areas are shown in Figures 13-19.

Area I (Figure 9) includes the Chukchi Cap, the western margin of the Chukchi Rise, the Charlie Gap leading north from the Chukchi Plain to the Mendelejev Plain, and the eastern margin of the Mendelejev Ridge. The Mendelejev Plain, described here for the first time, has gradients of about 1:1000 and lies at a depth of about 3300 meters. Its gradient barely classifies it as an abyssal plain. On the west, the Mendelejev Ridge rises 2500 meters above the adjacent plain to form three isolated plateaus. Two of these are named for the submarine U. S. S. Sargo and Ice Station Arlis II (this plateau is off the map), from which they were discovered (DeLeeuw, 1967). A third plateau was discovered in this investigation, located still further north around 79°N and 176°W, and at a slightly greater depth of around 1100 meters. It is proposed that this plateau be named the T-3 Plateau.

The transition from the ridge to the plain is gradual in the parts surveyed. To the north, the ridge is paralleled by a 600 meter high scarp which faces the ridge across a trough. This ridge disappears to the north, being absent altogether in a traverse 50 kilometers away. This feature, shown in cross section in Figures 13, 14, and 35, is interpreted as a fracture zone, associated with the Alpha Cordillera, which locally parallels the Mendelejev Ridge. The name Mendelejev

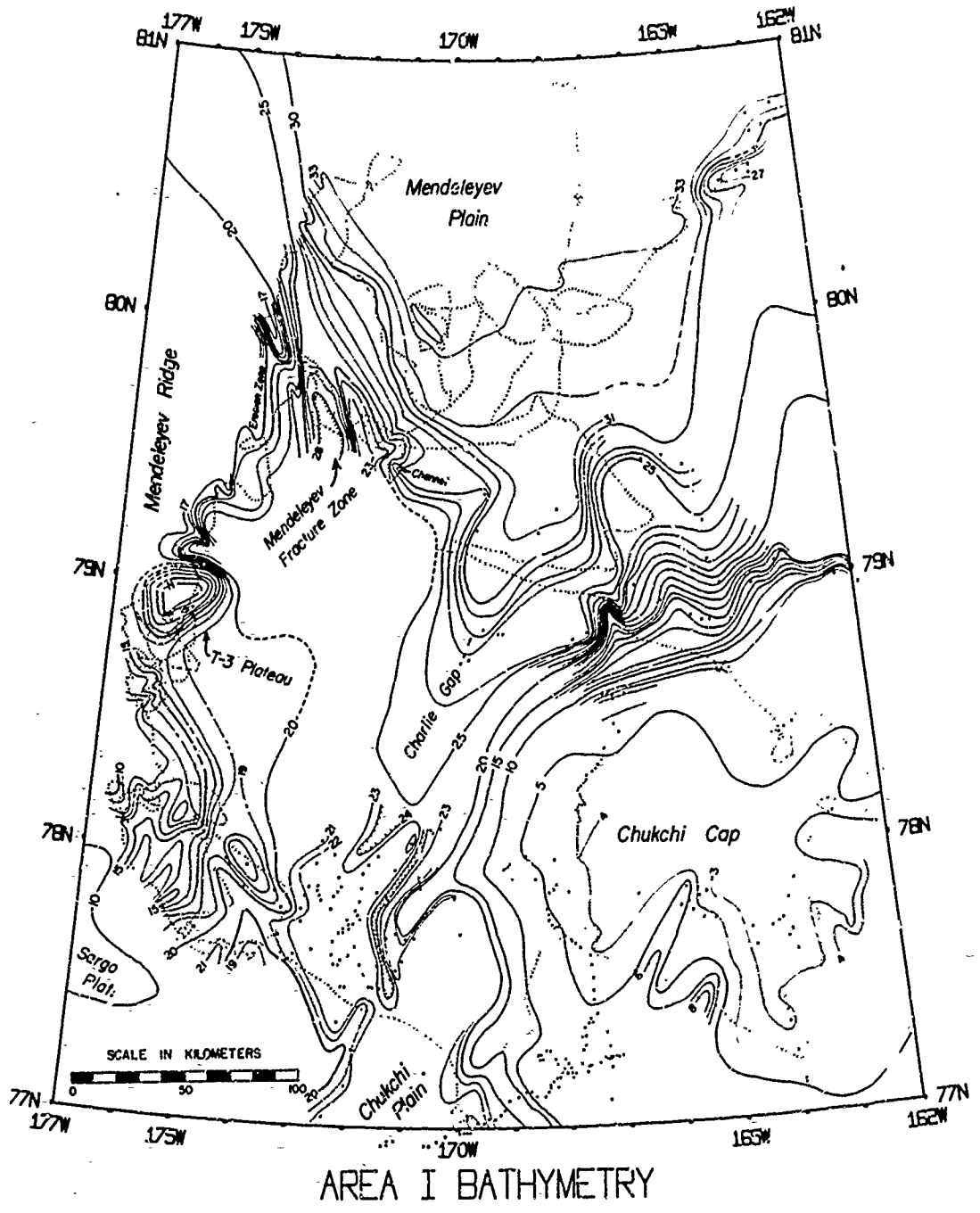


Figure 9

Fracture Zone is proposed for this feature. Along the ridge flank the topography appears to trend NNW-SSE, paralleling the fracture zone.

Area II bathymetry is shown in Figure 10, with selected profiles in Figure 15. Principal features in this area are the northwestern part of the Canada Plain, the northern extremities of the Chukchi Rise, and the southern flank of the Alpha Cordillera. The Canada Plain in this area lies at approximately 3800 meters, becoming slightly shallower toward the cordillera. A small isolated depression was discovered on the northern margin of the Chukchi Rise.

Three topographic highs with crestral depressions were traversed in Area II. These are interpreted as seamounts, although from the crossings it is uncertain whether they are isolated features. This interpretation is supported however, by the observation in the nuclear submarine bathymetric profiles of similar structures, which Beal (1968) considered to be volcanic. One seamount, 600 meters high, was crossed on the northern margin of the Chukchi Rise. Although submarine morphologists generally consider a relief of at least 700 and preferably 1000 meters necessary for classification as a seamount, it is suggested from Profile X-Y-Z in Figure 15 that this is a true seamount which has been partially buried by the sediments forming the plain.

Two other seamounts, 1200 meters in height, were crossed on the lower flank of the Alpha Cordillera. On the Canadian chart (DeLeeuw, 1967) these features appear as the southern end of a long NNW-SSE trending ridge. In this paper they have been reinterpreted as seamounts, probably volcanic in origin, because of their crestral depressions (see Profile A-B in Figure 15), the associated magnetic anomaly (Figure 16 and Figure 26), and because of the very low heat flow measured on their flanks by Lachenbruch and Marshall (1966). Subsequent heat flow measurements over the Alpha Cordillera have shown the heat flow to

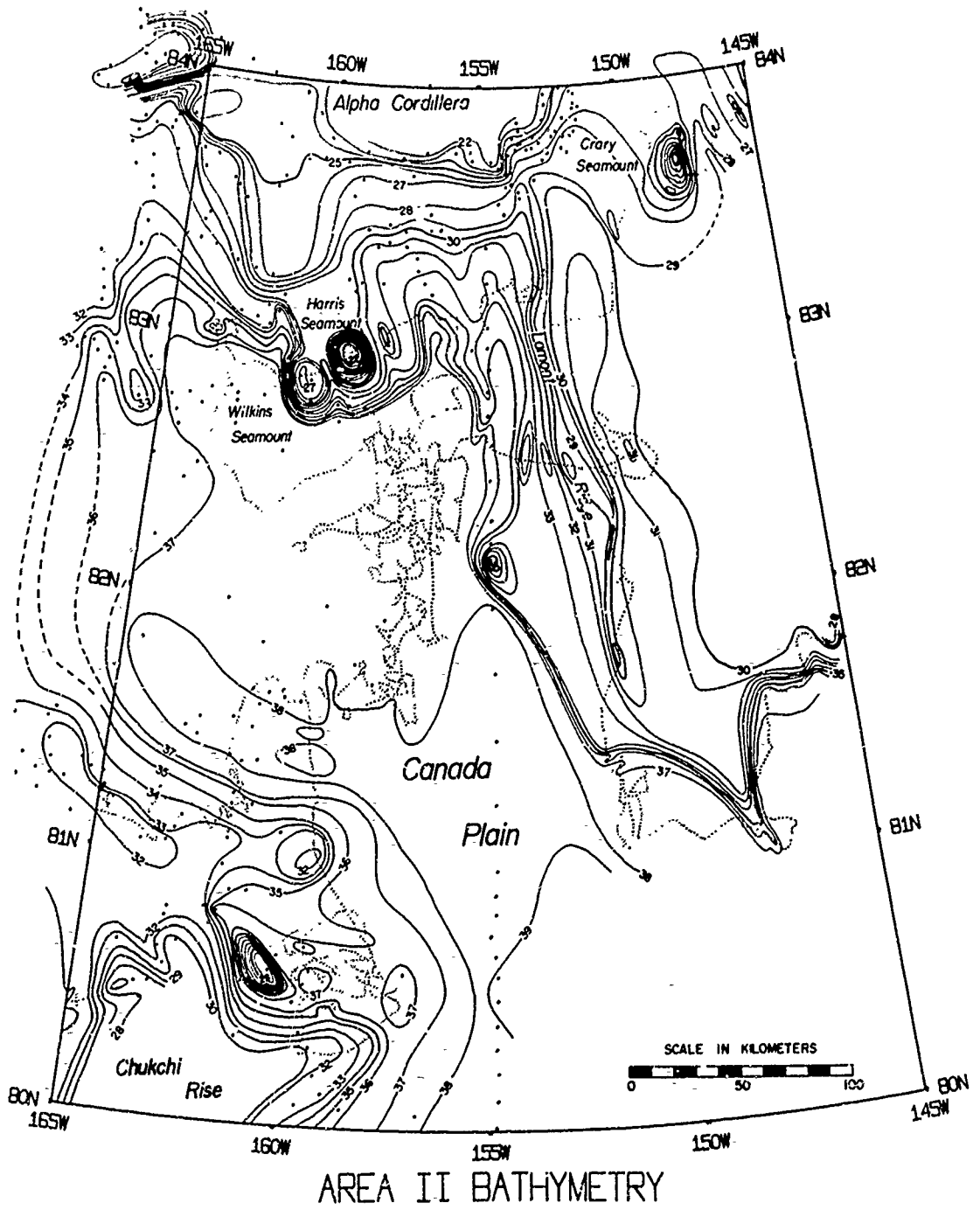


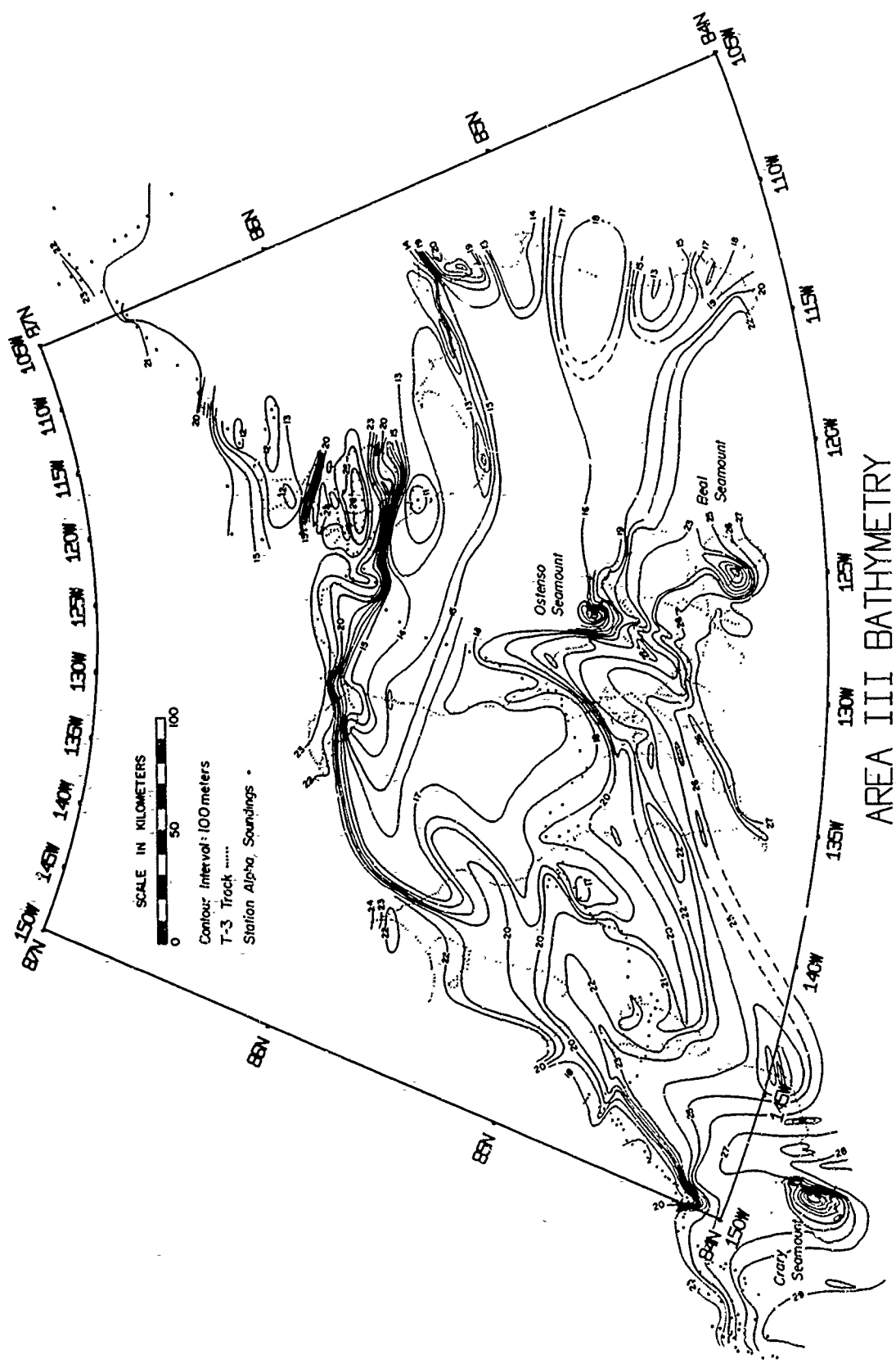
Figure 10

be generally normal and uniform (Dr. A. Lachenbruch, personal communication), which suggests that the low observed heat flow values could be the result of low conductivity volcanic material.

Names are proposed for these seamounts, to honor scientists involved in the exploration of this part of the Arctic Ocean. The largest seamount on the flank of the Alpha Cordillera is named after Rollin Arthur Harris (1863-1918), who in 1904 proposed the amphidromic regime of tides and predicted the existence of the Lomonosov Ridge from tidal observations. The nearby seamount is named after Sir Hubert (George H.) Wilkins (1888-1958) who pioneered the use of aircraft and submarine for Arctic Ocean exploration.

East of the plain, a rectangular region juts south from the cordillera, rising 800 meters above the adjacent plain. On the western edge of this upland, paralleling the plain, is a narrow ridge which rises to a depth of less than 2900 meters. Named the Lamont Ridge by DeLeeuw (1966), this narrow ridge is clearly seen in seven crossings spaced over a distance of 200 kilometers (see Figure 15). Steep slopes are observed on both flanks of this ridge at its southern end. In the northeast corner of this area, an isolated seamount was delineated when the ice island followed an "N" shaped track. Steep sides were observed on the northeast and southeast sides of the flat-topped structure, shown in Profile C-D in Figure 15, suggesting that it is bounded on the east by a fracture striking in the direction of a steep valley observed by Hunkins (1961) from Station Alpha. This valley appears in Area III (Figure 11). This seamount is named after Albert P. Crary, whose early geophysical measurements from T-3 delineated the North American terminus of the Alpha Cordillera.

Area III comprises the flank and crestal regions of the central section of the Alpha Cordillera. Soundings reported by Hunkins (1961) from the drift of Station Alpha have been included in the contouring of this area. The general trend of the topography is NE-SW, paralleling the trend of the cordillera. Two seamounts were traversed on the upper



AREA III BATHYMETRY

Figure 11

flank of the cordillera. The one to the south, over 700 meters high, is named after M. Allen Beal, who was one of the first to suggest that the Alpha Cordillera is a fossil mid-oceanic ridge, and whose contribution to our knowledge of the physiography of the Arctic Ocean Basin has already been acknowledged. To the north, a second seamount rising nearly a kilometer above the surrounding topography is named after Ned A. Ostenso, whose aeromagnetic, airlifted gravity, and other marine geophysical measurements from Ice Station Arlis II have added significantly to our knowledge of the Arctic Basin. A depression was observed at the summit, suggesting that Ostenso Seamount is also volcanic.

In the central part of the area, the crestral regions are characterized by extensive, rather level areas of low relief. This crestral plateau is cut on the west by depressions that run subparallel to the trend of the cordillera. On the central crossing, seen in Figure 17 as Profile K-P, this plateau dips toward the south, dropping off at its northern and highest edge through a series of northward dipping step faults to a partially surveyed plain at 2300 meters. To the east, a fourth crossing (Figure 18) showed alternating crestral plateau and deep graben-like valleys. A pronounced characteristic of the soundings on the crestral plateau was the appearance of numerous hyperbolic echoes, which are discussed in some detail in the second part of this paper.

A general profile across slightly more than half of the cordillera is shown in Figure 12 (see Figure 4 for the location of this profile). This projected profile runs in a straight line from the northern margin of the Chukchi Rise to just beyond the apparent axis of the cordillera as indicated by the bathymetry, gravity, and magnetics. Since the projected track overlapped itself in several places, a choice of bottom traces was offered. Sections containing exaggerated relief were rejected in favor of those showing a more general trend. In this profile, the Alpha Cordillera appears as a rounded feature, rising nearly 2 kilometers above the Canada Plain. To the east of this profile the crestral regions are higher still, reaching depths of less than 100 meters. Of note

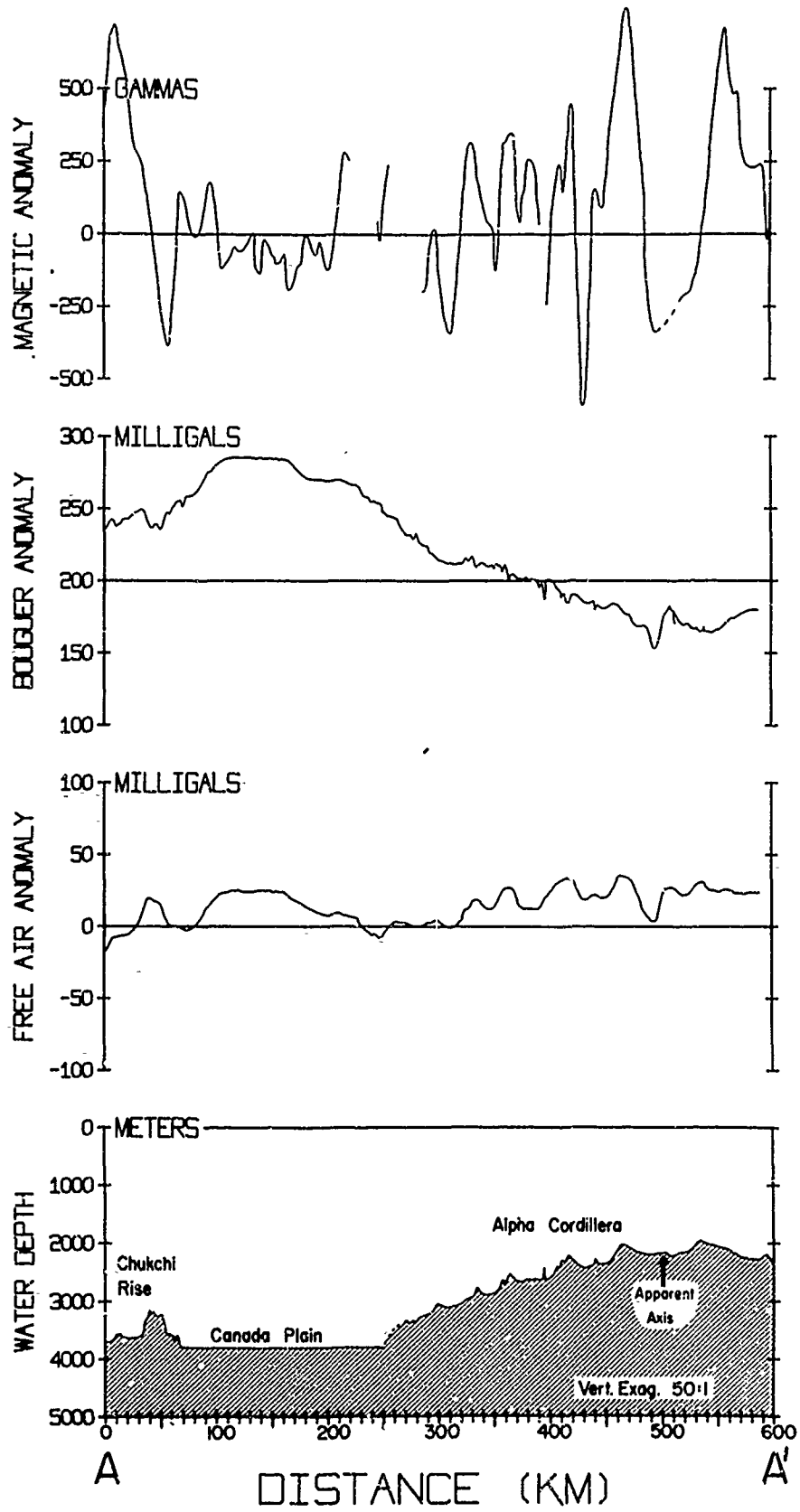


Figure 12.

is the concordance of heights of five elevated portions of the southern flank of the cordillera along an inclined line of  $0^{\circ} 23'$  slope. This slope is identical to that given by Beal (1968) from an analysis of nine submarine crossings of the Alpha Cordillera.

#### Seismic Reflection Measurements

The results of the seismic reflection measurements are shown in Figures 13 through 18. With the exception of Figure 16, which is derived from explosive soundings, these profiles were obtained with the 9000 joule sparker system. The records were digitized and projected in order to remove the effects of the erratic ice motion, and to provide some continuity by joining segments obtained during different periods of drift. A comparison of Profile C-C' in Figure 13 with the actual records used in its construction (Figures 33 and 35) will show the type of interfaces chosen for digitization. In these profiles, what is interpreted as basement -- the basaltic layer with 4.5 - 5.5 km/sec compressional wave velocity observed to underlie the sediments in other oceans -- has been blackened. Its upper surface is usually recognized as the beginning of a series of large hyperbolae.

Three segments of track crossed the Mendelejev Fracture Zone, a high scarp and trough paralleling the Mendelejev Ridge. Figure 13 shows these segments projected onto a common fixed plane. From this figure it is apparent that the fracture can be traced over a distance of at least 80 kilometers. Differences in stratigraphy across the scarp, discussed in some detail in Part II of this paper, indicate that these sediments were deposited after the formation of this fracture. The topography of the basement is quite rough. In Profile A-A', the top layer consisting of several hundred meters of conformable sediment, overlies relatively flat sediments which appear to have undergone considerable erosion. Higher on the Mendelejev Ridge (Figure 14), reflection measurements along a zig-zag track (Profile j-s) show

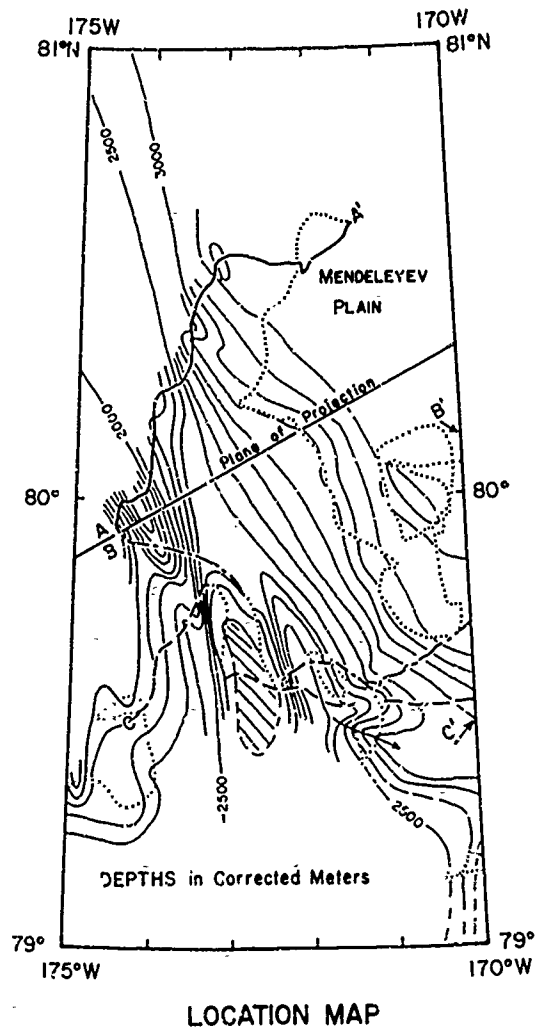
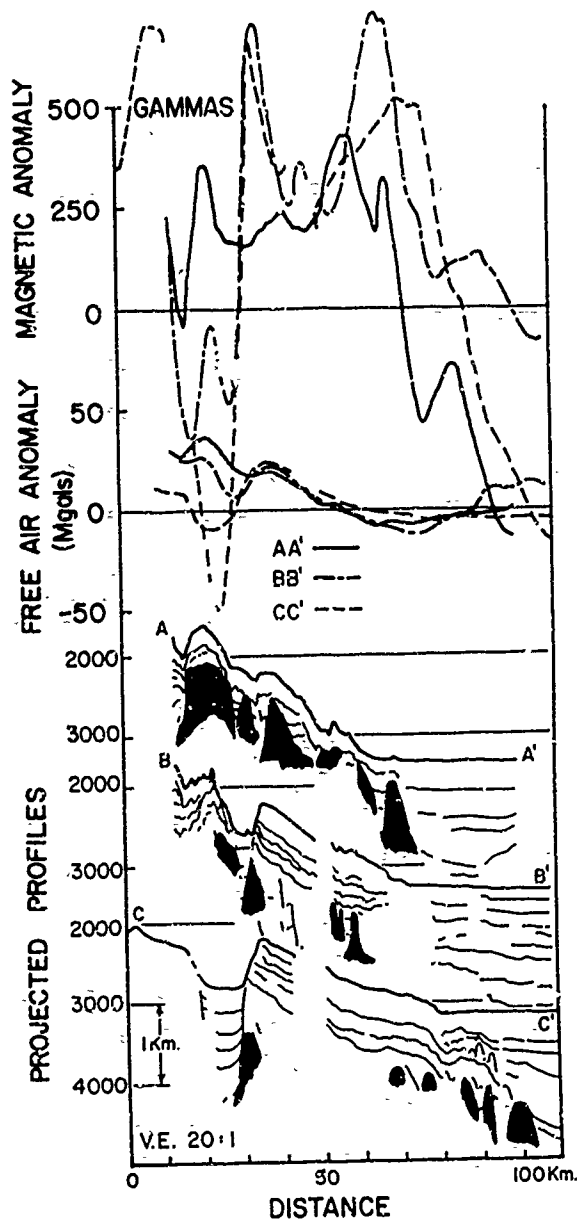


Figure 13



the Mendelejev Ridge to have a relatively thick and highly variable sediment cover. Steep slopes and rough topography within the basement are reflected in the surface topography, even though large volumes of sediment have partially filled some of the valleys.

More than two kilometers of sediment were observed beneath the Mendelejev Plain, with no indication of basement. Kutschale's (1966) measurement of at least 3.5 km of sediment beneath the Wrangel Plain, across the Mendelejev Ridge approximately 300 kilometers to the northwest, suggests that considerably more sediment exists. Beneath the Mendelejev Plain, about 100 km east of the fracture zone, the deepest interfaces appear to rise slightly, perhaps reflecting a similar rise in the underlying basement.

On the northern margin of the Chukchi Rise (Figure 15) the profiles reveal a basement topography which is considerably less rough than that over the Mendelejev Ridge. The sediment cover generally varies between 500 meters and more than a kilometer. The tightly grouped profiles reveal a succession of basement highs and lows which appear to trend north-northwest. Over two kilometers of sediment were observed beneath the northern Canada Plain. Again no basement reflections were observed. The basement appears to drop precipitously north of the Chukchi Rise. Dipping interfaces beneath the plain, more than 50 kilometers further north, suggest that a considerable thickness of sediment exists beneath that already observed.

The individual reflection measurements from the 1962-63 drift (Figure 16) show a thick sediment cover extending onto the Chukchi Cap, with approximately 500 meters on the Cap itself.

The seismic reflection profiles from the Alpha Cordillera (Figures 17 and 18) show the sediment cover to vary from as little as 100 meters to more than 1200 meters. The thickness increases toward the east, probably as a result of increased deposition near the continental shelf. Toward the west, sedimentation appears to be partially controlled by bottom currents, which have redistributed the available sediment.

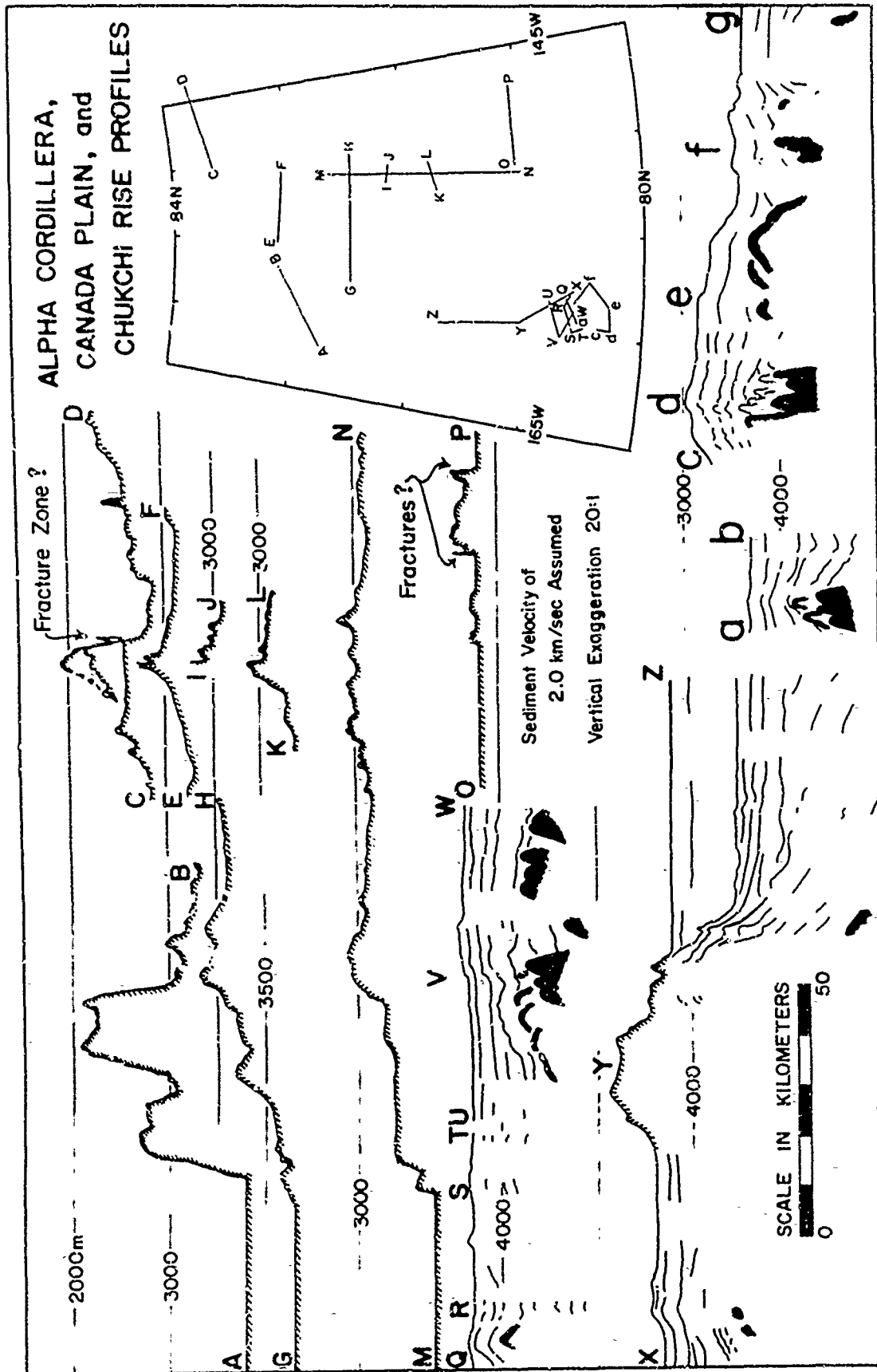


Figure 15

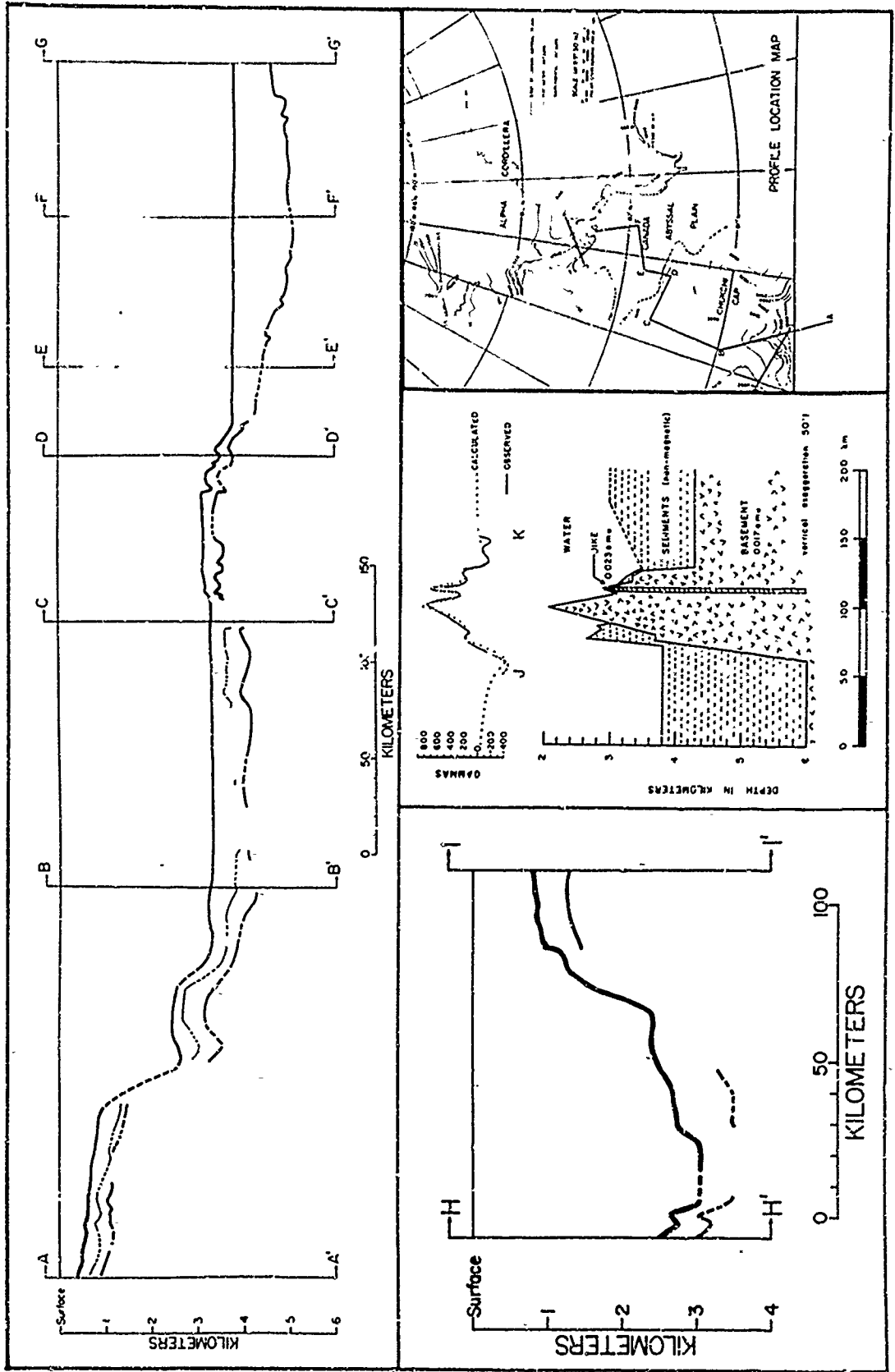


Figure 16



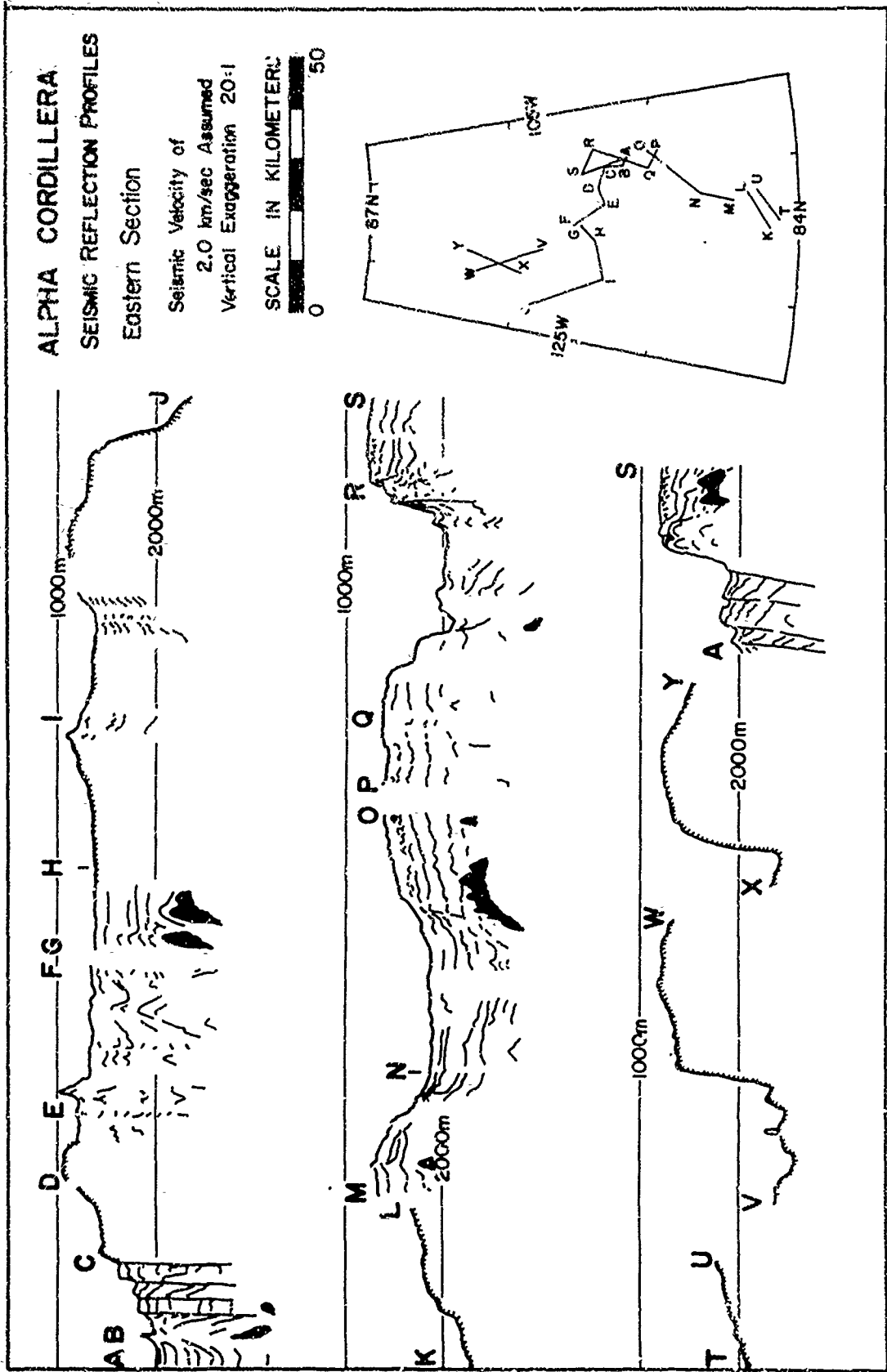


Figure 18

This sedimentation is discussed in some detail in Part II.

Beneath the sediments a rough basement topography is indicated. A comparison of the observed basement topography with that of the Mid-Atlantic Ridge as given by Heezen et al. (1959) reveals a similarity (Figure 19). In this part of the Alpha Cordillera only the higher portions of the high fractured plateau province, and the rift valley and rift mountain provinces appear to be represented. Within the rift mountains (Profile 2 in Figure 19 or Profile B-E in Figure 17), the ridges are topographically higher and of greater wavelength while the high fractured plateau (Profile 1 in Figure 19 or Profile Q-T in Figure 17) is lower, and exhibits a shorter wavelength. The boundary between the two provinces appears to be the small ridge seen on the southern flank in all profiles at the 2500 meter contour, which is a reflection of a similar buried basement ridge.

Two steep-sided depressions up to a kilometer deep were traversed over the crest of the cordillera in the eastern part of Area III. Step faults bound these depressions, and there is some suggestion (Figure 18 (bottom), Profiles V-W and A-S) that the floor of these depressions is also faulted. The fault traces appear to extend to the surface, suggesting that tensional forces continue to act on the cordillera. These depressions show some resemblance to the sediment-filled rift valleys found on land (Holmes, 1965).

#### Gravity Measurements

Figures 20, 21, and 22 show the free-air gravity over the area of investigation, contoured every 5 milligals. A map with all three areas combined is shown in Figure 28b. The isogals generally follow the topography, with a maximum of more than +80 milligals occurring on the crestral highs of the Alpha Cordillera, and minima of -30 milligals within the depression on the southern margin of the Chukchi Rise, and along the crestral rift of the Alpha Cordillera. The average gravity field is decidedly positive, a characteristic of the entire Arctic Ocean Basin.

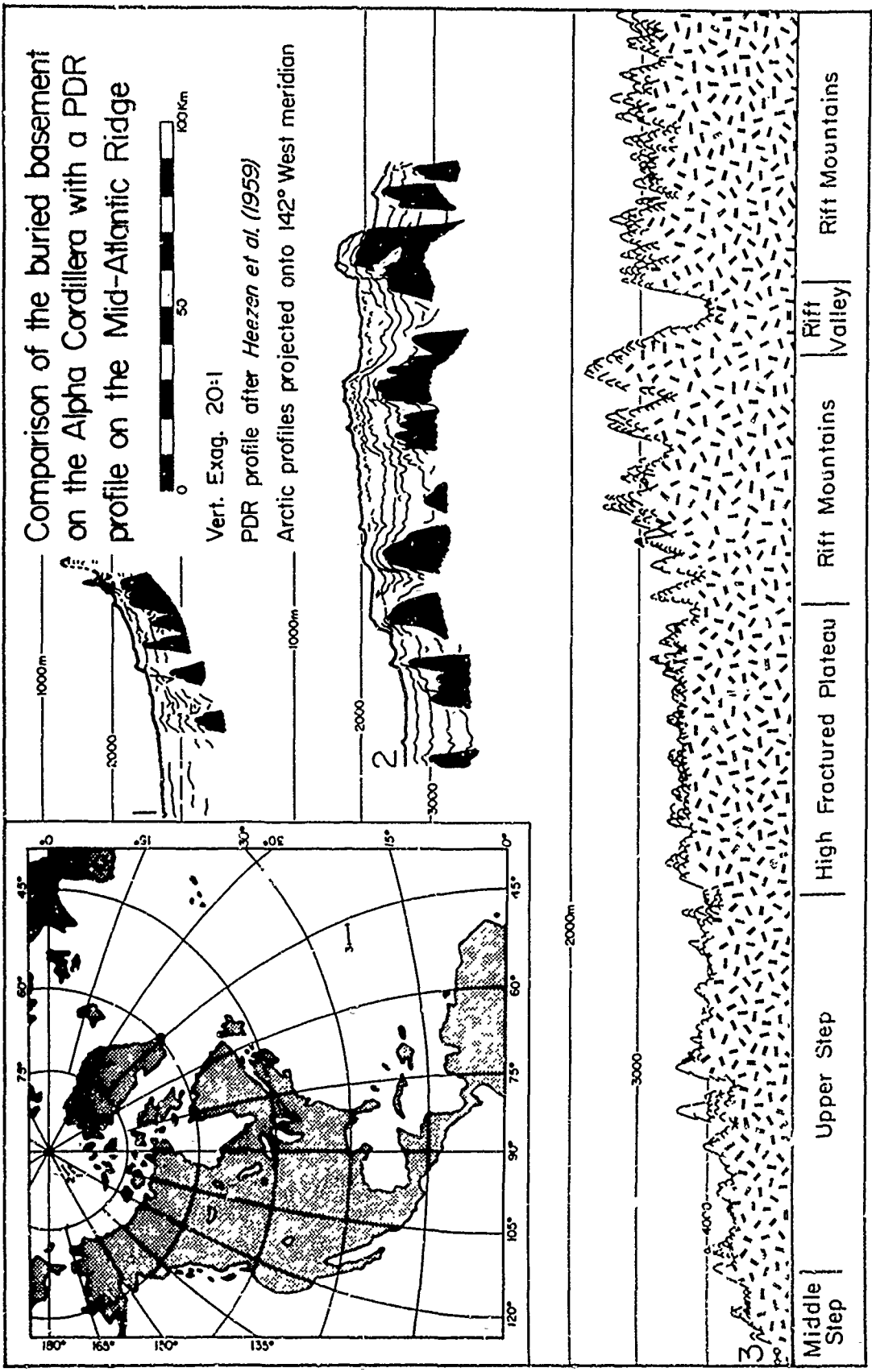


Figure 19

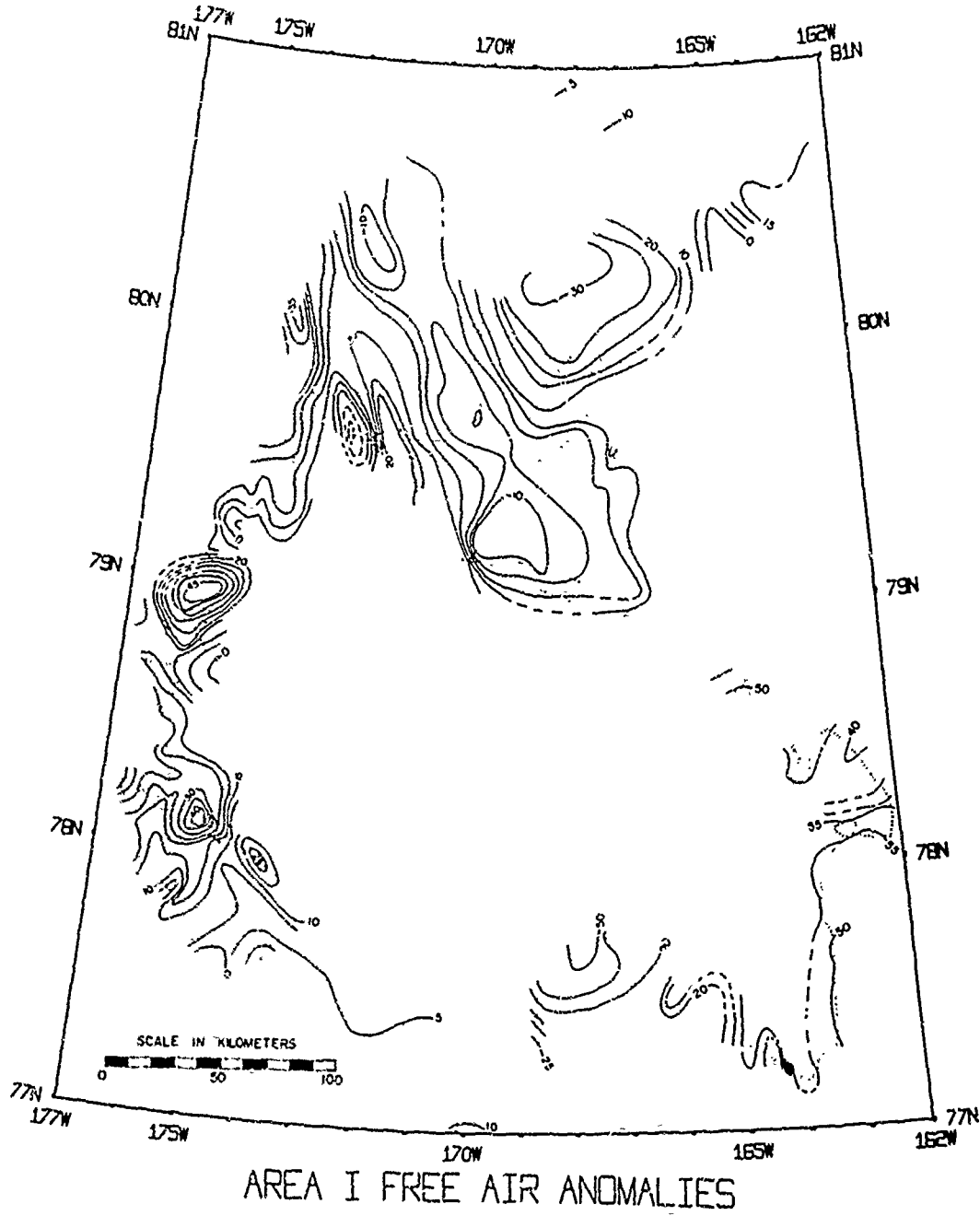
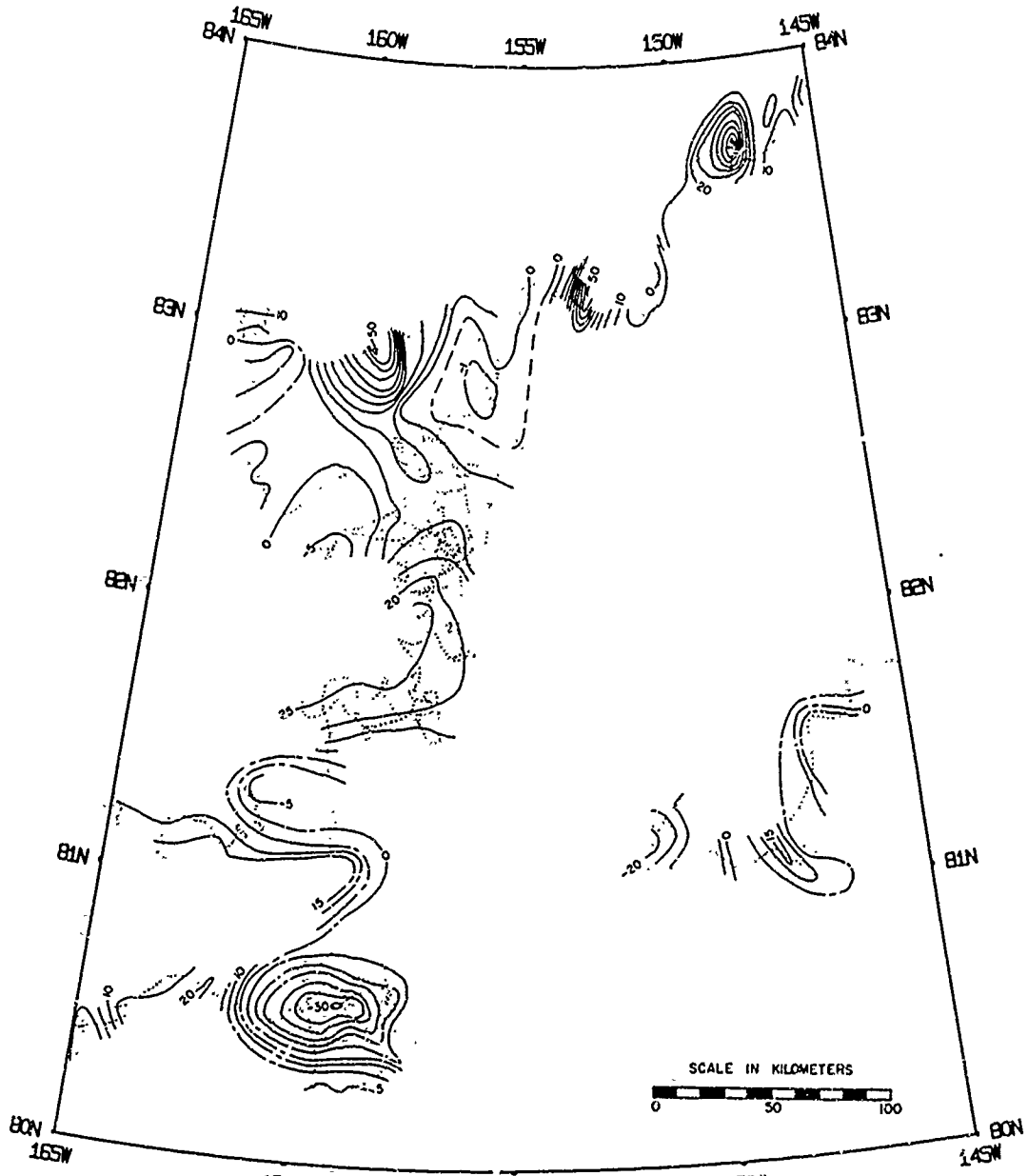


Figure 20



AREA II FREE AIR ANOMALIES

Figure 21

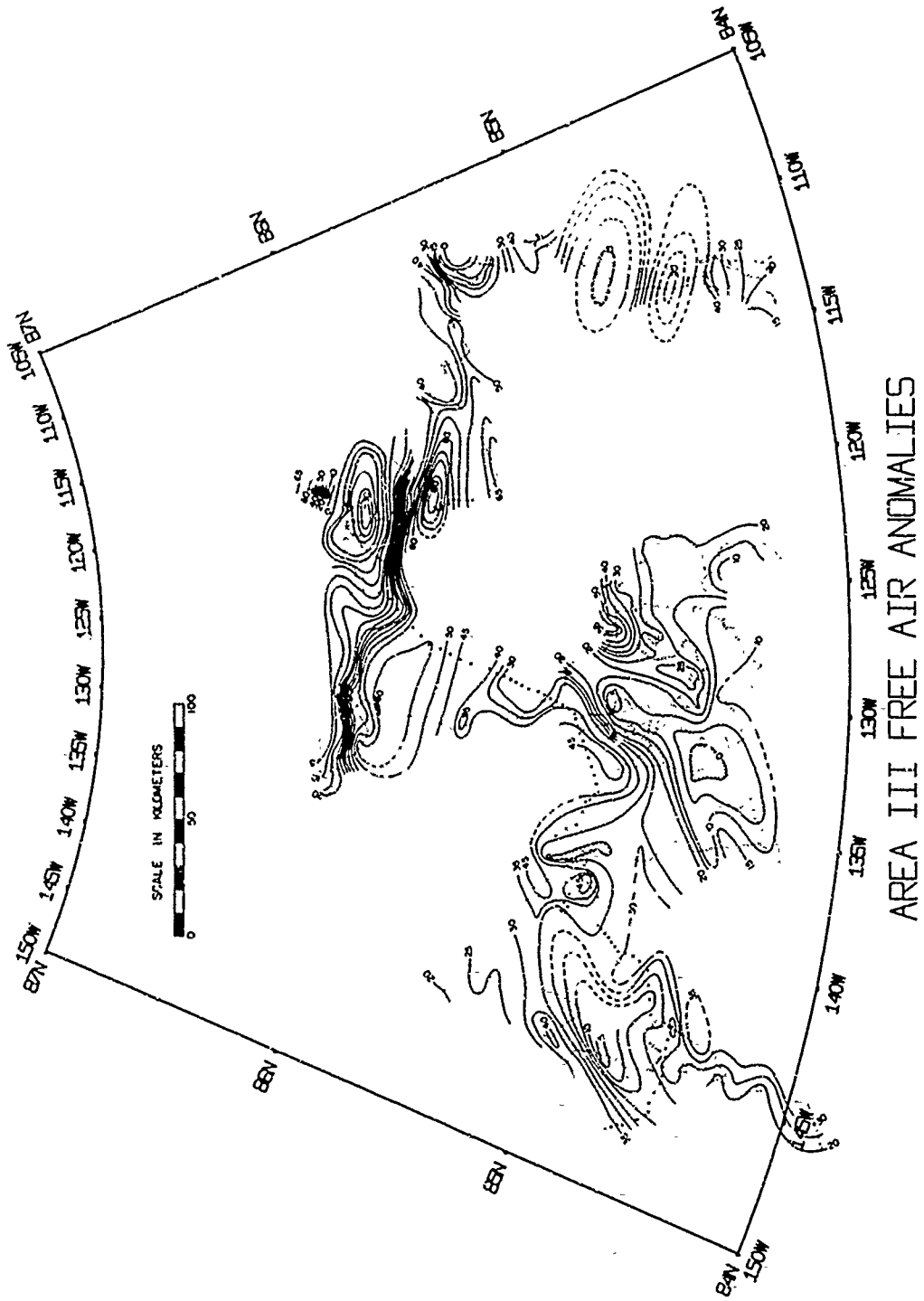


Figure 22

The Bouguer anomalies are generally smoother than the free-air in the immediate vicinity of topographic highs, suggesting that these features have densities near 2.67 g/cc. These effects can best be seen in the long Profile A-A' across the southern half of the cordillera (Figure 12), which shows a well developed Bouguer minimum at the crest. This minimum suggests mass compensation at depth, and is similar to that shown by Talwani et al. (1965) for the mid-oceanic ridges. The slope changes over the flanks are particularly evident.

A two-dimensional crustal model was fitted to this long profile using the procedures outlined by Talwani et al. (1959), and by Hayes (1966). Only one control point was available for this profile. Refraction Station 5, from the 1957-58 drift of Station Alpha, lies on the flank of a topographic high at  $85^{\circ}01.7'N$  between  $137^{\circ}54'W$  and  $139^{\circ}06'W$ , approximately 10 kilometers from the T-3 track (Figure 7). For this station, Hunkins (1961) reported 0.29 km of 2.0 km/sec sediment and 2.30 km of 4.70 km/sec "basement" material overlying an "oceanic" layer of 6.44 km/sec compressional wave velocity. The existence of a basement and oceanic layer in this refraction profile suggested that a multilayer crustal section such as that used by Talwani et al. (1965) might be more appropriate than one using a single crustal block with varying thickness and density around 2.87 g/cc. The reflection data shows considerably more than 0.29 km of sediment in many areas on the cordillera, but the control from the seismic reflection measurements is unfortunately not continuous, so that sediment and basement have been lumped together into a single layer of density 2.30 g/cc. This density is roughly equivalent to sediment and basement in the ratio 1:2, since the measured velocities correspond to densities of 1.90 and 2.50 g/cc on the Nafe and Drake (1963) curve. The oceanic layer was assumed to have a constant thickness of 5 km under the cordillera and adjacent plain. This thickness is based upon the average for this layer in the other world oceans (Worzel and Shurbet, 1955). A similar layer pinches out over the crest of the Mid-Atlantic Ridge, but is continuous over the East Pacific Rise. A density of 2.80 g/cc was given to

this layer, roughly corresponding to its 6.44 km/sec seismic velocity. Additional compensation under the cordillera was assumed to result from a low density root consisting of 3.15 g/cc "anomalous" mantle, overlying a normal mantle with density 3.40 g/cc.

The crustal section is shown in Figure 23. The sediment-basement layer was assumed to thicken in the direction of the neighboring plain, primarily due to thickening sediments observed by the reflection measurements. The depths to the layers were specified at inflection points in the free-air, Bouguer, and topographic trends, and adjusted so that the pressure of the layers, less the observed free-air gravity, would balance a standard crustal section consisting of 32 km of 2.87 g/cc crust overlying a mantle of 3.40 g/cc density. The level of compensation was arbitrarily set at 45 km, where the pressure is  $136.04 \times 10^5$  g/cm<sup>2</sup>. A pressure of  $10^5$  g/cm<sup>2</sup>, equivalent to that produced by a layer 1 km thick with unit density, corresponds to a gravity anomaly of about 42 milligals.

The Bouguer anomaly was computed assuming the water layer to have density 2.67 g/cc, in order to match the assumptions used in computing the observed anomaly. Any comparisons of these Bouguer gradients with those from other ridges should be made with this in mind.

The computed model agrees reasonably well with the observed gravity. The smaller deviations are probably the result of basement topography. Buried fractures, which should make an angle of about 28° with the profile according to the inferred pattern in Figure 28, might be responsible for the larger deviations, particularly that occurring around 500 km. This particular model, similar to that of Talwani et al. (1965) for the East Pacific Rise, shows that the observed gravity is consistent with the hypothesis that the Alpha Cordillera is a fossil mid-oceanic ridge. One must remember however, that this model is only one of a number which could be tailored to satisfy the small number of available constraints. Any refinement will require additional

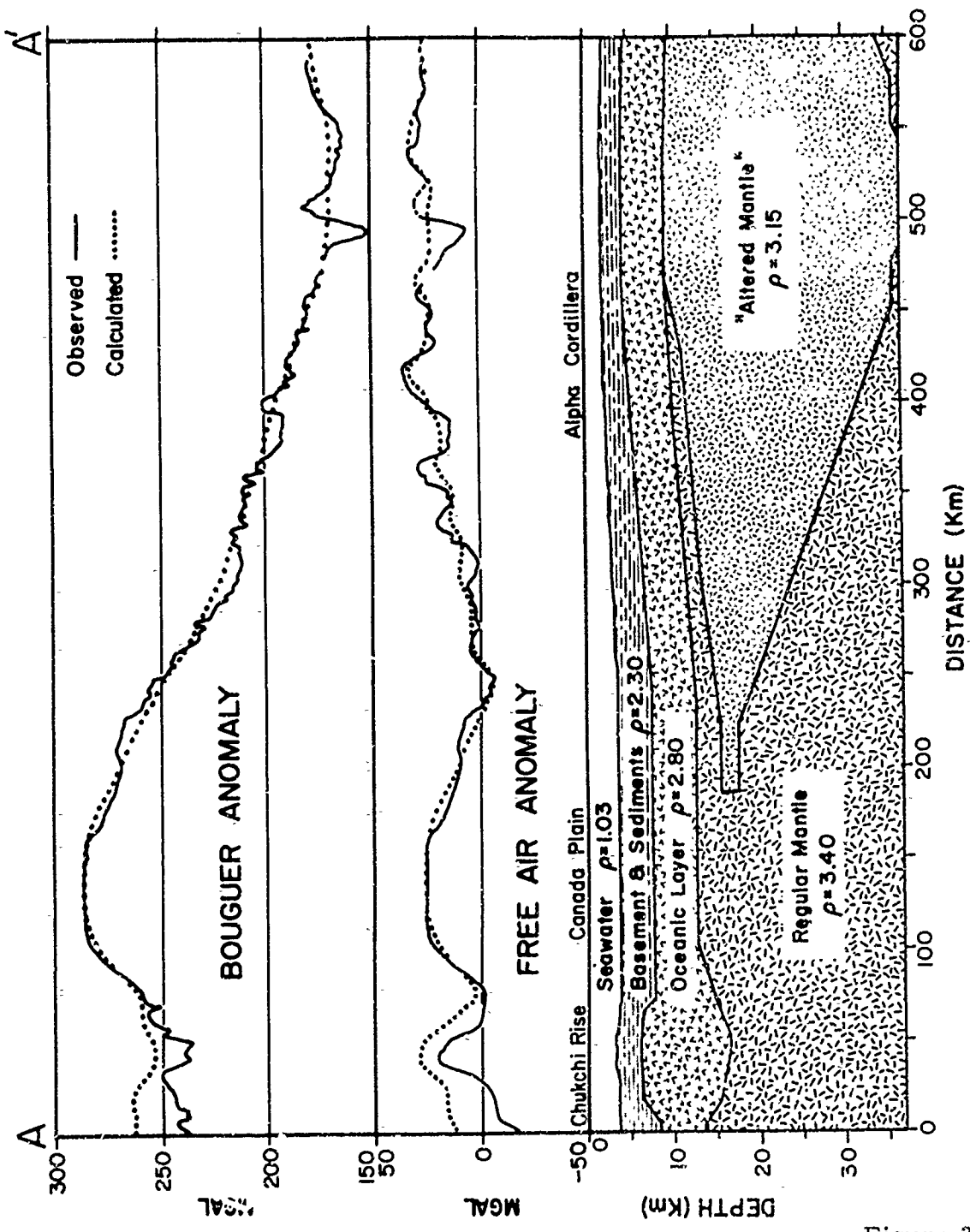


Figure 23

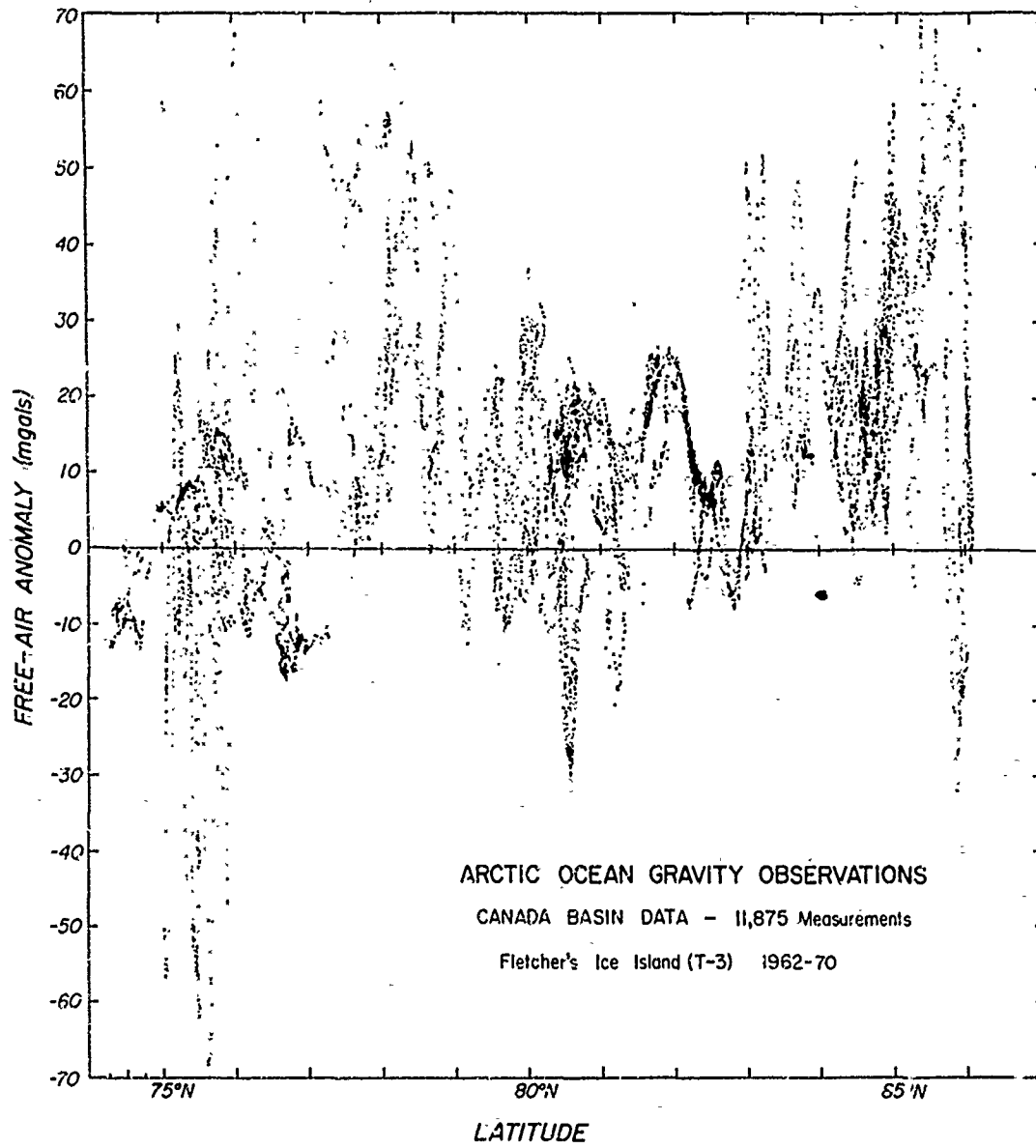


Figure 24

refraction and reflection measurements.

The free-air gravity anomalies have been plotted against latitude in Figure 24. For this side of the Amerasia Basin the average field is decidedly positive, with some tendency to increase toward the north. This increase might be due to the Alpha Cordillera, which marks the northern limit of all these measurements. The cause of the regional high is unknown, but its existence is worth noting.

#### Magnetic Measurements

The magnetic anomalies for each area were contoured at 100 gamma intervals. The results are combined into one map in Figure 28c. In Area I (Figure 25), closely spaced high amplitude (1000 gammas) anomalies showing an ENE-WSW trend are observed in the southwest over the Mendelejev Ridge. To the north, the trend is generally north-south, centered about a large 1400 gamma anomaly associated with the Mendelejev Fracture Zone (Figure 13). On the Mendelejev Plain, a large NW-SE trending anomaly is possibly related to the basement ridge in Figure 14, which appears in Profile j-s at point q, and Profile f-i at point g.

In Area II (Figure 26), the anomaly pattern appears to show two orientations. The most prominent orientation is normal to the trend of the Alpha Cordillera, and is represented by linear anomalies extending SSE from Harris Seamount, along the Lamont Ridge, and over the eastern scarp of Crary Seamount to the northeast. The second orientation is rather weakly developed parallel to the cordillera between the three sets of transverse anomalies, and together they suggest the striping pattern observed in the fracture-offset flanks of the present mid-oceanic ridges.

Area III magnetics are shown in Figure 27. Good coverage to the northwest and in the southern part of this area allows a relatively detailed look at the heart of the Central Magnetic Zone of King et al. (1966). In the northwestern part, data from T-3 has been supplemented

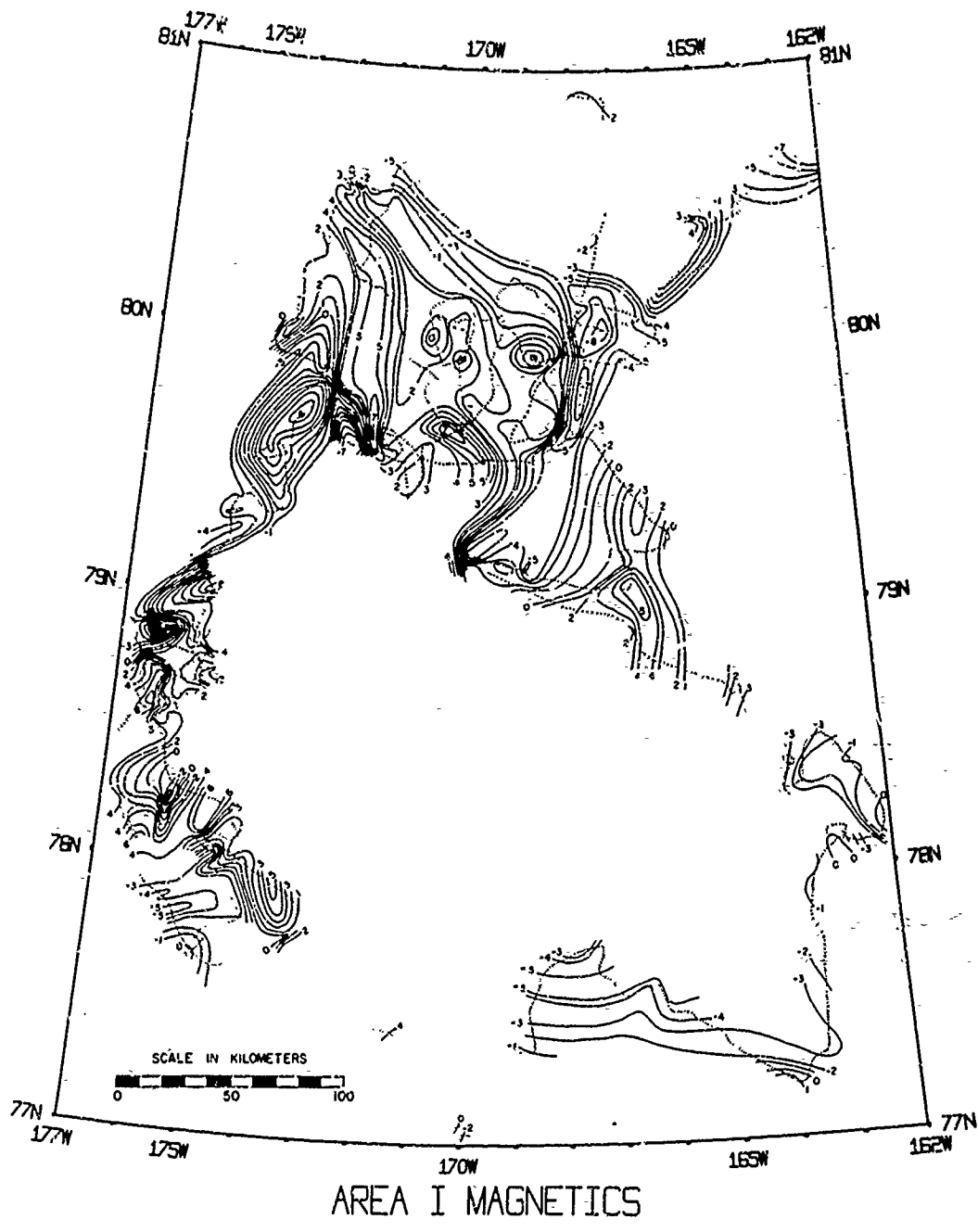


Figure 25

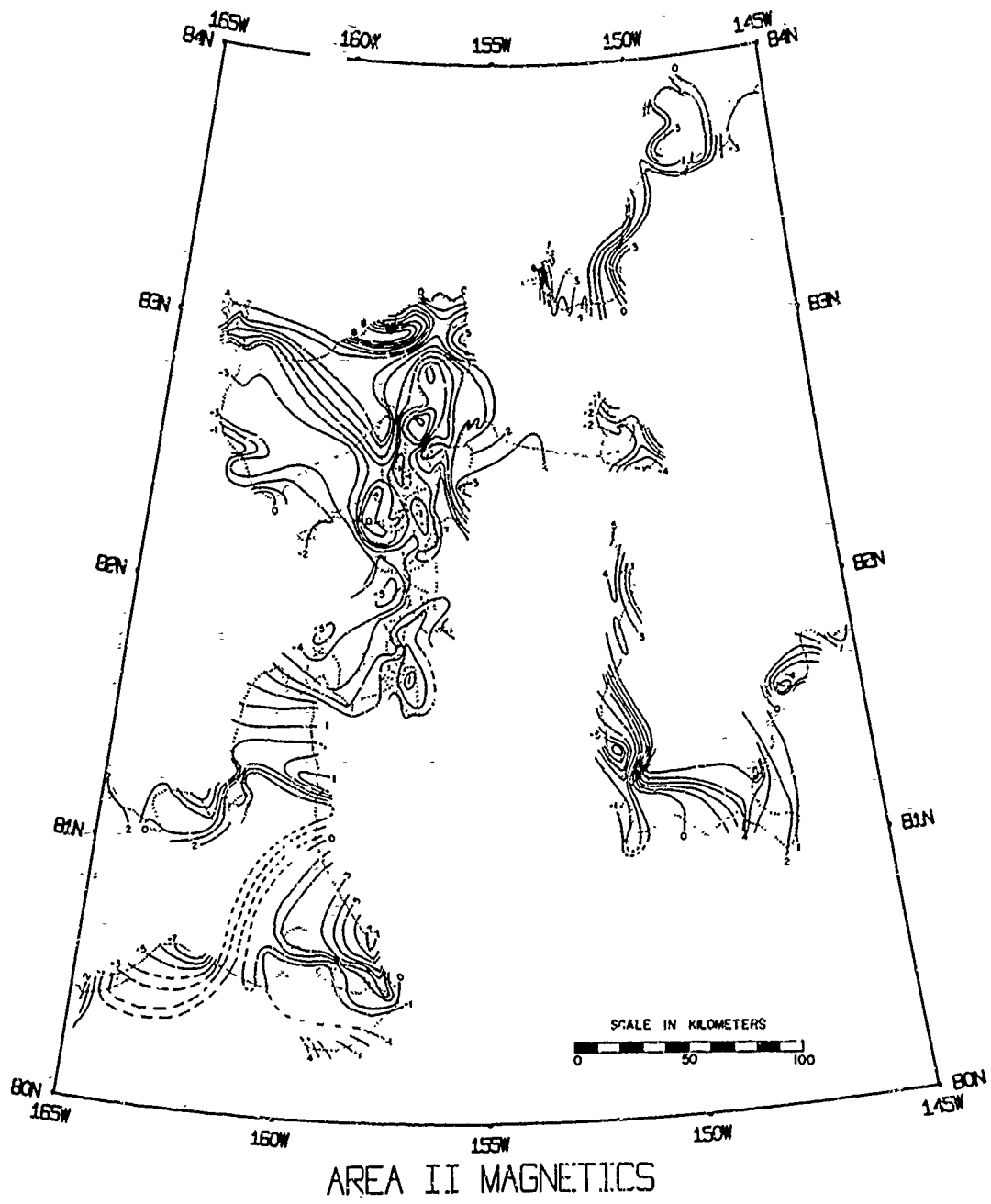


Figure 26

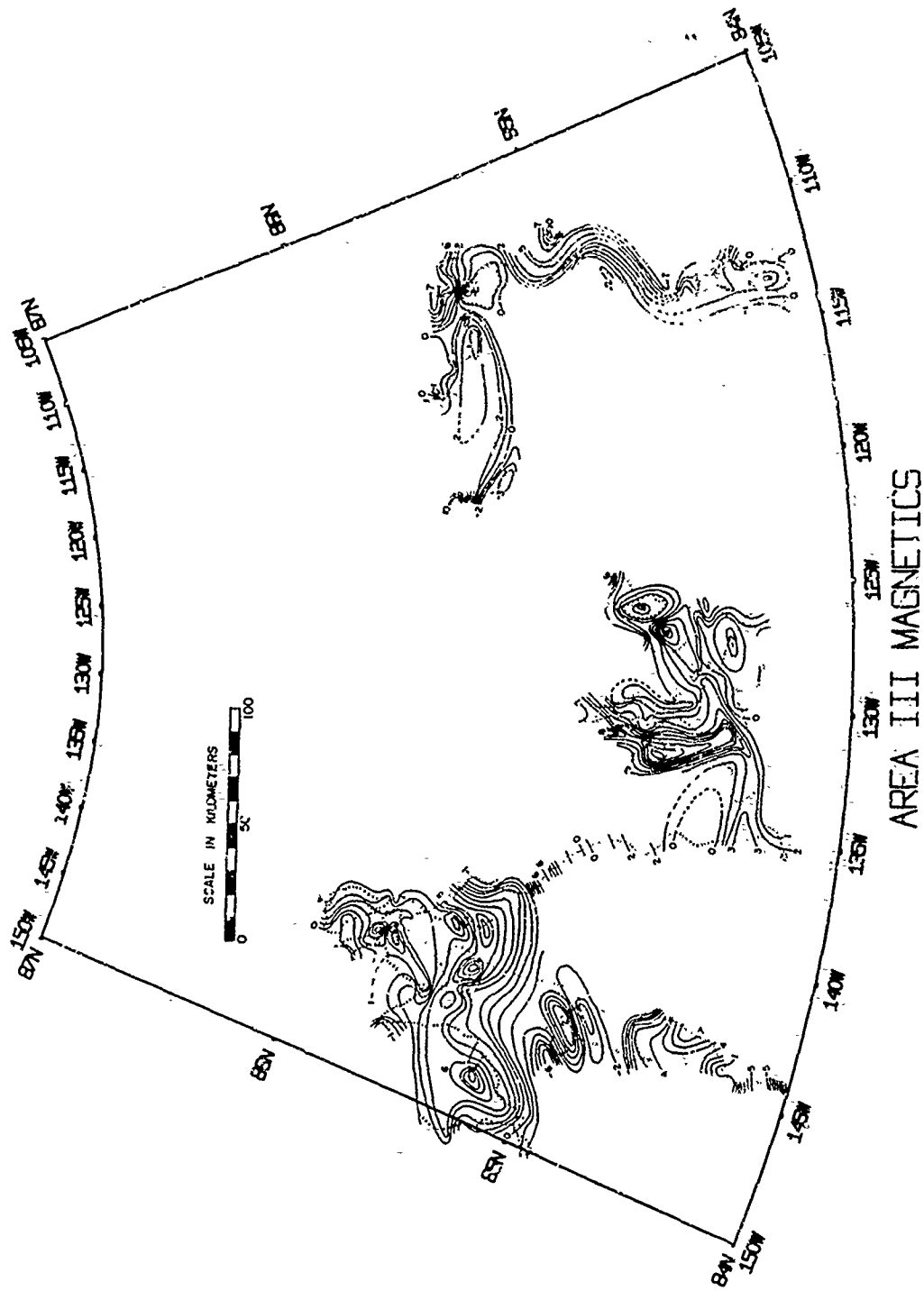


Figure 27

by observations taken during the winter drift of the BTAE. Two pattern orientations are again evident, but in this case the anomalies paralleling the cordillera are the most prominent. In the northwest portion, a wavy pattern of NE-SW trending anomalies follow the cordillera, but exhibit sufficient complexity to make correlation of individual anomalies between profiles very difficult. This particular problem was encountered by Vogt and Ostenso (1970).

In the south-central part of Area III, along the 132° West meridian, a transverse band of anomalies was delineated, possibly produced by a buried fracture bounding the valley which runs into the cordillera just to the east. A similar lineation appears to bound the eastern side of the valley, passing alongside Ostenso Seamount.

A general profile of the magnetic anomalies across the southern half of the Alpha Cordillera is shown in Figure 12. The magnetic anomalies appear to show symmetry about an apparent axis at 510 kilometers, corresponding to the Bouguer minimum in the profile. The observed symmetry is limited however, to one sharp high-amplitude anomaly with a bump on its flank slopes, because of the absence of data from the northern flank of the cordillera.

There is evidence, from other magnetic profiles which are not shown here, that there is another negative anomaly, bounded by two positive anomalies, which appears within the central negative anomaly in Figure 12. These anomalies were removed from Figure 12 because of their extremely ragged appearance, possibly caused by the contorted nature of the track, and also by the possibility (suggested by the gravity measurements) that the track crosses a fracture here. However these central anomalies do appear in short segments of profile (not shown) from the eastern part of Area III, and particularly in Ostenso's (1962) aeromagnetic profile 61-523 which appears to cross normal to the cordillera axis in the vicinity of 84°N and 165°E.

The magnetic anomalies might help explain the angular relationship between the Mendeleev Ridge and the Alpha Cordillera. The anomaly

pattern for the Soviet Arctic (Figure 3) shows lineations trending approximately north-south along the Mendeleev Ridge just east of 180°. The presence of the Mendeleev Fracture Zone shows that these anomalies could not reflect a north-south trending axis for the Mendeleev Ridge, for this would imply that any spreading must occur across rather than parallel to the fracture zone. Instead it suggests that the Mendeleev Ridge represents a portion of the Alpha Cordillera which has been offset toward the south along a series of en echelon transform faults, one of which is the Mendeleev Fracture Zone. The large anomalies associated with these fractures (Figure 25 around 170° West for example) might tend to overwhelm the narrow offset sections of smaller anomalies which parallel the cordillera axis, giving the pattern shown by Rassokho et al. (1967) in Figure 3. The suggested configuration for the ridge is shown in Figure 26.

The magnetic data generally supports, and certainly does not conflict with, the application of the seafloor spreading hypothesis of Vine and Matthews (1963) to the Alpha Cordillera. In fact, the presence of some degree of symmetry about the apparent ridge axis, plus the parallelism of the anomalies with the axis (except in the vicinity of fractures), argues for this hypothesis.

#### Inferred Fracture Zone Pattern

According to the seafloor spreading hypothesis, the ocean basins consist of basaltic material which is introduced at the axis of a mid-oceanic ridge. With time, this material moves away from the axis, gradually cooling and subsiding to give the ridge its characteristic shape. Newly forming seafloor takes on a remanent magnetization corresponding to the existing geomagnetic field: as reversals occur in the earth's field, the normal and reversely magnetized bands paralleling the ridge will give a striped appearance, with the "stripes" showing symmetry about the ridge axis. If the reversal chronology is known, then a magnetic profile normal to the ridge should indicate the approximate age of the seafloor at any point, as well as the rate at which

seafloor is produced.

When the ridge axis is offset, the pattern becomes more complicated. That part of the offset joining the displaced axes is called a transform fault, and represents an area of relative strike-slip motion of the spreading blocks. Outward from the transform the offset flanks spread together, separated by a lineation or fracture zone which dislocates the magnetic striping pattern. Fracture zones are inactive traces of transform faults and are often observed as basement ridges normal to the ridge axis. Delineation of these fractures defines the direction of spreading.

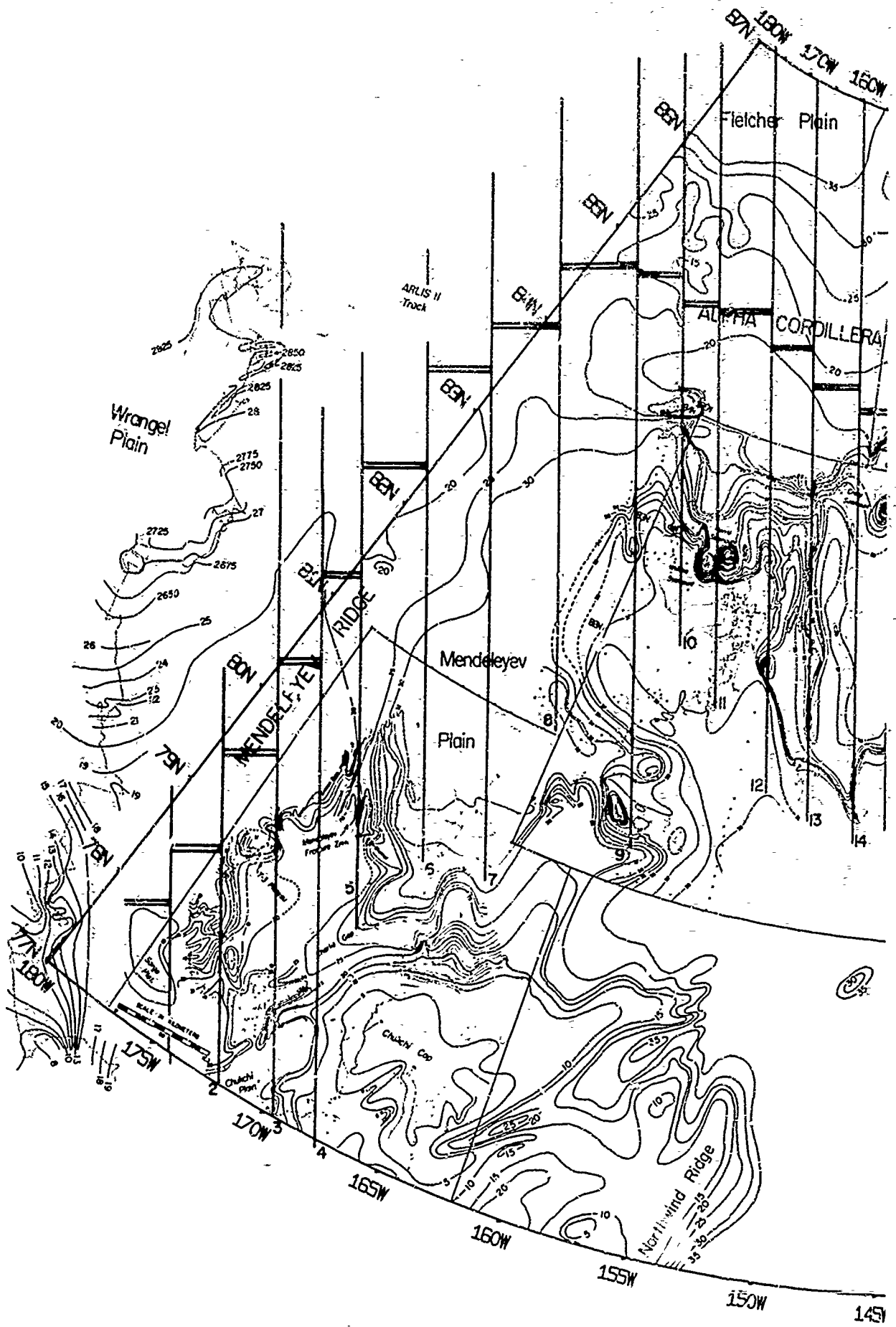
The bathymetric, seismic, gravity, and magnetic data were used in conjunction with the above to prepare maps showing the inferred fracture zone pattern and location of the ridge axis over the Alpha Cordillera and the Mendeleev Ridge (Figures 28a, 28b, and 28c). The observations underlying the inferred existence of each fracture are tabulated in Table I. Bathymetric and gravity data from the drift of Ice Station Arlis II (Black and Ostense, 1962, and Kutschale, 1966) have been included in these maps. The orientation of the fractures appears to parallel the 142° West meridian, which, for ease of reference, is about the orientation of the Alaska-Yukon boundary. No evidence of curvature was noted for these fractures, but any existing curvature is unlikely to be observed by so coarse a survey so close to the ridge axis. The 1961, 1963, and 1964 aeromagnetic profiles published by Ostenso and Wold (1970) were used in locating fracture crossings (usually identified by sharp anomalies or a break in the pattern) and the ridge axis (evidenced by some anomaly symmetry and a maxima in the anomaly envelope). The basement ridge observed by Kutschale (1966) appears to be a result of a large offset, paralleling the Mendeleev Fracture Zone, and indicating a high-low basement configuration consistent with the inferred ridge offsets.

Table I

## Basis for Inferring Fracture Zones

<u>Zone</u>	<u>Bathymetry</u>	<u>Magnetics</u>	<u>Aeromagnetics</u>	<u>Gravity</u>
1	(L)			
2	L	(L)		L
Wrangel Plain Buried Ridge (Kutschale, 1966)				
3	(L)-SP	L		L
4	(L)	(L)		(L)
Mendeleev Fracture Zone				
5	L-SP	L	Prof. 61-609	L
6	SP	L		L
7	GT	(L)	61-609, 523	
8	(L)		Prof. 61-609	(L)
9	L	(L)		
10	L-GT	(L)		
Wilkins and Harris Seamounts				
11	L-GT	L	Prof. 61-609	L
12	L	(L)	Prof. 61-609	(L)
Lamont Ridge				
13	L-250km	L-100km	Prof. 61-609	L
14	L-Scarps	L		L
Crary Seamount - Truncated on the Eastern Flank				
15	L	L		(L)
16	L-GT	L		(L)
17	L-GT	L		L
18	L	L		L
19	L	(L)		(L)
20	L-Valley	L		L
Ostenso Seamount				
21	L-Valley	(L)		L
Beal Seamount				
22	L		Bouguer Trough	(L)
23	GT			
24	L-Trough	L		L

( ) = Weak, L = Lination, GT = Gross Topography, SP = Seismic Prof.



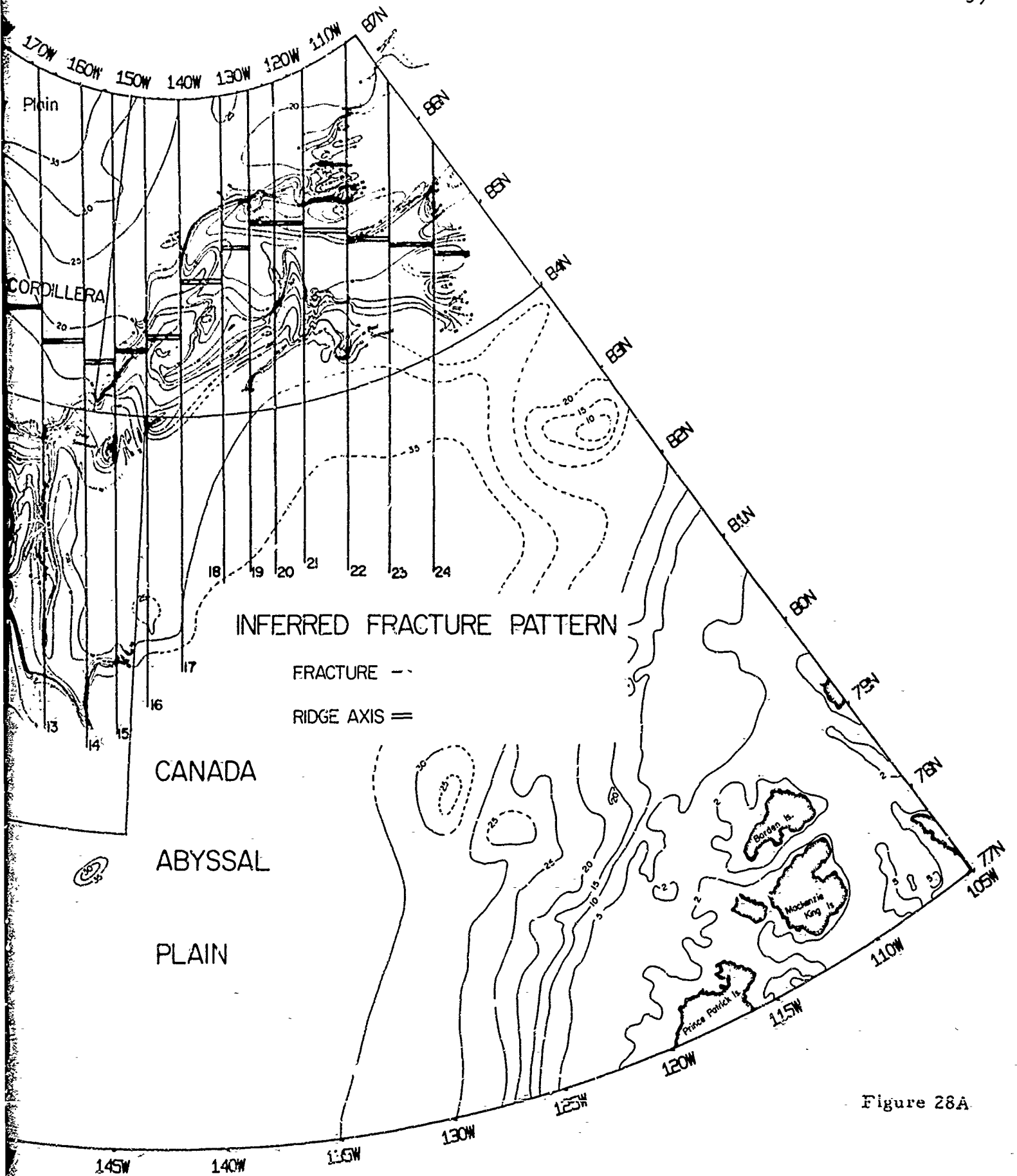
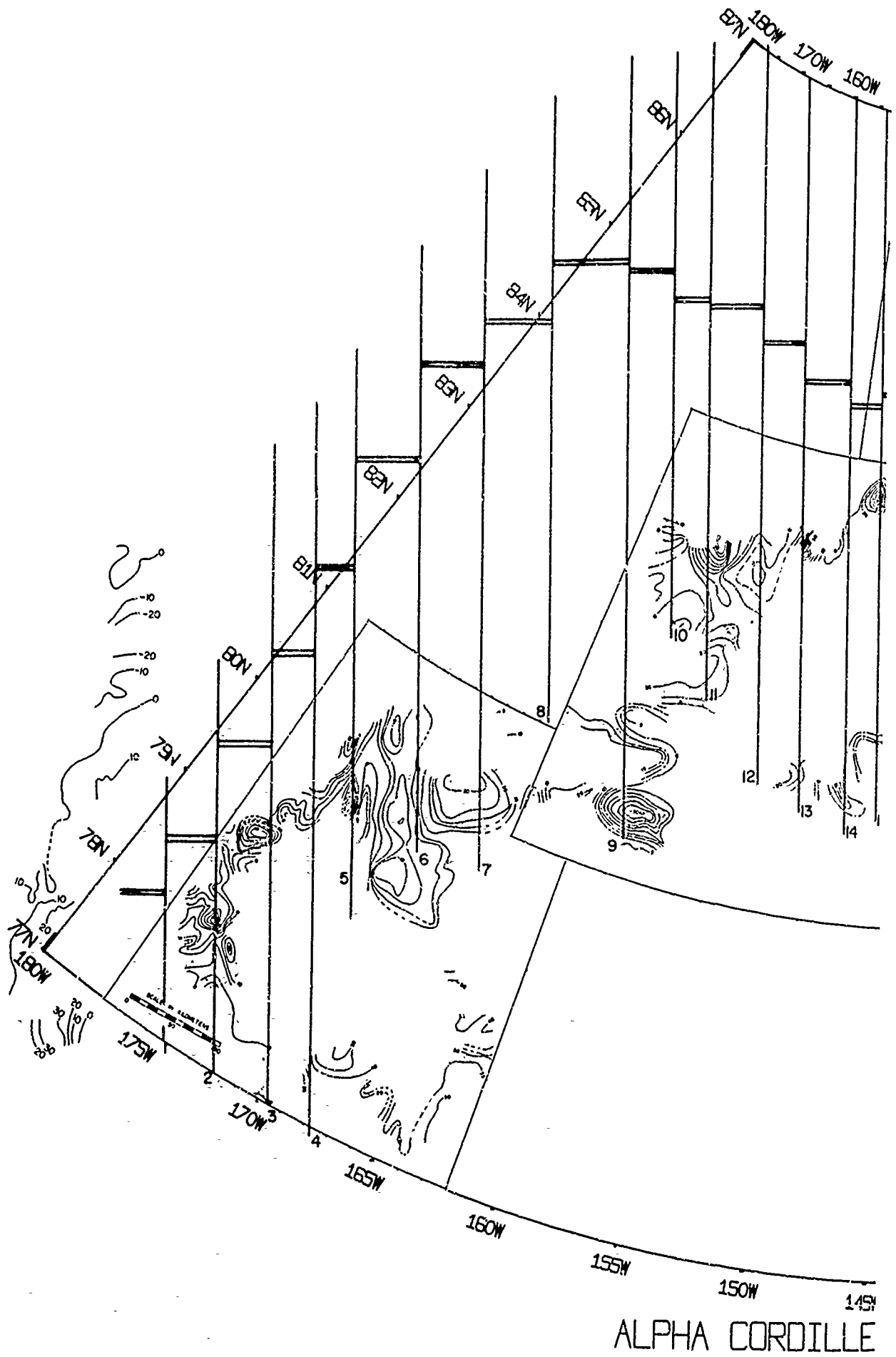
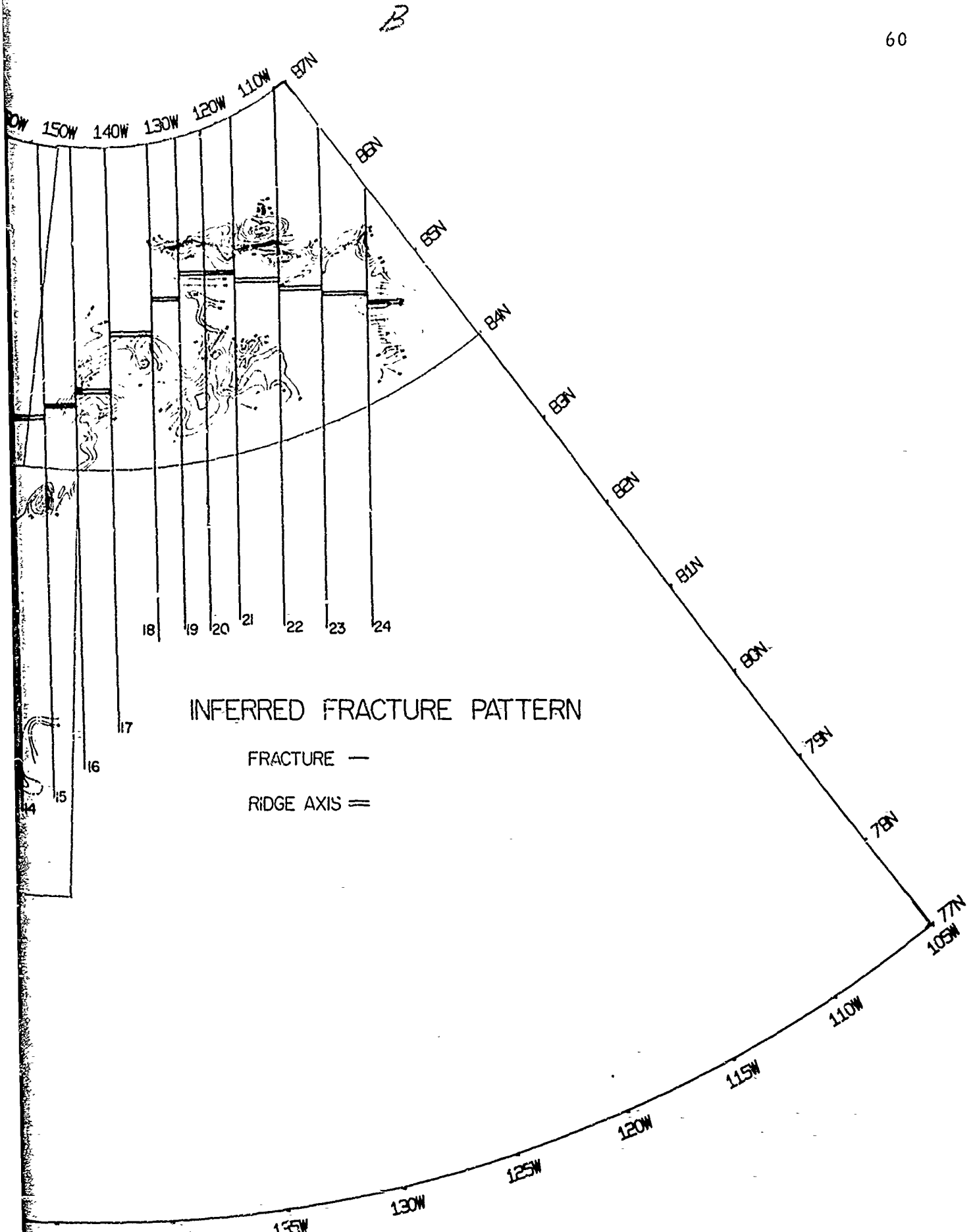


Figure 28A

A

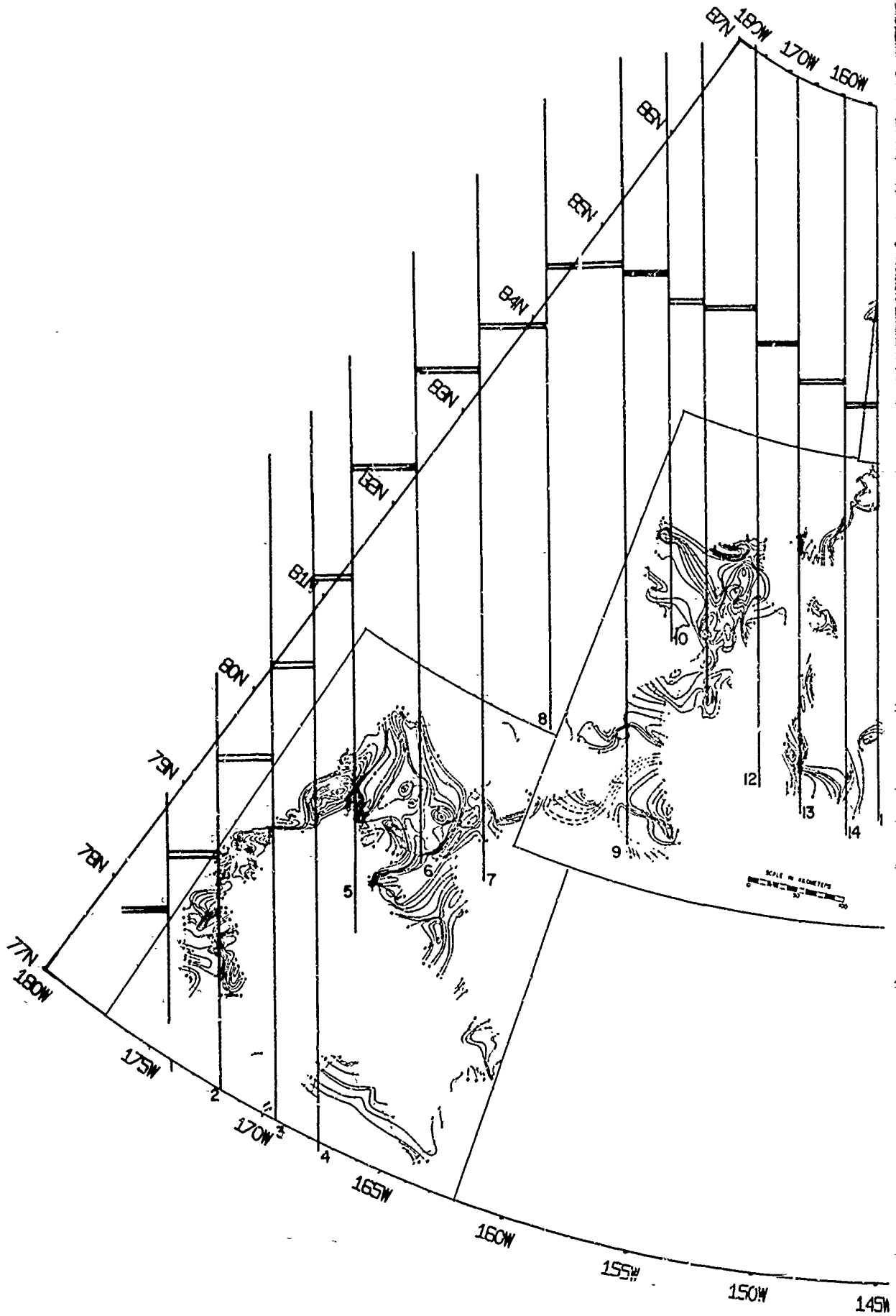




INFERRED FRACTURE PATTERN

FRACTURE —  
RIDGE AXIS ==

MLERA FREE-AIR GRAVITY



ALPHA CORDI

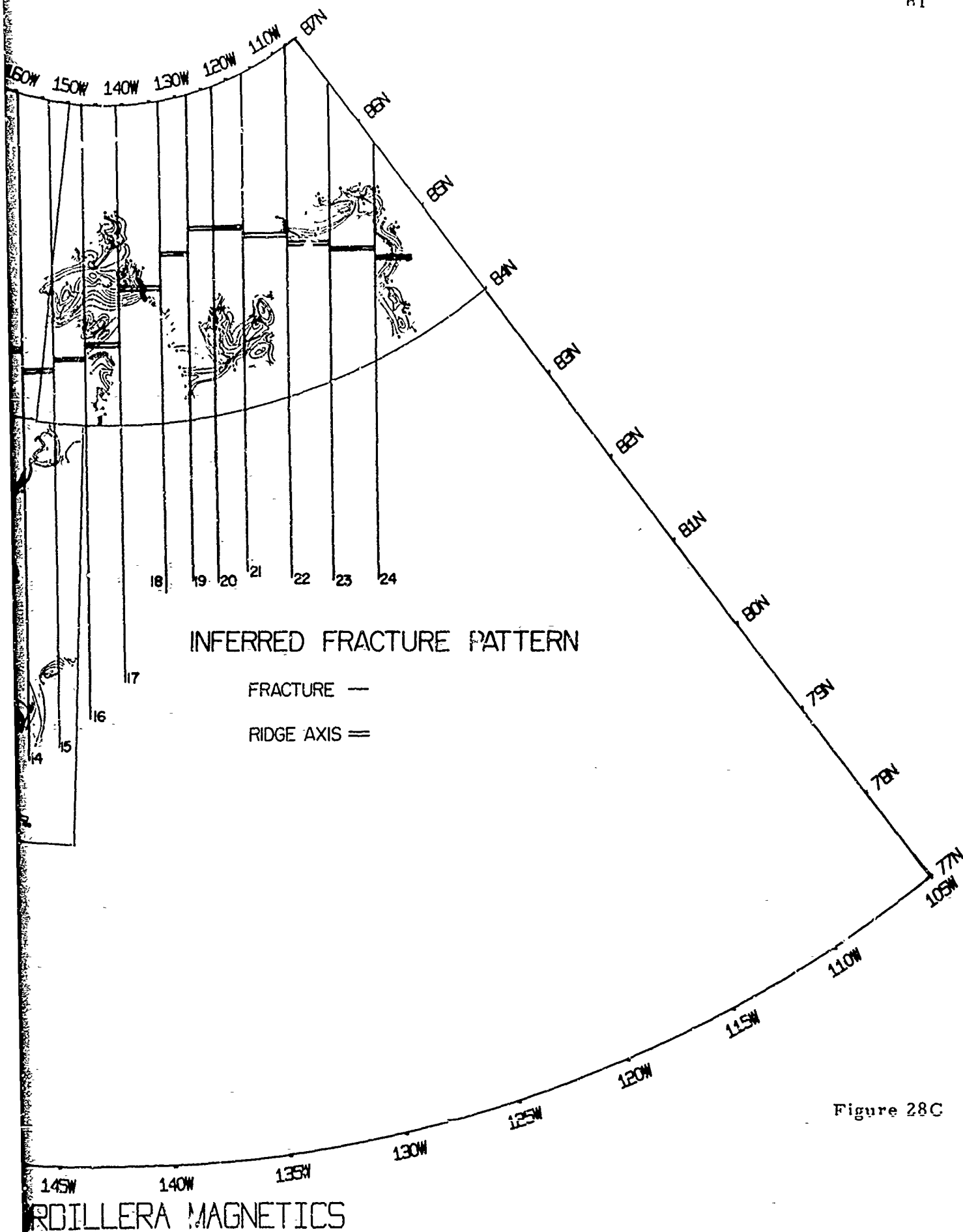


Figure 28C

### Speculations concerning the Alpha Cordillera as an Inactive Center of Seafloor Spreading

The previous sections have presented bathymetric, gravity, seismic, and magnetic data which support the contention of earlier investigators that the Alpha Cordillera is an inactive center of seafloor spreading. This section will propose a model for the development of this cordillera or ridge which suggests that the Alpha Cordillera represents the northernmost segment of an oceanic ridge which was active at various times in the Paleozoic, and in the Late Mesozoic and early Tertiary.

#### Proposed Model

Figure 29 shows the Amerasia Basin as it would appear following the closing of the Atlantic Ocean and the Eurasia Basin, about 80 million years ago. This reconstruction generally follows that of Bullard et al. (1965) based upon the computer matching of bathymetric contours, and also the reconstruction of Pitman and Talwani (1970) from fracture zone orientation and magnetic anomaly in the North Atlantic. Slight changes have been made to assure the fit of the sinuous Lomonosov Ridge against similar indentations along the Barents Shelf. The rotation of Ellesmere Island and northern Greenland will be described later, and the position of Siberia relative to Alaska is certainly in error.

This reconstruction shows that the Amerasia Basin is essentially rectangular in shape. On the east the basin is bordered by the Inuitian (pron. like Aleutian) system of folded geosynclinal belts along the northern margin of the Canadian Arctic Archipelago and Greenland. On the south lies the Yukon and northern Alaska, the site of the Brooks Range Orogen. The continental margin of Siberia, which is bounded by the Chukotka Geosyncline on the northeast, lies to the west. To the north is the Lomonosov Ridge, which Wilson (1963) and later investigators have considered to have once been the outer margin of the Barents Shelf. Within the Amerasia Basin, the results of this investigation suggest that, in the vicinity of the crest of the Alpha Cordillera at least, seafloor spreading has occurred parallel to the present 142° West meridian, along the long axis of the basin.

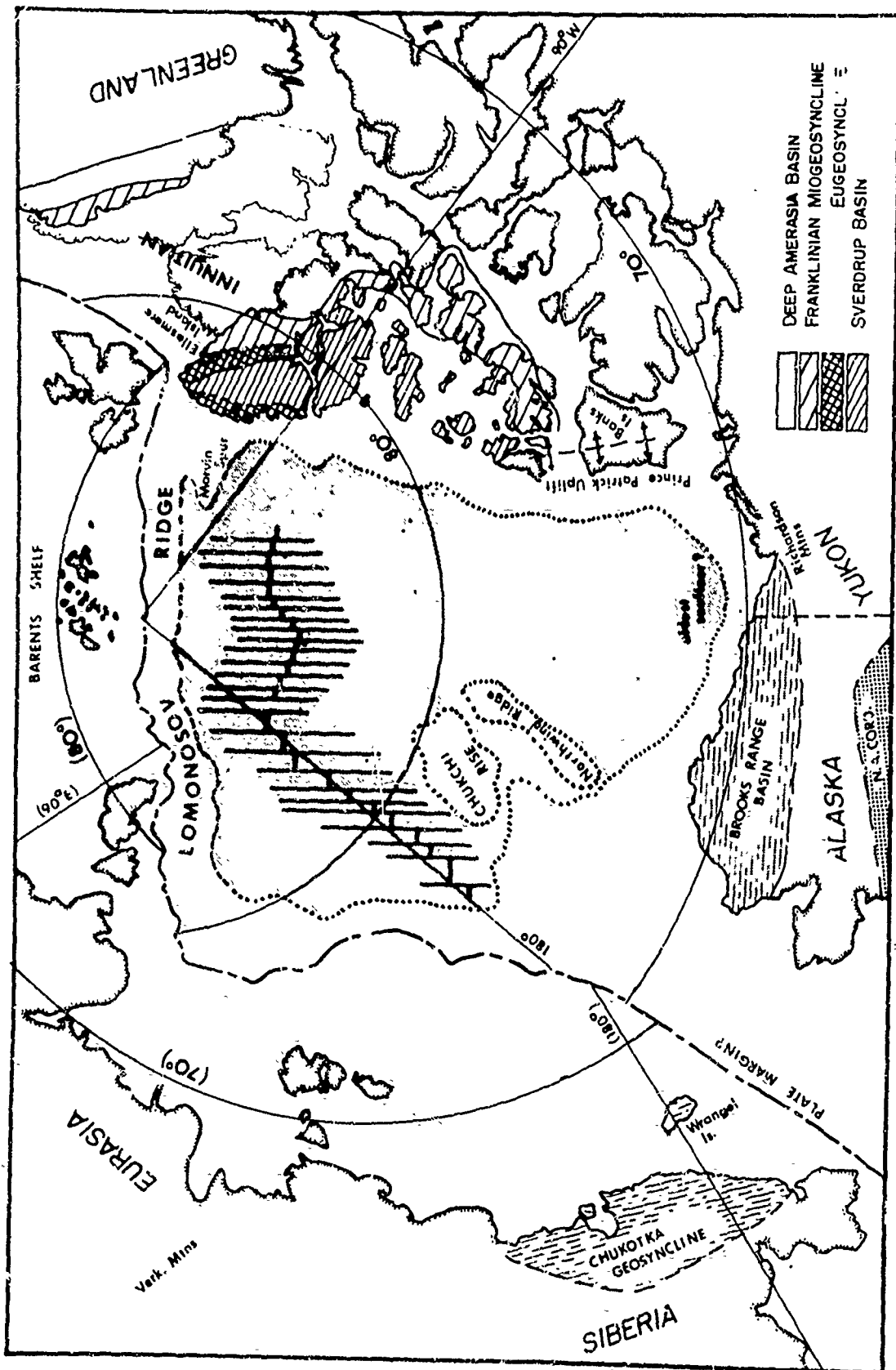


Figure 29

The marginal geosynclines bordering the Amerasia Basin indicate a depositional and deformational history which is quite similar to that of the Appalachian/Caledonian Orogen. In the reconstruction of Bullard et al. (1965) this orogen extends from Spitsbergen to Florida. Dewey (1969) and Bird and Dewey (1970) have related the events in the southern part of this orogen to an opening and closing of a Proto-Atlantic Ocean in the Lower Paleozoic following a suggestion set forth by Wilson (1966). The model proposed here suggests that the Alpha Cordillera was an integral part of this early spreading episode, as well as a forerunner of the opening of the Eurasia Basin.

The continuation of the Appalachians into the Caledonian belts of Scotland, Scandinavia, eastern Greenland, and Spitsbergen has been reasonably well documented (Wilson, 1966; Dewey, 1969). However a continuation into the Arctic further north presents some problems:

1) On the northern coast of Greenland, a Caledonian belt in Peary Land strikes at approximately right angles to the Caledonian belt on the eastern coast. Any continuation must account for this angularity.

2) Any Paleozoic continuation between the Proto-Atlantic and the Amerasia Basin presumably passed somewhere between the present Barents Shelf in the vicinity of Spitsbergen, and northern Greenland and Ellesmere Island. However any expansion and contraction in this vicinity would not be normal to the arcuate Inuitian System in northern Greenland and the Canadian Archipelago.

3) Late Mesozoic separation of Greenland from Labrador suggests that a continuation of the Atlantic Ridge with the Arctic at this time might have passed through the Labrador Sea, and thence into the Amerasia Basin where it connected with the Alpha Cordillera. However attempts at a continuation via transform faulting through the Robeson Channel separating Greenland from Ellesmere meet with geological evidence that does not allow more than a few kilometers of strike-slip movement (Kerr, 1967). Furthermore, any continuation beneath Ellesmere must pass beneath areas of undisturbed Lower Paleozoic sediment

(Thorsteinsson, 1961).

4) Finally, the tectonic history of the bordering belts is similar for all periods of deposition and orogeny except the Early Jurassic through Early Cretaceous, when northern Alaska went through an extended period of uplift, with the formation of a tectonic welt beneath the present Brooks Range.

Many of the above problems are obviated by the continental reconstruction and history of Atlantic-Arctic spreading, contraction, and renewed spreading proposed below.

1) Prior to the early Tertiary, the Caledonian/Appalachian orogen extending from Florida to Spitsbergen continued northwest and west through the Inuitian System in northern Greenland and Ellesmere, forming one continuous and relatively smooth arcuate belt around eastern and northern North America. West of Prince Patrick Island another belt continued through the Yukon and northern Alaska, and perhaps across northeastern Siberia by the Chukotka Geosyncline.

2) Between the Late Precambrian and the Ordovician, following the model of Bird and Dewey (1970), a Proto-Atlantic Ocean opened along the full length of the Appalachian/Caledonian orogen. The Amerasia Basin may have existed prior to this opening. This opening was accomplished through plate accretion (seafloor spreading) along a fracture in an older North American/African/European continent, and was accompanied by subsidence of the separating continental margins and generally uninterrupted sedimentation.

3) Commencing with the Ordovician in the south, this ocean began to close. Oceanic plate consumption was accomplished through the development of marginal trenches and underthrusting along Benioff Zones. This underthrusting and associated granitization produced the Caledonian orogeny.

4) Closing continued until the Devonian, when a collision of the continents, probably as far north as eastern Ellesmere, produced the Late Caledonian Spasms (Haller and Kulp, 1962) in the Greenland and Inuitian belts and the Acadian orogeny to the south.

5) Minor movements occurred along the belts in the Late Paleozoic

and Early Mesozoic, and these may have been the precursor of the present opening of the Atlantic Ocean. Some spreading may have occurred in the Amerasia Basin.

6) In the Jurassic and Cretaceous, the Brooks Range geanticline was produced as a result of the Nevadan Orogeny along the Western Cordillera. At about the same time the Atlantic began to open in the far south, and by Late Cretaceous had progressed as far north as Greenland.

7) Between 80 and 60 million years BP Greenland separated from Labrador, rotating approximately 11 degrees east about an apparent pole in Ellesmere Island (Le Pichon et al. , 1970).

8) From some time before 60 and until 40 mybp, spreading occurred on the Alpha Cordillera (Vogt and Ostenso, 1970), parallel to the present 142° West meridian. The amount of spreading apparently exceeded the opening of the basin, producing compressional structures in the marginal geosynclines south of the Alpha Cordillera.

9) Between 60 and 40 mybp Greenland (less the northern Greenland belt) also moved north about 500 kilometers about an apparent pole of rotation in the vicinity of Hudson Bay (Le Pichon et al. , 1970). This motion was predominantly strike slip along the Davis Strait. This northward movement resulted in the deformation of the eastern Franklinian Geosyncline and the northern Greenland Caledonian belt, through a kinking of the belt about two hinges or pivots in northeastern Greenland and the Sverdrup Basin. Bending of the Sverdrup Basin produced folding transverse to the earlier Paleozoic and early Tertiary folds, thrusting, and diapirism (Keen et al. , 1969). The latter part of this northward movement resulted in the accretion of the northern Greenland Caledonian belt with the central and southern part of Greenland. The northward movement was possibly accommodated through deformation of the Greenland end of the Lomonosov Ridge, which was then the outer margin of the Barents Shelf.

10) About 40 million years ago the movements of Greenland ceased, except for slight rifting along the Robeson Channel (Keyr, 1967). Spreading ceased on the Alpha Cordillera about this time (Vogt and

Ostenso, 1970), and was replaced by opening of the Greenland Sea and the Eurasia Basin.

#### Alternative Proposals

The events south of Spitsbergen appear to be reasonably well explained by the formation and contraction of a Proto-Atlantic Ocean (Dewey, 1969). However, other proposals have been, or might be called upon, to explain the events recorded in the belts around the Arctic. Three of these are discussed below.

1) Tailleir (1969b) has speculated that the Canada Basin may have formed through episodic Early Jurassic to Early Cretaceous rifting, similar to the Arctic Sphenochasm proposed by Carey (1955). According to Tailleir's (1969b) speculation, the basin opened approximately along the present 145° West meridian, by rotation about an apparent pole in east central Alaska. Total opening was estimated at about 32°. Arguments for this speculation lie in the fact that geologically, the newly parallel Brooks Range and Franklinian Geosyncline/Sverdrup Basin would have developed alongside a tectonic source area that could have supplied the clastics comprising the thick Devonian and Mississippian deposits. Rifting would also allow the straightening of the bends Tailleir (1969a) reports in the western Brooks Range orogen, account for extensive lateral foreshortening due to thrusting, and allow an original connection of these sutured belts with the Canadian Cordillera to the southeast. Tailleir (1969a) supports this last suggestion by noting the close similarities between the Devonian and Mississippian carbonates along the front of the Brooks Range and those found at Nation River on the Yukon.

However, this speculation has several failings. First it suggests no mechanism of rifting, such as seafloor spreading or the relative rotation of blocks, which might dovetail with the known history of the basin. Moreover it does not explain the absence of basinal deposits between Prince Patrick Island and the Mackenzie Delta, or the lack of deformation of the Sverdrup Basin accumulations analogous to that found

in the Brooks Range in the Mesozoic. And finally, there is no evidence for the remains of the central tectonic lands within the basin, nor an explanation for their disappearance.

2) Harland (1965) has postulated that the Caledonian belts of eastern and northern Greenland resulted from two stages of deformation; an east-west compression which was gradually replaced by a north-south component which produced the Innuitian fold system.

Both this, and the case where both belts were produced simultaneously in their present orientation, seem unlikely for several reasons. First, if the development of these belts is a result of spreading followed by contraction, as has been suggested for the southerly belt, then it is difficult to imagine a spreading geometry which would give such an orthogonal deformation pattern. The closest possible geometry would, of course, be a triple ridge junction off the northeastern coast of Greenland. However this seems unlikely in the absence of any supporting evidence from Eurasia. Second, the curvature of the fold belts in the Franklinian Geosyncline and the Sverdrup Basin does not suggest that the direction of compression was uniform along the geosyncline, as might be expected by a north-south component presumably resulting from plate movements. Finally, Kerr's (1967) conclusion that relative motion between northern Greenland and Ellesmere is extremely limited, plus the mounting evidence that Greenland experienced a large northward movement, suggests that any deformation prior to Greenland's movement was within a different geometrical framework.

3) Beal (1968) suggested a continuation of the Alpha Cordillera through the Canadian Arctic Archipelago to the buried ridge in the Labrador Sea observed by Drake et al. (1963). The suggested continuation was presumably beneath Ellesmere Island by way of Eureka Fjord (Nansen Sound) and Baffin Bay. This will be called proposition a). Other continuations might consist of b) a more roundabout path through the archipelago, such as the passage of the "Mediterranean-Greenland Branch of the World Rift System" through the Parry Channel proposed

by Dementitskaya and Dibner (1966), or c) an offset of the ridge around Ellesmere by means of transform faults along the Robeson Channel (Wilson, 1963) and then back along the shelf margin north of Ellesmere.

In all three cases the evidence for a continuation seems doubtful. The existence of undisturbed Lower Paleozoic sediments on eastern Ellesmere and Devon Island makes a) quite unlikely; the lack of any evidence of an extended tensional zone anywhere in the archipelago does the same for b), and c) would imply that a ridge crest lies in line with the Lomonosov Ridge for a short distance. This is quite unlikely. Finally, the work of Le Pichon et al. (1970), suggesting an opening of the Labrador Sea which is best explained by a rotation of Greenland about Ellesmere, may make such a continuation less compelling.

#### Geological Evidence

This subsection describes the geological history of Greenland, the Canadian Arctic Archipelago, and northern Alaska and the Yukon for three time periods from Late Precambrian to the present. Unless otherwise noted, summary accounts by Koch (1961), Haller (1961), Haller and Kulp (1962), Thorsteinsson and Tozer (1961), Tailleux (1969a) and Churkin (1969) have been used. In particular, a paper by Keen et al. (1969) examines the continental margin of Eastern Canada, considering the opening of the Labrador Sea, and offering the first suggestion that Ellesmere experienced a rotation along with Greenland which produced the bend in the Innuitian System. Keen et al. (1969) also present a bibliography of recent geological and geophysical investigations.

For locating some of the more obscure areas or locations the reader is referred to the World Map of the National Geographic Society (1966), or other comparable polar maps.

#### Precambrian to Carboniferous

Dewey and Bird (1970) have related the development of mountain belts to plate tectonics. In some earlier papers, they developed models, based upon these relationships, for the evolution of the Appalachian/Caledonian Orogen. The part of the orogen in the British Caledonides

was covered by Dewey (1969) and that part in Newfoundland and New England by Bird and Dewey (1970). They showed the development of the orogen as a result of an opening and closing of a Proto-Atlantic Ocean similar to that suggested by Wilson (1966). In their model, the ocean opened in Late Precambrian time, and spread to its maximum breadth around Late Cambrian time. Subsidence along the continental margins provided areas of accumulation for detrital sandstones and shales, covered by shales, limestones, and dolomites. In the south, Bird and Dewey (1970) show the closing accommodated by the development of a slab of downgoing oceanic crust or Benioff Zone along the western margin. In Late Ordovician time this resulted in the formation of a volcanic arc along the western margin which produced Taconian folded mountains, westward overthrusting, igneous intrusions and metamorphism. The Acadian Orogeny marked the final closing through continental collision in the Late Devonian.

In the British Caledonides the postulated events were more complex, with the development of three Benioff Zones, two on the east and one on the west by Upper Ordovician (Dewey, 1969). Further north Dewey (1969) shows the development of the East Greenland-Norway belt through one simple Benioff Zone to the west. The present eastern Greenland belt was thought to represent the far western part of Zone A, an area of high temperature/pressure metamorphism.

This paper suggests that the development of the Innuitian System and perhaps northern Alaska follows a similar evolutionary model, with the exception that in the western part of the Innuitian belt and northern Alaska there probably was no continental collision.

Summing up the Paleozoic orogenic episodes in eastern Greenland Haller and Kulp (1962) note a main Caledonian orogeny which rapidly produced the principal fold belt at the end of the Silurian and was responsible for the vast regional metamorphism. This may mark the closing of the ocean. This was followed by the "Late Caledonian Spasms", an orogenic decline which, with the minor succeeding episodes, lasted

for almost 100 million years. Dewey (1969) suggests that the long thermal history associated with this orogenic cycle is "related to the rise of magmas and volatiles from an underlying Benioff Zone progressively later on the continental side". These Late Caledonian Spasms were only found south of  $76^{\circ}\text{N}$ . The opening of the Proto-Atlantic along eastern Greenland may be recorded in the block-faulting of the older Precambrian Carolinian structural system and subsequent post-orogenic generation of basalt in the form of extensive dikes (Haller, 1961).

The northern Greenland geosyncline was the site of sedimentation from Precambrian through Silurian time. Movements during this time were slight, and paraconformities are apparent between formations. The Upper Silurian graptolite shales become very sandy, and are overlain by several hundred meters of sandstone of increasing coarseness. Koch (1961) interpreted this as a flysch facies associated with the initial folding. Folding is observed along a zone 530 km long, with fold intensity increasing toward the east. In the east, thrusting and metamorphism is observed, and the metamorphic rank increases toward the north. In eastern Ellesmere, between  $78^{\circ}$  and  $78^{\circ}15'\text{N}$  the original rifting of the Proto-Atlantic may also be recorded in a sequence of 620 meters of Late Precambrian sandstones and shale, tuff and volcanics which are intruded by diabase dikes, and overlain by another 1240 meters of light sandstones, red shales, and thick lava beds (Christie, 1962).

Just to the west of the North Greenland belt, in the shape of a reverse "L" is the Franklinian Geosyncline. This was formed by great subsidence between Cambrian (or earlier) and the Upper Devonian. Sediment thicknesses within the geosyncline increase toward the east, with up to 60,000 feet deposited on northwestern Ellesmere Island. A miogeosynclinal belt is found on the south and east next to the interior Arctic Lowlands, and has been traced over a distance of more than 1600 kilometers. A eugeosynclinal belt lies seaward of the miogeosyncline, and is seen in exposures on northern Ellesmere and Axel Heiberg Islands. The boundary shown in Figure 29 marks the transition from some clastics which show some Ordovician and Silurian fossils to the

miogeosynclinal limestones and shales. Paleozoic volcanics are identified further to the northwest on northern Axel Heiberg and on the northern coast of Ellesmere Island.

The Franklinian Geosyncline was the site of diastrophism several times in the Paleozoic. Deformation of limited extent occurred near the Siluro-Devonian boundary, resulting in northerly trending structures which form the Cornwallis fold belt on Cornwallis and Bathurst Islands. Shallow folds are observed, along with some normal faults but no thrusting. The Boothia Arch was formed south of this belt at about the same time, and both structures are related to movements within the basement by Thorsteinsson and Tozer (1961).

A second period of deformation resulted in the east-west trending structures which form the Parry Islands fold belt on the southern side of the miogeosyncline, and the fold belts paralleling the arcuate miogeosyncline on northern Devon Island and eastern Ellesmere. The miogeosynclinal deformation is dated stratigraphically as being between Upper Devonian and Middle Pennsylvanian. The Parry Islands belt shows increasing fold intensity toward the north, and the shape of the folds suggests forces acting from north to south. The Ellesmere folds are not continuous with the Parry Islands belt because of the Cornwallis belt, but are considered to be contemporaneous.

Intense deformation is observed in the eugeosyncline to the north. No date is available for this deformation but the event can be bracketed. Basic lavas are observed to overlie rocks containing Middle Silurian graptolites, which are themselves overlain by Middle Pennsylvanian limestones, indicating that the deformation was post-Middle Silurian and pre-Middle Pennsylvanian. The uplift and deformation of the eugeosyncline may have been pre-Middle Devonian, as a thick sequence of Middle to Upper Devonian clastics, extending from southern Ellesmere to Banks Island, indicate a provenience to the north of the miogeosyncline. Within the eugeosyncline the degree of metamorphism increases to the northwest, away from the miogeosyncline.

In northern Alaska the interpretable record begins in the Silurian or Devonian, and indicates a tectonic evolution similar to the Canadian Arctic Archipelago. Dated granitic plutons (Baadsgaard et al., 1961) and the discovery of argillite beneath Mississippian sediments in wells along the northern coast suggest evidence of a northerly ancestral Brooks Range orogen which was uplifted, deformed, and intruded by granitic plutons. This orogen may have provided a northerly source of sediment to build a thick clastic wedge or delta toward the south in Late Devonian time. Similar wedges have been described in the Innuitian System above, and are reported in Chukotka and Wrangel Island on the west (Churkin, 1969). The constituents of this ancestral geosyncline may be represented in the Richardson mountains in the northern Yukon to the east. From the Cambrian through the Devonian the Richardson Trough was the site of deposition of limestone, shale, argillaceous limestone, chert, and other shelf deposits (Gabrielse, 1967).

The geologic data for the Lower Paleozoic in the Innuitian and northern Alaskan geosynclines suggest, within the framework of plate tectonics, that these areas mark margins with oceanic plate underthrusting. The granitic intrusions of northern Alaska and the formation of arches and uplifts in the Canadian Arctic Archipelago is suggestive of the magmatic rise associated with the development of a Benioff Zone. In northern Ellesmere and Greenland's Peary Land the suggested Upper Silurian age of deformation and metamorphism may mark an early closing of the Proto-Atlantic relative to Acadia. Further delineation of events in this area must await a much better knowledge of the geology, plus a reconnaissance of the matching margin across the proto-ocean. Presumably this margin is now part of the Barents Shelf.

The geometry of the lithospheric plates suggests that an ocean remained along the coast of northern Alaska and perhaps by the western Franklinian Geosyncline. This old ocean may have been separated from the continent by an uplifted belt which shed clastics to the south to form the ubiquitous Middle to Upper Devonian clastic wedges. The seafloor remaining within this basin would have to be Cambrian or older.

The lack of deformation along the archipelago between Prince Patrick Island and the western Yukon may be a result of strike-slip motion of the seafloor along this line, with separate Benioff Zones below the eastern Canadian Archipelago and northern Alaska.

#### Carboniferous to Upper Mesozoic

With the exception of northern Alaska, this period was one of sedimentation and minor tectonic movements. Eastern Greenland lay alongside Norway, experiencing the final movements associated with the lengthy Caledonian orogeny, a period of faulting lasting through the Carboniferous to Middle Permian. Some of these movements may have been related to deformation within the Ural Mountains geosyncline, the completion of the Variscan chains across western Europe, or the final uplift and deformation of the Appalachian Geosyncline. Following a Middle Permian marine transgression eastern Greenland witnessed numerous transgressions during the Mesozoic which deposited coastal sediments indicative of tectonic quiescence.

Within the Franklinian Geosyncline, the Sverdrup Basin was developed through essentially uninterrupted sedimentation from Middle Pennsylvanian to the Tertiary. During this time more than 40,000 feet of both marine and non-marine sediment was deposited. Along the margins of the basin there is some evidence of a hiatus. An angular unconformity occurs between Middle Pennsylvanian and Permian formations, with evidence of folding and faulting of the underlying rocks in northwestern Melville and southern Ellesmere Island. This uplift was apparently enough to seal off the basin, for evaporites were formed in the Pennsylvanian and/or Permian. Gypsum and anhydrite are observed, but no halite. Masses of gabbro and volcanics are commonly observed in the Tertiary diapiric structures produced from these deposits, and are apparently Tertiary in age themselves.

In northern Alaska, this period was one of subsidence and deposition along the present site of the Brooks Range which lasted until the Jurassic. In the Early Jurassic a tectonic welt began to form in this basin, devel-

oping by early Early Cretaceous into a volcanic province which shed debris into a flanking basin on the north. Large scale foreshortening, uplift of the Brooks Range Geanticline, and depression of the flanking foredeeps occurred in late Early Cretaceous. By Late Cretaceous these foredeeps had been filled, and in latest Cretaceous and early Tertiary were deformed along with the anticline, to form the present Brooks Range and adjacent foothills (Tailleur, 1969a).

During this period, the Permo-Carboniferous angular unconformity found along the margin of the Sverdrup Basin may indicate a period of spreading within the basin, or perhaps just the final episodes of the Caledonian Orogeny. The evidence is hardly conclusive. In Alaska however, the Jurassic and Cretaceous development of the Brooks Range geanticline coincides with the development of other geanticlines to the south (Eardley, 1962), and with a period of great tectonic activity (The Nevadan Orogeny) along the Western Cordillera. Gabrielse (1967) notes two periods of regional metamorphism and as many as six episodes of granitic intrusion accompanied by regional uplift in the south central Yukon.

These events would appear to be related to underthrusting of the Pacific oceanic crust and development of a Benioff Zone beneath southern Alaska. Mafic and ultramafic intrusions emplaced in one area of the Brooks Range in the Late Jurassic (Eardley, 1962) may be the result of mobilization of the inactive south-dipping underthrust Arctic oceanic plate by the active north-dipping underthrust Pacific oceanic plate. In any case the absence of Jurassic-Cretaceous tectonic activity in the Sverdrup Basin makes underthrusting of northern Alaska unlikely at that time.

#### Upper Mesozoic to Present

The exact sequence and time of tectonic events during this period is not known, however a general pattern of early Tertiary deformation is observed. In eastern Greenland the formation of extensive plateau basalts and local acid plutons may herald the opening of the present

Atlantic Ocean. In the south some of these basalts occur over a sedimentary series extending to lowest Eocene (Wenk, 1961). In southwest Greenland, the rifting from Labrador may be recorded in a swarm of olivine-doleritic dikes, dipping at  $45^\circ$  to the southwest or west-southwest, which are confined to the seacoast region. Berthelson (1961) tentatively attributes a Tertiary age to these. On the western side of Baffin Bay another area of probable Tertiary volcanics is seen on Baffin Island.

In northern Greenland, sediments of Cretaceous to Tertiary age are found in eastern Peary Land. These have been faulted and mildly folded along a general southeast trend sometime in the Tertiary, and may be related to the postulated collision of northeast Greenland with the Lomonosov Ridge on the Barents Shelf, or perhaps the Alpha Cordillera. West of Peary Land no post-Caledonian sediments are known. Between Hall Land and J. P. Koch Fjord, a striking thrust-fold system is reported (Haller and Kulp, 1962), wetting the North Greenland fold belt. Structural relations indicate a post-Paleozoic origin, resulting from forces directed toward the south.

Sedimentation in the Sverdrup Basin continued into the Tertiary. In the Tertiary (probably early Tertiary) folding and thrust faulting occurred throughout much of the Queen Elizabeth Islands. Ellesmere and Axel Heiberg show the effects of more intensive movements. Many of the folds are superimposed upon the older Paleozoic belts, but not all. Folds and thrusts in central and southern Ellesmere generally follow the older Caledonian structures. To the west, similar superpositions appear, but folding is of lower amplitude. Numerous folds with diapiric cores are developed in Amund and Ellef Ringnes and western Axel Heiberg Islands along the trend of the Boothia Arch. Numerous large diapiric intrusions of Permo-Carboniferous evaporites are also observed in this area, as well as on eastern Axel Heiberg Island. The age of the Tertiary deformation is not precisely known, however a post-Paleocene-Eocene age is suggested by the deformation of the Eureka Sound formation which is partly, or perhaps wholly of

this age. The deformation zone, transverse to the Sverdrup Basin along the trend of the Boothia Arch, may possibly be a result of the postulated rotation and bending of Ellesmere between 60 and 40 million years ago.

In northern Alaska the main phase of the Brooks Range orogeny occurred in the late Early Cretaceous with metamorphism and establishment of an east-west structural pattern. Uplift throughout the Late Cretaceous filled the flanking basins (the Colville and Kobuk), and in latest Cretaceous and early Tertiary these were deformed with thrusting possibly as late as the Late Paleocene (Eardley, 1962).

On the eastern slope of the Richardson Mountains in the northern Yukon, Jeletzky (1961) reports major north-south dislocations of post-mid-Upper Cretaceous (? Tertiary) age. These structures appear to be related to movements of basement blocks, possibly along reactivated Precambrian faults.

Vogt and Ostenso (1970) compared aeromagnetic profiles from the Alpha Cordillera with profiles from the North Atlantic. They found a best match with those anomalies presently found between 300 and 500 kilometers from the crest of the Reykjanes Ridge. From this they tentatively concluded that the Alpha Cordillera was actively spreading from at least 60 my to 40 mybp, at which time spreading probably began in the Eurasia Basin. This spreading episode appears to be consistent with the early Tertiary deformation in the Canadian Archipelago, the Yukon and Alaska. At present it is impossible to determine when this last episode of spreading began, but it appears possible that the post-mid-Upper Cretaceous movements along the eastern slope of the Richardson Mountains (Jeletzky, 1961), or post-Lower Cretaceous extrusion of evaporite structures along the northern slope of this range (Kent and Russell, 1961) may be related to an initial compressive pulse caused by underthrusting.

Milne (1965) may have provided evidence of underthrusting with an unreversed refraction profile across the continental shelf NNE of Point Barrow, Alaska. He shows a 2.5 km thick (sedimentary) layer of 2.40

km/sec compressional wave velocity overlying 8.68 km of 4.40 km/sec "basement", which is underlain by a 7.47 km/sec mantle. There was no evidence of the usual 6.50 km/sec oceanic layer. It was considered possible that the low velocity mantle was a result of a dip to the SSW. However, in a reversed refraction profile, Hunkins (1966) reported a 7.4 km/sec layer dipping south from a depth of 20 kilometers near the shelf edge to 32 kilometers near Barrow, suggesting that anomalous mantle is dipping beneath the continental margin.

During the suggested northward movement of Greenland between 60 and 40 million years ago (Le Pichon et al., 1970), it is proposed that the Inuitian-eastern Greenland belt was bent from a relatively linear feature into a reverse "Z". Within the Sverdrup Basin the bending may be recorded in the extensive folding, thrusting, and diapirism along the inferred axis of compression (Keen et al., 1969). Tensional features observed by Kerr (1967) at the southern end of the Nares Submarine Rift Valley may also be related to this proposed bending. In northwestern Greenland there is no suggestion of rotation other than strike-slip movements along reactivated Caledonian faults. The inferred hinge or pivot may lie beneath the sea somewhere north of Kronprins Christian Land, or preferably near the ice-covered area at the end of Hagens Fjord (Mylius Ericksens Land), while the areas of compressional deformation should be concealed by the permanent ice cover.

North of Greenland, deformation of the Lomonosov Ridge by the northward movement of Greenland may have produced the Marvin Spur. The faulted depressions observed on the Alpha Cordillera and noted in an earlier section may also be a result of this motion.

#### Age of the Canada Basin

The proposed history of the basin would indicate that the Amerasia Basin is very old, and that it might also contain very old seafloor. Speculations on how old, of course, will depend upon the interpretation of events around the basin. The inferred direction of spreading and

location of the ridge axis (Figure 29) suggest that, in the absence of a change in spreading direction, the oldest oceanic crust should be located near the Mackenzie Delta in the Yukon. This length of oceanic crust is about 1700 kilometers. A visual inspection of the correlated Alpha Cordillera/Reykjanes Ridge magnetic profiles (Ostenso and Wold, 1970) shows that the anomaly wavelengths, and therefore spreading rates, are similar. Although this spreading rate is appreciably less than 2 cm/year, let us assume this value to be on the safe side. At 2 cm/year it would take about 85 million years to produce 1700 kilometers of seafloor. The geological evidence suggests that the most recent episode was perhaps half that, leaving about 850 kilometers to be produced in an earlier episode.

When was that episode? The geologic record indicates that spreading might possibly have occurred in the Permo-Carboniferous, and quite possibly in the Cambrian, with the evidence of the Cambrian episode outweighing the later event.

The magnetic data from the basin would tend to support a conclusion that the basin is quite old. Ostenso and Wold (1970) show, in a figure presenting the overall physiography of the magnetic field, based upon their extensive aeromagnetic data, that the magnetic field becomes very subdued for a distance of up to 800 kilometers out from the Alaskan continental margin. This subdued zone generally parallels the ridge axis shown in Figures 28 and 29, and was observed from T-3 during its 1964-66 drift over the Canada Plain. In this zone anomalies are less than 100 gammas. It is quite possible that this quiet zone represents an elevation of the Curie point isotherm resulting from the thick sediment cover, but this is considered unlikely in view of the large anomalies observed on the thickly blanketed Mendelejev and Wrangel Plains. Instead the subdued field may reflect long periods of constant polarity such as the Late Triassic-Jurassic normal interval (DeBoer, 1968), the fifty million year long reversed Kaiman interval in the Upper Pennsylvanian and Permian (Irving and Parry, 1963), or an even older period when the area was situated much closer to the magnetic equator.

The sedimentary cover in the Canada Basin could be consistent

with such a great age when it is considered that the marginal geosynclines and troughs surrounding this basin could have intercepted much of the sediment which otherwise would have entered the deep basin. This is presently happening in the Pacific.

#### A Final Note

It should be pointed out that the bordering geosynclines and marginal basins hold great promise as habitats of petroleum. The large sedimentary accumulations offer a potential source rock, while the observed thrusting, folding, diapirism, marine transgressions, and the possibility of landward continuation of oceanic fractures as wrench faults, present the possibility of structural and stratigraphic traps.

One final speculation is in order. According to the proposed development of the Amerasia Basin, the Eurasian continental margin was also a zone of ocean floor consumption, a suggestion reinforced by the asymmetrical position of the Alpha Cordillera. Possibly the Lomonosov Ridge is a northern analog to the Barrow Arch, and similarly a geosynclinal basin may lie beneath the Barents Shelf. Just such a configuration has been shown in a hypothetical model for the Barents Shelf transition zone by Demenitskaya et al. (1968). Seismic investigations across this shelf should confirm or deny this speculation.

## INTERPRETATION

## PART II: SEDIMENTARY FEATURES

Hyperbolic Echoes observed on the Precision Depth Recorder

The echo sounding records show the crestral regions of the Alpha Cordillera as a series of large overlapping hyperbolae (Figure 30). These hyperbolae are the result of a highly irregular seafloor. They are produced by strong specular echoes from the crests and troughs of the irregularities as the sounder moves overhead. The difference in depth between the higher crestral hyperbolae and the lower, often obscured ones from the troughs gives the approximate amplitude of the irregularities. This will be the amplitude referred to in relation to these hyperbolae, or hyperbolization as they will be collectively called.

The areal distribution of the hyperbolization, according to amplitude range, is shown in Figure 31. Within this area, the hyperbolization appears to be bounded on the north by the 2200 meter contour, and by the 2500 meter contour on the south. Between these boundaries it is observed everywhere on those parts of the crestral plateau traversed, with but two exceptions; the small spur running SSW from Ostenso Seamount, and on the SSW-NNE trending ridge on the northern margin around 85°N, 145°W. On the southern side of the cordillera hyperbolization is observed at depths in excess of 2700 meters. In the submarine sounding records obtained from nine crossings of the Alpha Cordillera, Beal (1968) noted similar hyperbolae occurring as minor relief superimposed upon extensive, rather level areas near the crest.

The hyperbolization appears to be best developed in areas with gentle slopes on the southern sides of local topographic highs, and on the southern edge of the crestral plateau. The largest hyperbola observed (Figure 30, at 16 kilometers) has an amplitude of 55 meters, and a width of about one kilometer, giving quite steep slopes of more than six degrees.

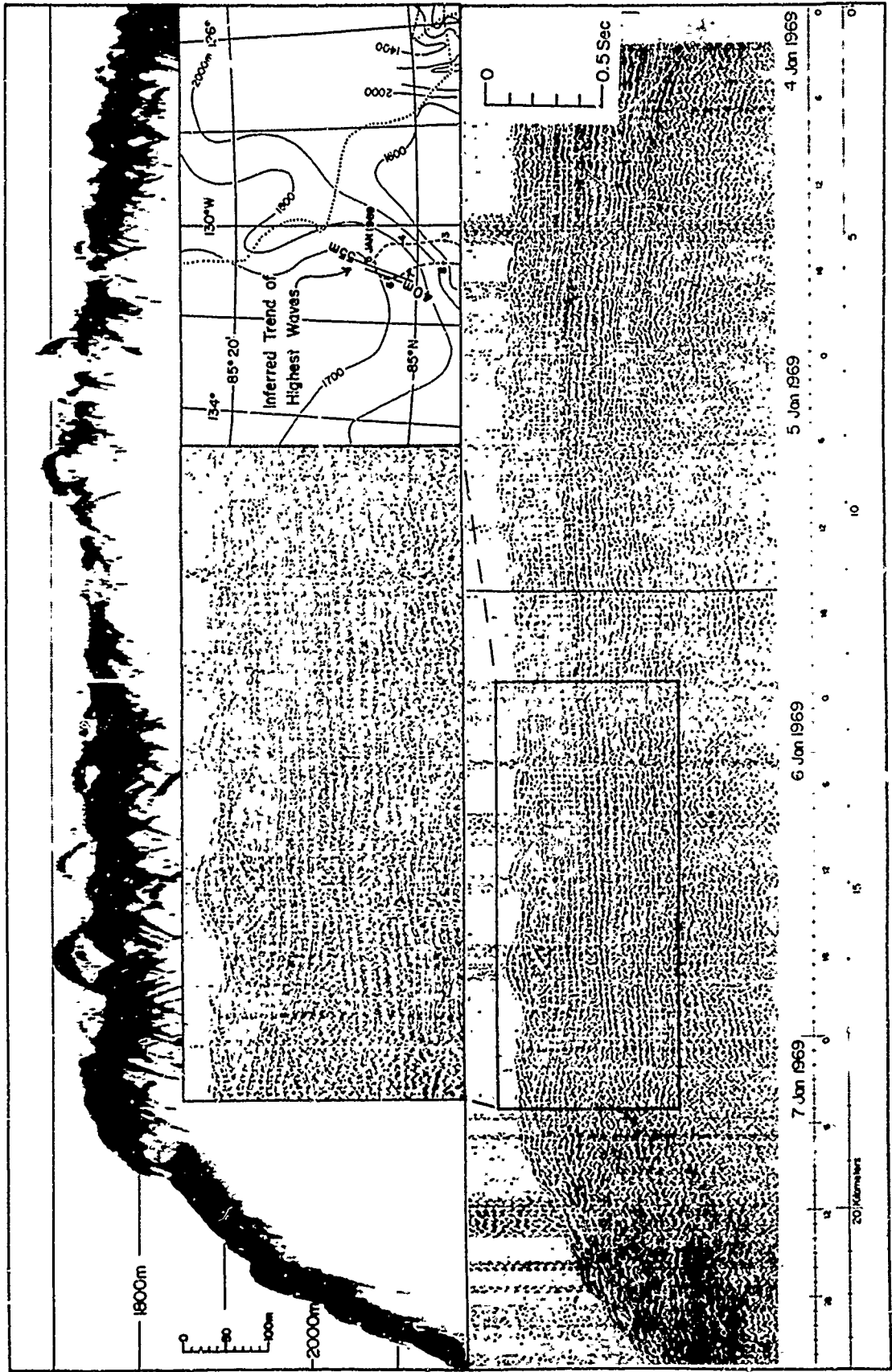


Figure 30

## Data bearing on the Origin of the Hyperbolization

### Seismic Reflection Measurements

The seismic reflection measurements (Figures 17, 18, and 30) show the hyperbolization to be confined to a layer about 100 meters thick. This layer is underlain by numerous relatively flat horizons extending down, in some cases, to more than a kilometer. From this observation, and the observation by Hunkins (1961) that the Alpha Cordillera is overlain by an average of 380 meters of low velocity (2.0 km/sec) material, it can be concluded that the hyperbolization is sedimentary in origin.

Is the hyperbolization a result of depositional or erosional processes? The reflection data suggest that it is predominantly depositional. Profile B-C-D-E in Figure 17, which has hyperbolization everywhere above 2200 meters, shows that deep horizons tend to come closer to the surface, and perhaps even outcrop, on the northern edge of the crestral highs, while the southern sides are covered with thick accumulations of confused hyperbolized deposits. Along the southern margin of the crestral plateau, these measurements indicate (Profile K-P, Figure 17) that a considerable shelf-like accumulation has occurred. These profiles suggest that sediment has been moved across the cordillera from north to south, with topographic highs experiencing little or negative deposition, and depressions and the southern edge of the crestral plateau acting as areas of accumulation.

The hyperbolization might be the result of linear sediment "ridges" such as those presently found in other oceans (Ewing and Ewing, 1964, and Johnson and Schneider, 1969). The largest hyperbolae were observed when the ice island crossed the southern flank of the cordillera, looped around a small part of the crestral plateau, and then passed out over the flank again (Figure 30). During this loop, two prominent hyperbolae, 40 meters and 55 meters in amplitude, were twice observed, suggesting that they result from linear features. If

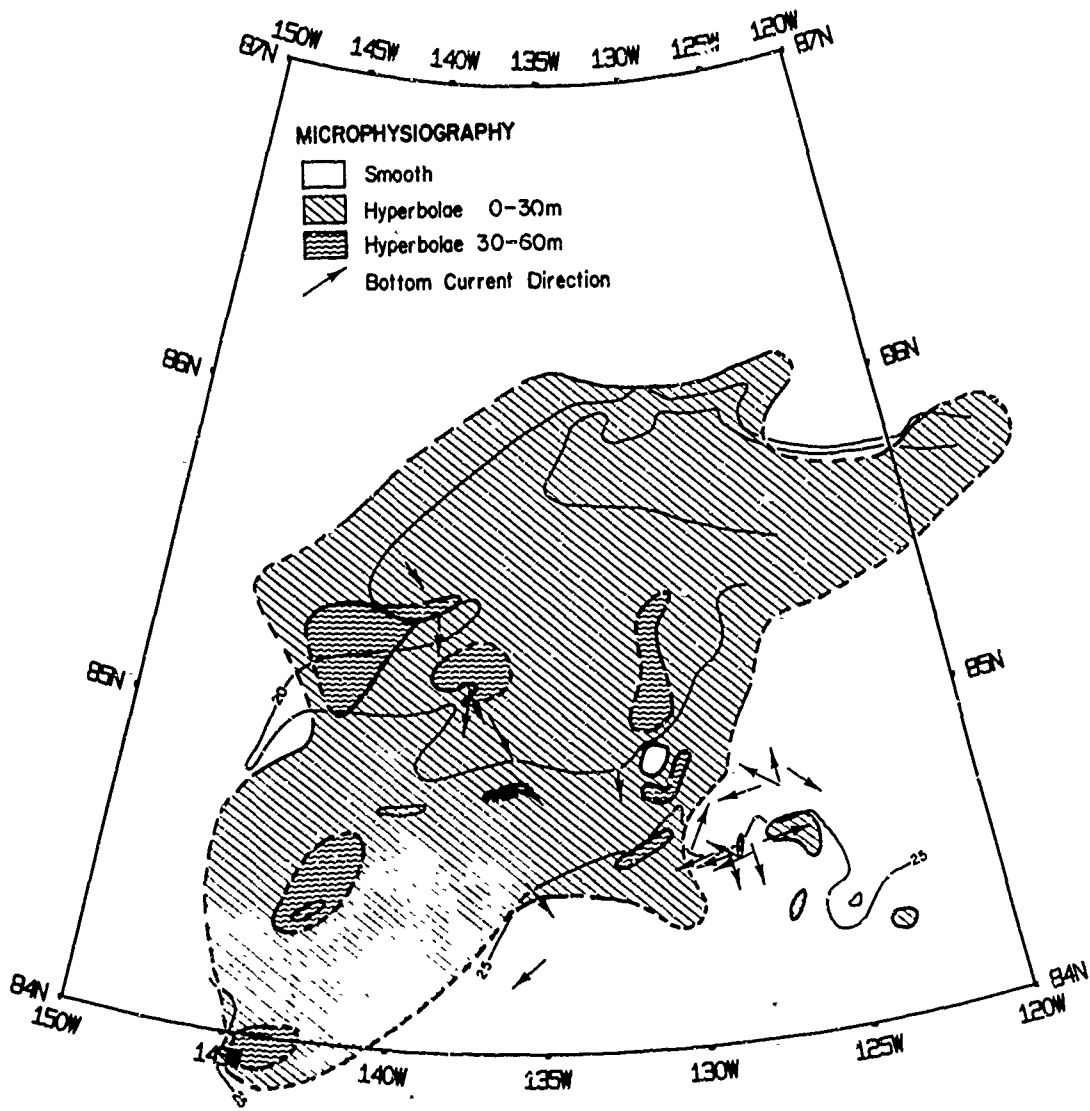


Figure 31

the points of crossing are connected, the crests of the "ridges" are found to strike slightly east of north, with the highest ridge nearest to the edge of the plateau. This strike agrees with the trend of the long axis of the elongate region of high amplitude hyperbolae shown in Figure 31.

A second indication of linearity was observed along the southern flank, around  $84^{\circ}40'N$  and  $137^{\circ}W$ , where the width of the hyperbolae increased considerably along part of a loop, suggesting that the ice island was briefly drifting parallel to a ridge. The inferred trend in this deeper location is again northeast. These indications are based upon scanty data, but in the absence of a more detailed survey they offer the suggestion that these features are ridges, formed at a large angle to the inferred direction of sediment drift.

#### Sediment Cores

Scientists on Station Alpha raised fourteen cores from the Alpha Cordillera to the west of Area III. These cores are described and discussed by Ericson et al. (1964), and by Hunkins and Kutschale (1967). The cores showed alternating dark and light brown lutites, easily correlated between cores, which are interpreted as evidence of continuous accumulation uninterrupted by slumping or intercalation of turbidity current layers. The top 10 cm consisted of dark brown foraminiferal lutite mixed with ice rafted sand and pebbles, overlying a light brown sand with ice rafted material but few foraminifera that extends to a depth of 40 cm. These layers are interpreted to be a result of normal pelagic sedimentation continuing to the present, but diluted by glacial marine accumulations. Another foraminifera-rich lutite is found below 40 cm. Carbon 14 dating on these cores showed the sediments between 7 and 10 cm to be around 30,000 years old.

Ku and Broecker (1967) used the uranium series method to date another core raised from T-3 in 1963 from the lower flank of the cordillera. Their measurements showed an age of 70,000 years at the first horizon, located at a depth of 15 cm in this particular core,

and indicated an age of 220,000 years at the lower lithological boundary at 45 cm. These and the other  $C^{14}$  measurements indicate that the rate of deposition has remained essentially constant at a very low rate of 2 mm/1000 years for at least 150,000 years.

While none of these cores is definitely known to have come from an area exhibiting hyperbolae, primarily because of the inability of the explosive sounding method used on Station Alpha to recognize this type of feature, there is good evidence that these cores do contain the types of sediment found in the area of hyperbolization. A tripod camera equipped with three trigger cores obtained short cores from an area with hyperbolae up to 30 meters high on October 28, 1968. These cores showed a sharp boundary between dark and light brown foraminiferal and sandy lutites like that in the Alpha cores. In addition, Beal (1968) reported hyperbolae south of the cordillera crest on a profile obtained by the submarine U.S.S. Sargo in 1960, and part of this profile traverses the Alpha drift area from which the cores were raised.

If the Alpha cores are representative, as the short cores suggest, then the relatively well correlated sediments and uniform sedimentation rates indicate that no non-uniform horizontal transport has been taking place, certainly for the last 150,000 years, and probably much longer.

#### Camera Stations

Eighty-two camera stations were occupied over the Alpha Cordillera during the present drift of T-3. Two types of camera were used. An impact-triggered Thorndike bottom camera, equipped with a separate photographic nephelometer (Thorndike and Ewing, 1967) for the measurement of light scattering intensity, was used at thirty-nine stations. Of these, twenty-two yielded useful scattering measurements. Forty-three stations were occupied with a tripod camera, an apparatus consisting of a deep-sea camera suspended from the apex of a rigid tripod which is placed on the ocean floor. The tripod permits closeup photographs and provides a rugged platform to which a compass and various other devices may be affixed. Photos were taken every 130

seconds, and a number of sites were usually occupied at each station.

The bottom photographs reveal a contrast between the seafloor on the deep plains and that on the high ridges and rises (Hunkins et al., 1960, 1970). The ridges and rises are found to be littered with small fragments of ice-rafted pebbles and seashells, and a few larger angular cobbles (Figure 34). Scour marks indicate the presence of bottom currents. Abundant animal life is found, with animal tracks and burrows, as well as brittle stars, medusae, amphipods, crinoids, sponges, and sometimes even fish being photographed. The plains, on the other hand, show a veritable mosaic of animal tracks, but relatively few animals, and practically no ice-rafted material.

Photographs obtained from the present drift of T-3 over the Alpha Cordillera do not reveal any appreciable differences between areas with hyperbolization and those without. Although large variations in debris concentration are observed, the variability over the course of a single lowering in a single province only points out the random nature of the accumulation of ice-rafted debris. The regions of maximum hyperbolization show no consistent increase in fine sediment relative to debris. These observations support the suggestion that the present area is quite similar to that from which the Alpha cores and photos were obtained. It would appear that while the irregularities are being perpetuated by the conformal pelagic and glacial marine sedimentation, the sedimentary processes which produced the bottom irregularities are presently inactive.

#### Bottom Current Measurements

Current measurements were made at twenty-two locations in Area III with the tripod camera, first using visual observations of a direction vane and later of a dissolving dye pellet. Directional measurements were referenced to true north by comparing the current directions with a compass in the field of view, and then correcting the compass for magnetic variation. No quantitative measurements were made, but the currents were sufficiently strong and persistent to give generally consistent results with the vane at different sites occupied at each

station, and consistent results with the dye pellets. Such currents are most likely of the order of 1 cm/sec. The nine stations traversing the cordillera showed currents (Figure 31) flowing south and southeast, indicating a weak general flow over the cordillera from northwest to southeast. Other current measurements were made on the southern flank just below the crestal plateau; current directions are scattered, perhaps indicating that these weak currents are controlled by the local topography, or are caused by tidal motions.

Hunkins et al. (1960) reported several quantitative measurements of bottom currents to the west of the present area, with speeds of 0.3 to 0.6 cm/sec obtained by tracking clouds of stirred up sediment seen in the bottom photographs. The new measurements from the cordillera probably have similar velocities.

The observed current directions are consistent with those which might be expected to produce the distribution of hyperbolae observed on the cordillera. However, the observed speeds are much too small, indicating that the drift process is presently inactive but raising the possibility that a similar circulation with considerably higher speeds was once at work.

#### Nepheloid Measurements

Hunkins et al. (1969) reported the results of all the light scattering observations made from T-3 between 1965 and early 1969. In all stations over the ridges and rises, a deep zone of light scattering, called the bottom nepheloid layer, was observed to occur below an intermediate scattering minimum. The degree of scattering increases with depth below this bottom nepheloid layer. This layer is absent over the Canada Plain, where the scattering was found to decrease slightly with depth from 2000 meters to the bottom. These observations, plus the spot measurements of relatively weak 4-6 cm/sec bottom currents at four stations on the Mendelejev Ridge and of less than 1 cm/sec at one station on the Canada Plain, led Hunkins et al. (1969) to conclude that the ridges and rises are being presently swept by bottom currents

which keep the fine material in suspension by turbulent flow, eradicating some of the animal tracks and keeping the glacial debris exposed. In contrast to the high areas, the plains receive sufficient turbidites to bury the randomly distributed ice rafted material, but infrequently so that the animal tracks produced by a smaller animal population are preserved.

The locations of the nephelometer and camera stations are shown in Figure 32. Two characteristics of the bottom nepheloid layer, determined from an analysis of the nephelometer records, are contoured in the figure. Considerable liberty has been taken in contouring the sparse data, but the contours appear valid where the control is good, and they are reasonable insofar as they relate to the other data available along the same track. The thickness shows a tendency to increase with water depth. The R value for the measurement, defined as the ratio of the densitometer deflection at the bottom of the layer to the deflection at the depth of maximum clarity, and therefore a measure of the strength of the turbidity, is contoured on a 10% difference interval. A comparison of the R value contours with the microphysiography (Figure 31) shows that the R value has an inverse correlation with the degree of hyperbolization. A good example is found below the crestal plateau at about  $85^{\circ}\text{N } 130^{\circ}\text{W}$  where the highest R value observed ( $R = 2.1$ ) is surrounded by lower values, and is associated with an isolated area with little or no hyperbolization.

The meaning of this correlation is uncertain. If it represents cause and effect, then this might suggest that very weak deposition is occurring where hyperbolae have previously been formed, and that small amounts of fine material are being swept up in turbulent flow, or at least held in suspension, where hyperbolae are scarce. While the cores do not indicate that hyperbolae are presently being formed, this interpretation would suggest that the present circulation could account for the distribution of hyperbolae if the currents were appreciably stronger. Alternatively, the correlation may be a result of other unknown factors.

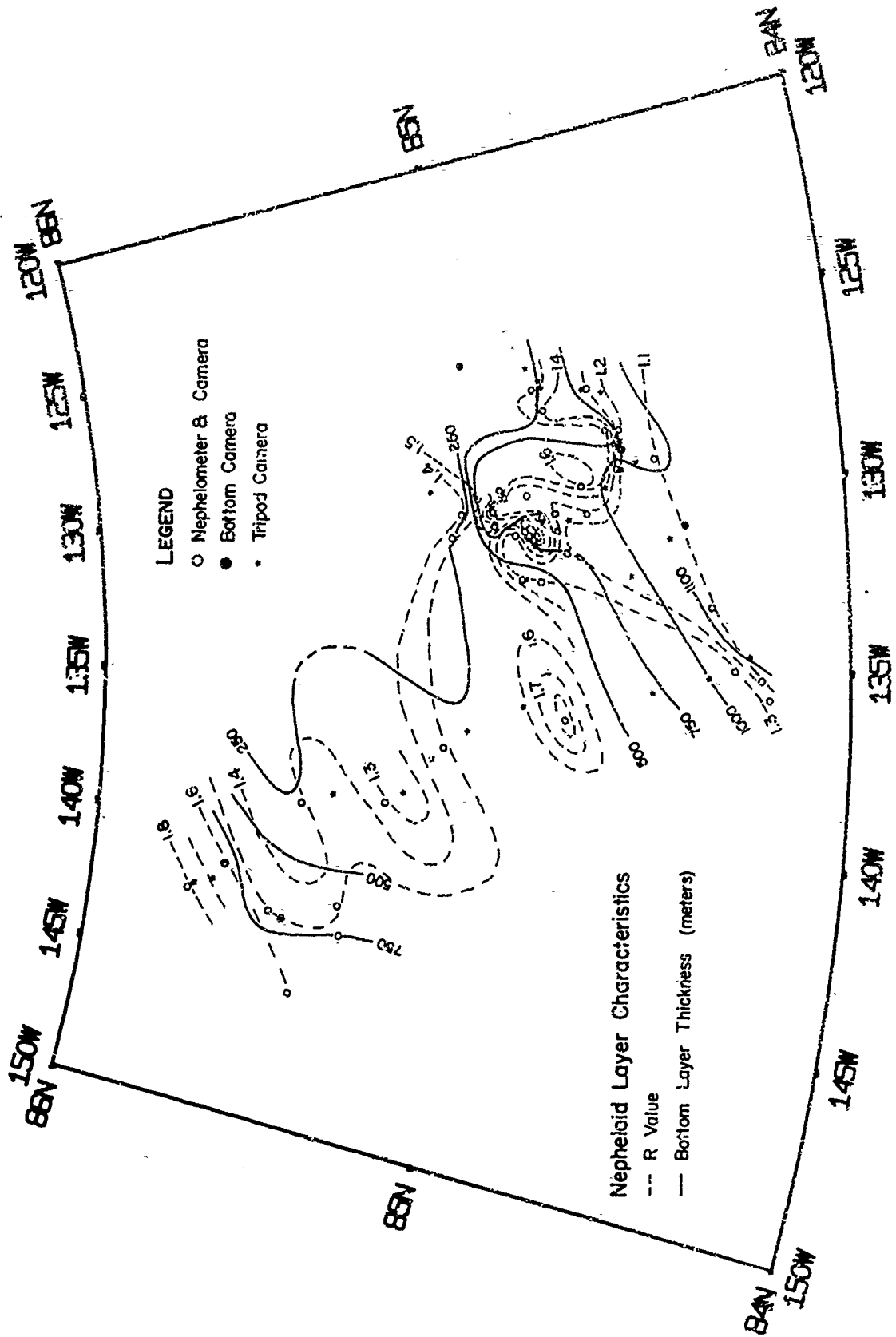


Figure 32

### Discussion

In summary, these data suggest that the hyperbolization reflects the presence of elongate sedimentary structures, formed by the bottom-current-related transport of fine sediment across the crest of the Alpha Cordillera from northwest to southeast. The weakness of the observed currents, the uniform sedimentary cover considered to blanket these features, the random distribution of ice rafted debris in the photographs, and the low strength of the turbidity of the bottom nepheloid layer indicate that this process is presently inactive. However, the present circulation inferred from the bottom currents and nepheloid layer observations appears to be capable of producing the observed hyperbolization if the currents are increased considerably.

It is tempting to speculate that such an increase in circulation without appreciable change in pattern would attend an ice-free ocean where greater coupling between the atmosphere and ocean was possible. If this is so, then we are presented with a method of dating this event, by coring the uppermost uniform blanket and dating the current deposited sediment beneath. Denton (1969) has suggested from glaciological investigations that North American glaciation has occurred intermittently, not since the beginning of the Pleistocene, but probably since the Upper Miocene, some 10 million years ago. Assuming a constant sedimentation rate of about 1 mm/1000 years which Steuerwald et al. (1968) have shown to hold for the past 4 million years in a magnetically dated 5.54 meter long core from the northern margin of the Chukchi Rise, we arrive at a possible blanket of 10 (or perhaps 20) meters of uniform sediment overlying the current-deposited material. This thickness represents the first dark band on the seismic profiler, and may explain why the profiler appears to show active hyperbolization extending right to the surface.

### The Mendelejev Plain and Buried Hyperbolization

Figure 33 is a drum recorder profile across the edge of the Mendelejev Plain. This profile is the same as Profile b-c-d-e in Figure 14. The record, obtained over a two week period, is displayed as a function of time, and therefore does not have a linear distance scale. Horizontal time lines are printed every second, so that the subbottom depth in seconds can reasonably be assumed to represent the depth in kilometers.

A particularly clear section through the plain is seen at about 115 km on the distance scale in Figure 33. This section is shown in more detail in Figure 34. Five layers are distinguished. The top layer is approximately 550 meters thick. The top of this layer is the present plain surface, and is recorded as three strong closely spaced horizons followed by numerous weaker horizons, indicative of turbidity deposits. Two moderately strong reflectors 150-160 meters below the bottom can be traced over the whole profile. This uppermost layer is observed everywhere on the Mendelejev Ridge, with the exception of the erosion zone along the ridge flank, to be discussed later.

The second layer, beginning at a depth of approximately 550 meters, is about 300 meters thick, regionally smooth, and is recorded as two sequences of hyperbolic reflections. The top of this layer is well defined as a number of closely spaced strong reflectors, and this horizon, and the layer it marks, will be called A (not to be confused with similarly named horizons in other oceans). The hyperbolic reflections, observed throughout the plain at this depth, are similar to the hyperbolization on the crestal plateau of the Alpha Cordillera, and probably result from a similar sedimentary process. If an average sedimentation rate of about 1 cm/1000 years is assumed for most of the overlying sediment, one might speculate that this hyperbolization is a result of a strong bottom circulation brought about by the opening of the Atlantic Ocean about 60 million years ago.

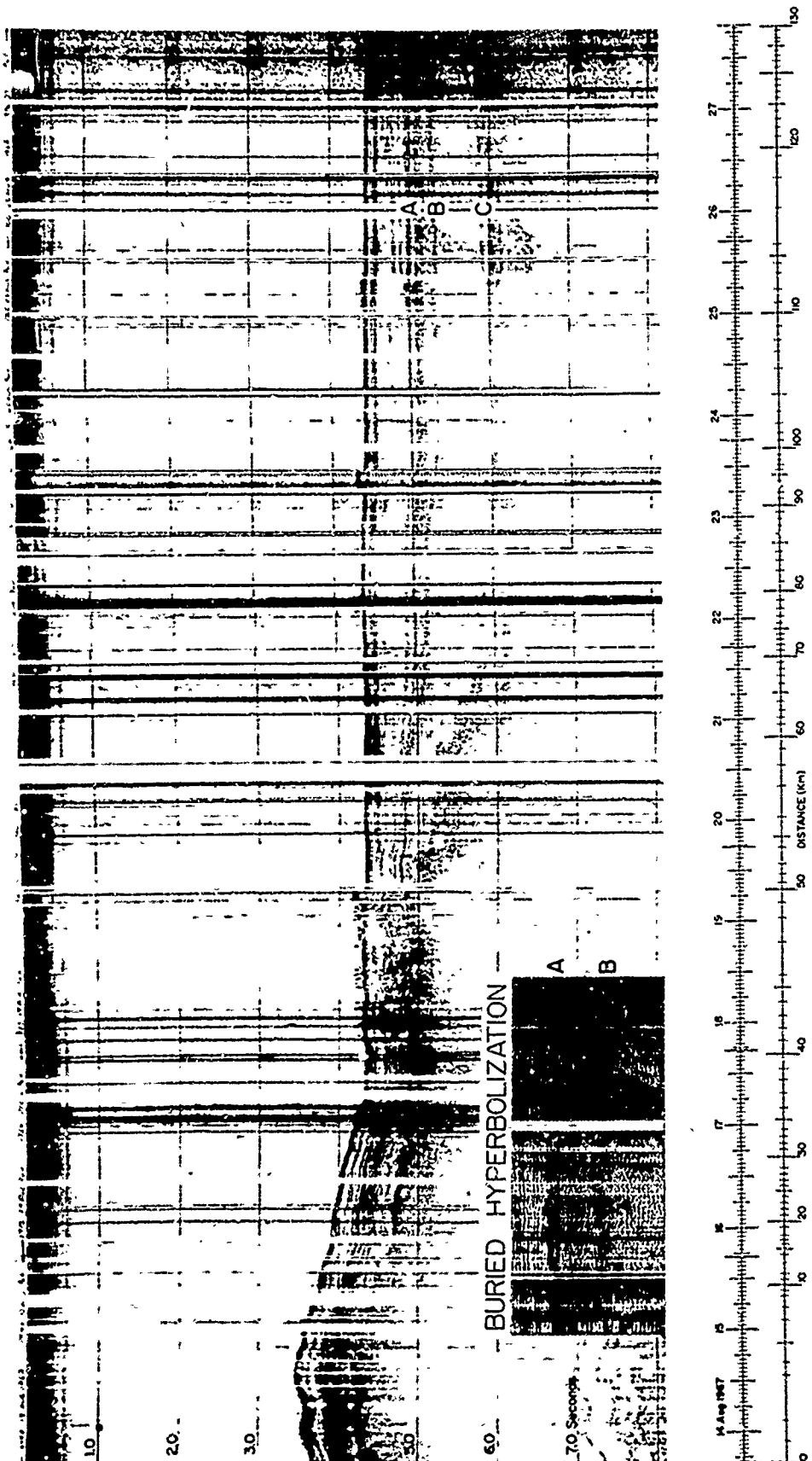


Figure 33

The third layer, 600 meters thick, extends from about 900 meters to a depth of about 1500 meters below the seafloor. The top of this layer is distinguished by two strong and continuous reflectors overlying a transparent layer. This horizon is regionally smooth, but regionally not as smooth as the A horizon above. This horizon, which will be called B, appears to merge with A on the ridge flank. Although the exact point of transition is obscured in this profile, it is apparent in several other profiles. The double reflecting horizon seen at about 400 meters depth on the ridge flank is probably A with B just below.

The fourth layer in this section appears to extend from a depth of around 1500 meters to approximately 2100 meters, where another strong sequence of reflectors is encountered. This layer, which we shall call C, is remarkably smooth and consists of a 600 meter thick sequence of weak reflecting horizons. This layer appears to drape the rising basement in Figure 33 at 50 km, forming the deepest layer observed on the ridge flank.

The fifth layer, below 2100 meters, contains few reflectors. No underlying sedimentary or basement interface is seen, possibly as a result of a large thickness of sediment below, absorption of the signal, or both.

On the ridge flank, the strongly reverberant and rough boundary observed beneath the sediments between 0 and 50 km looks like basement, but is probably layer C in close proximity to the basement. Evidence for this is seen in Figure 35.

Figure 34 compares seismic reflection profiles from the four plains within the Amerasia Basin where measurements have been made. Comparisons are made difficult by the different frequency ranges at which the reflections were recorded, and the different types of sound source used, but one conclusion can be drawn. The three plains bordering the Alpha Cordillera - the northern Canada Plain, the Mendeleev Plain, and the Wrangel Plain (data from Kutschale, 1966) - show similar stratigraphy in the form of a thick

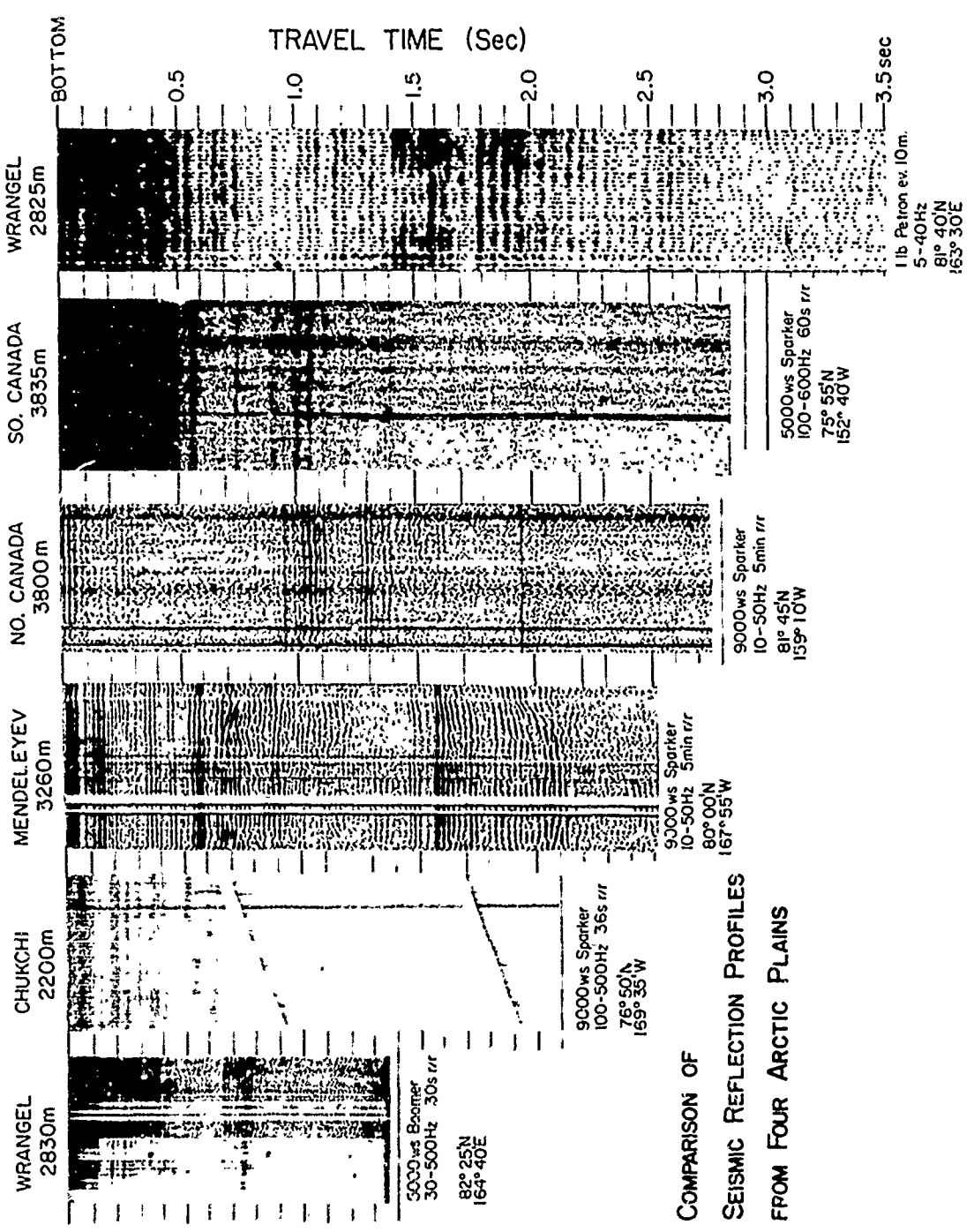


Figure 34

uppermost layer overlying a closely spaced A and B layer. The relative thicknesses of the three layers vary, probably as a function of sediment supply from bordering shelves, but stratigraphic similarities illustrate that both basins flanking the cordillera experienced a similar change in sedimentation. The opening of the Atlantic Ocean might have produced such a sequence of events.

#### The Mendeleev Fracture Zone

The linear nature of the Mendeleev Fracture Zone is shown in the three projected profiles in Figure 13. Figure 35 shows the original chart profiler record upon which Profile C-C' in Figure 13 is based. Three explanations for the development of the scarp appear possible: 1) that it is the result of transcurrent motion which brought topographically different areas into juxtaposition, 2) that it was produced by vertical movements, or 3) that it is a sedimentary feature which reflects an older buried basement ridge produced by 1) and/or 2) above.

An examination of Figures 13 and 35 supports the third explanation. Transcurrent motion during or following the deposition of some or all of the sediments seems unlikely in the absence of a vertical disturbed zone in any of the profiles in Figure 13. Vertical movements resulting directly in formation of the scarp are ruled out by the thickening of the sedimentary section across the scarp, and by the thinning of the layers in the trough where they abut the trace of the scarp. A stratigraphic interpretation which supports explanation 3) is given below.

On the high side by the scarp, approximately 700 meters of sediment are found overlying another strongly reflecting interface. Two horizons are observed at 300 and about 425 meters, with perhaps another weak one at 550 meters. The strong horizon at 700 meters consists of three closely spaced reflectors overlying an opaque layer. This interface is much too smooth to be basement, and from the projected profiles in Figure 13, would appear to correlate with horizon C on the plain. Away from the scarp there is a suggestion of stratification deep below this strong interface.



Figure 35

Within the trough adjacent to the scarp, a 900 meter thick sequence of sediments, stratigraphically similar to those on the high block, is found to overlie a strong interface similar to C east of the scarp. The 30% thickening of the section is considered to be a result of sediment ponding within the trough, and is evidence that a scarp existed throughout the period represented by this section. The uppermost layer shows little thickening, which might indicate predominantly pelagic sedimentation for this layer.

East of the scarp, the uppermost layer is highly conformal to the reflectors below, again suggestive of pelagic sedimentation. Against the face of the scarp these reflectors bow downward and show some distortion. This appears to be a result of post-depositional slumping. No accumulation of slumped material is seen however, suggesting that bottom currents have transported the sediment away from the scarp and distributed it over the trough. Bottom currents also appear to have been responsible for maintaining a scarp long after the inferred fractured basement ridge (Figure 13) was buried. At present the scarp face appears to be thinly blanketed by the same veneer of surficial sediments seen elsewhere in the area.

Within the trough, the interface interpreted as being the top of layer C is underlain by a minimum of 400 and possibly up to 1000 meters of sediment with acoustic characteristics similar to those of C on the plain (Figure 33). These sediments, like those overlying them, dip away from the scarp. This, plus the tendency to thicken away from the scarp, appears to be a result of either differential compaction, or deposition on a slope, or both, and is evidence that the fracture predates these sediments too.

#### Bottom Erosion Zone along the Mendeleev Ridge

A zone of bottom erosion parallels the Mendeleev Ridge. On the north, this zone is evident between 30 and 50 km in Profile A-A' of Figure 13 (also shown as section n-o-p of Profile j-s in Figure 14, where the uppermost 300 meters of sediment appear to overlie un-

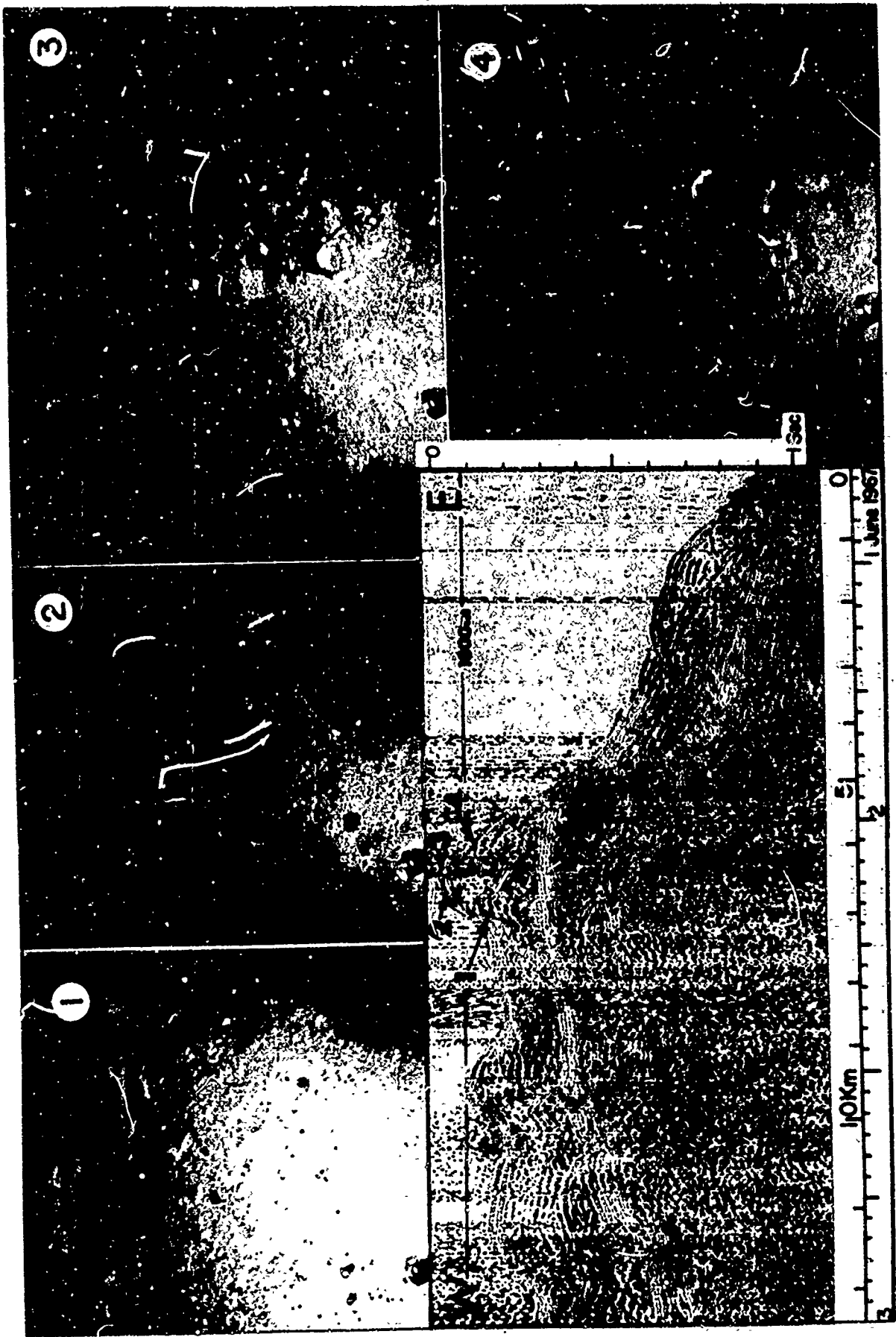


Figure 36

conformably layers A, B, and perhaps also C. However, A, B, and C appear to be mutually conformable and flat-lying, indicating that the erosion occurred at or near the end of the deposition of A, and perhaps contemporaneous to the development of the now-buried hyperbolization seen on the plain.

Two similar sedimentary features are developed on a ridge crest west and southwest of the area of unconformities. These are seen in sections l-m and n-o of Profile j-s in Figure 14. The original record of Profile n-o is shown in Figure 36. The present seafloor is a series of three topographic "megaripples" on a narrow eastward dipping shelf. In the profiles, the generally uniform top layer appears to thin, be deformed, and may disappear altogether. A series of bottom photographs taken over the summit of the highest peak in Profile l-m revealed several outcrops that Hunkins et al. (1970) suggested could be volcanic or perhaps carbonate rocks, and which the reflection profile, showing a thick sequence of strong reflectors beneath, indicates is probably consolidated sediment from layer A or B. The photographs from this lowering, the only outcrop photos known for the Canada Basin, are shown in Figure 36. In sequence, these photos show (1) ice-rafted angular cobbles and current scour marks, (2) sea lilies oriented with the current, some animal tracks, cobbles, and scour marks, (3) an encrusted outcrop, and (4) soft sediment with animal tracks and one ice-rafted cobble in an area that is probably not swept by currents.

The outcrop area, the rippled shelves, and the area with buried unconformities appear to result from erosion (and deposition) by bottom currents, which in places appears to continue to the present.

It is interesting to speculate on the source of such strong long-term currents. One possible explanation is the presence and close proximity of the Cooperation Gap, whose reported 2700 meter depth (Belov and Lapina, 1958) and presumed orientation (Figure 1) would allow bottom water in the northern Amerasia Basin and possibly the Eurasia Basin to pass through the Alpha Cordillera and be circulated

along the Mendeleev Ridge as a contour current. These currents would presumably be strongest near the gap, and confined to a narrow zone like that observed. Such currents could also be expected to exist for as long as there is a gap. A counterclockwise deep circulation like that observed and discussed by Hunkins et al. (1969) would be reinforced by deep water entering the basin in this manner.

#### Buried Channels through the Flank of the Mendeleev Fracture Zone

Figure 37 shows two crossings of a channel (No. 1) that appears to have once acted as a passage through the high side of the Mendeleev Fracture Zone, perhaps between the ridge and the plain. In both crossings the channel is seen impressed upon the sediment interfaces, to a depth of 700 meters in the upslope crossing, and to about 500 meters in the lower one. The channel appears to have first developed in layer C, have subsequently been filled with reverberent turbidites, rejuvenated at about the time that bottom currents were probably building up the sediment wedge observed in the high area between crossings (13 km), and then filled up with conformal (pelagic?) sediments that have preserved the outline associated with the time represented by the sediments at a depth of 270 meters. The downslope channel appears to have migrated north about one kilometer during its intermediate period of usage. The hyperbolization present in the plain sediments corresponding to this period suggests that the migration might somehow be related to bottom current scour and deposition. Enhanced hyperbolization appears adjacent to the downslope channels (23-35 km).

At the present time the gradient of the fossil channel (No. 1) is 1:32, corresponding to a reasonably steep slope of  $1.8^\circ$ . The sedimentary character of the smooth basal layer C is particularly evident from the presence of the channel, and under the sediment wedge, where horizontal stratification is observed 750 meters below C.

A second channel (No. 2) was traversed further to the north. The reflection record for this crossing is not as clear as for the others, but a development very similar to that of Channel 1 is indicated.

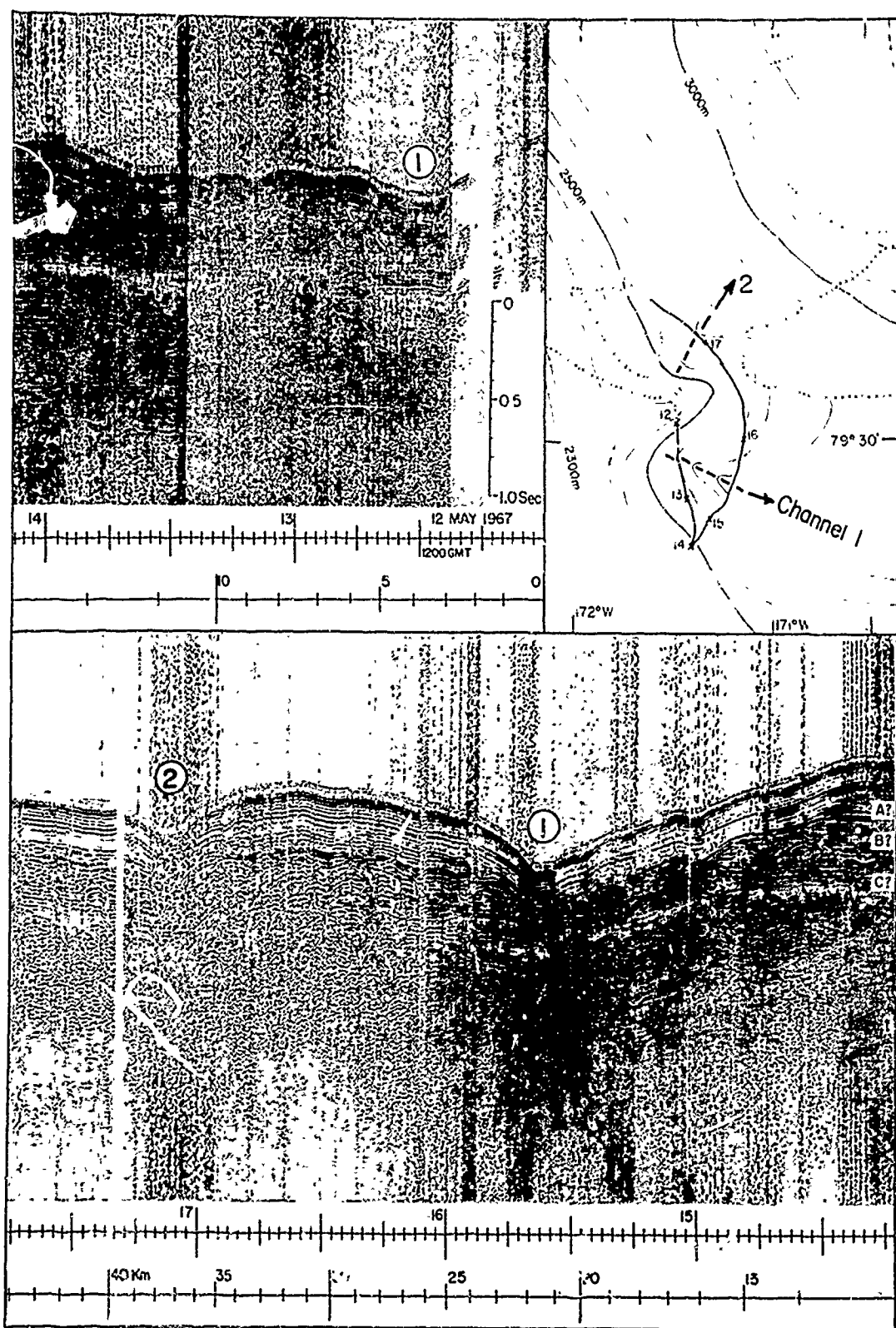


Figure 37

All three channel crossings show the channel floor to be higher on the right when the observer is looking downstream. This elevation becomes more pronounced with depth beneath the surface in the two downslope traverses. Several explanations might be possible. The dip at the surface might be a result of oblique crossings of the channels, always in a way so that they appear to dip north. However, this would not explain the increase in dip with depth, unless the deeper channels change direction in some consistent manner. Another possibility is that the thickness and velocity structure of the sediments covering the deep channels change horizontally so that a greater apparent dip is recorded. This appears unlikely however, as the northward migration of the channels has produced a uniform sediment thickness over the deepest channel which probably could not account for much of the additional tilt. A third possibility is that flow through the channel has produced a variable dip in the channel bottom. On the Wrangel Plain, Kutschale (1966) observed flat-bottomed channels with natural levees that were always higher on the right bank when facing downstream. These apparently result from channel overflow and accompanying sedimentation when pressure gradient and Coriolis forces cause tilting of the turbidity current - water interface during turbidity current discharges. Perhaps in the case of deeper canyons where levees cannot form it is possible to form a tilted channel floor. Another possibility, which is consistent with the observations but highly speculative, is that the tilts record the subsidence of the Alpha Cordillera and Mendelejev Ridge over the long time period following the cessation of spreading. In the absence of more data, no firm conclusions are possible.

## BIBLIOGRAPHY

- Baadsgaard, H., R. E. Folinsbee, and J. Lipson, Caledonian or Acadian granites of the northern Yukon Territory, in Geology of the Arctic, Vol. I, edited by G. O. Raasch, pp. 458-465, University of Toronto Press, Toronto, Ontario, 1961.
- Barazangi M., and J. Dorman, Seismicity map of the Arctic compiled from the ESSA, Coast and Geodetic Survey epicenter data, January, 1961 - September, 1969, Bull. Seismol. Soc. Amer., in press, 1970.
- Beal, M. A., Bathymetry and structure of the Arctic Ocean, Ph.D. thesis, Oregon State University, Corvallis, 204p., 1968.
- Belov, N.A., and N. N. Lapina, Bottom sediments in the central portion of the Arctic Ocean, Transactions of the Arctic Geology Institute, v. 85, Leningrad, 1958.
- Berthelson, Asger, On the chronology of the Precambrian of Western Greenland, in Geology of the Arctic, Vol. I, edited by G. O. Raasch, pp. 329-338, University of Toronto Press, Toronto, Ontario, 1961.
- Bird, J. M., and J. F. Dewey, Lithosphere plate-continental margin tectonics and the evolution of the Appalachian orogen, Bull. Geol. Soc. Amer., v. 81, 1031-1060, 1970.
- Black, D. J., and N. A. Ostenso, Gravity observations from Ice Island Arlis II, 6 October, 1961 to 8 April, 1962, University of Wisconsin Geophysical and Polar Research Center Research Report No. 62-8, 26p., 1962.
- Bullard, Sir Edward, J. E. Everett, and A. G. Smith, The fit of the continents around the Atlantic, Phil. Trans. Roy. Soc., A, 258, 41-51, 1965.
- Bushnell, Vivian, Scientific studies at Fletcher's Ice Island, T-3, (1952-1955), Geophys. Res. Pap. AFCRC-TR-59-232 (1) No. 63, 172, 1959.
- Cabaniss, G. H., Geophysical data from U. S. Arctic Drifting Stations, 1957-1960, Air Force Cambridge Res. Lab. U. S. A. F., Research Note AFCRL-62-683, 234p., 1962.
- Cabaniss, G. H., K. L. Hunkins, and N. Untersteiner, US-IGY Drifting Station Alpha Arctic Ocean, 1957-1958, Office of Aerospace Research, U. S. A. F., AFCRL-65-848, Special Reports No 38, 336p., 1965.
- Carey, S. W., The orocline concept in geotectonics, Proc. Roy. Soc. Tasmania, v. 89, 255-288, 1965.
- Carey, S. W., A tectonic approach to continental drift, in Continental Drift.- A Symposium, edited by S. W. Carey, pp. 177-355, Tasmania University, Hobart, Tasmania, 1958.

- Caulfield, D. D., Predicting sonic pulse shapes of underwater spark discharges, Deep-Sea Research, v. 9, 339-348, 1962.
- Christie, R. L., Geology, Alexandra Fiord, Ellesmere Island, District of Franklin, Geol. Surv. Canada Map 9-1962, 1962.
- Churkin, Michael Jr., Paleozoic tectonic history of the Arctic Basin north of Alaska, Science, 165(3893), 549-555, 1969.
- Crary, A. P., Bathymetric chart of the Arctic Ocean along the route of T-3, April 1952 to October 1953, Bull. Geol. Soc. Amer., v. 72, 1319-1330, 1954.
- Crary, A. P., and Norman Goldstein, Geophysical studies in the Arctic Ocean, Deep-Sea Research, v. 4, 185-201, 1957.
- DeBoer, Jelle, Paleomagnetic differentiation and correlation of the Late Triassic volcanic rocks in the Central Appalachians (with special reference to the Connecticut Valley), Bull. Geol. Soc. Amer., 79(5), 609-626, 1968.
- DeLeeuw, M. M., New Canadian bathymetric chart of the Western Arctic Ocean, north of 72°, Deep-Sea Research, 14(5), 489-504, 1967.
- Demenitskaya, R. M., A. M. Karasik, Yu. G. Kiselev, I. V. Litvinenko, and S. A. Ushakov, The transition zone between the Eurasian continent and the Arctic Ocean, Can. Jour. Earth Sci., 5, 1125-1129, 1968.
- Denton, G. H., and R. L. Armstrong, Miocene-Pliocene glaciations in southern Alaska, Amer. Jour. of Science, v. 267, 1121-1142, 1969.
- Dewey, John F., Evolution of the Appalachian/Caledonian orogen, Nature, v. 222, 124-129, 1969.
- Dewey, J. F., and J. M. Bird, Mountain belts and the new global tectonics, Jour. Geophys. Res., 75(14), 2625-2647, 1970.
- Dietz, R. S., and George Shumway, Arctic basin geomorphology, Bull. Geol. Soc. Amer., 72(9), 1319-1330, 1961.
- Drake, C. L., N. J. Campbell, G. Sander, and J. E. Nafe, A mid-Labrador Sea ridge, Nature, v. 200, 1085-1086, 1963.
- Eardley, A. J., Structural history of North America, Second edition, 743 p., Harper and Row, New York, 1962.
- Edgerton, H. E., and G. G. Hayward, The 'Boomer' sonar source for seismic profiling, Jour. Geophys. Res., 69(14), 3033-3042, 1964.
- Ericson, D. B., M. Ewing, and G. Wollin, Sediment cores from the arctic and subarctic seas, Science, 144(3623), 1183-1192, 1964.
- Ewing, M., and J. I. Ewing, Distribution of oceanic sediments, in Studies in Oceanography, edited by K. Yoshida, pp. 525-537, Univ. of Tokyo Press, Tokyo, 1964.

- Gabrielse, H., Tectonic evolution of the northern Canadian Cordillera, Can. Jour. Earth Sci., v. 4, 271-298, 1967.
- Guier, W. H., Satellite navigation using integrated Doppler data, the AN/SRN-9 equipment, Jour. Geophys. Res., 71(24), 5903-5910, 1966.
- Haines, G. V., A Taylor series expansion of the geomagnetic field in the Canadian Arctic, Publ. of the Dom. Obs., XXXV No. 2, 119-140, 1967.
- Hakkel; Ya. Ya., Signs of recent submarine volcanic activity in the Lomonosov Range, Priroda, v. 4, 87-90 (Defense Research Board Translation T296R by E. R. Hope, June 1958), 1958.
- Hall, J. K., Instructions for sparker cable construction, WHOI Tech. Memo. No. 13-64, 11 p., 1964.
- Haller, John, Account of the Caledonian Orogeny in Greenland, in Geology of the Arctic, Vol. I, edited by G. O. Raasch, pp. 170-187, University of Toronto Press, Toronto, Ontario, 1961.
- Haller, John, and J. L. Kulp, Absolute age determinations in East Greenland, 77p., Medd. om Gronland, v. 171, No. 1, 1962.
- Hamilton, Warren, The Uralides and the motion of the Russian and Siberian platforms, Bull. Geol. Soc. Amer., 81(9), 2553-2576, 1970.
- Harland, W. B., Discussion of the tectonic evolution of the Arctic-North Atlantic region, Phil. Trans. Roy. Soc. A, 258, 59-75, 1965.
- Hayes, D. E., A geophysical investigation of the Peru-Chile trench, Marine Geology, v. 4, 309-351, 1966.
- Heezen, B. C., M. Tharp, and M. Ewing, The floors of the oceans, I, The North Atlantic, 122 p., Geol. Soc. Amer. Spec. Paper 65, 1959.
- Holmes, Arthur, Principles of physical geology, Second edition, 1288 p., Ronald Press, New York, 1965.
- Hubbard, A. C., and B. Luskin, Sounding and magnetometer equipment for a drifting ice station, 8 p., Lamont Geol. Obs. Tech. Rept. 19, CU-52-59, NOBSR 64547, Geology, 1959.
- Hunkins, K. L., M. Ewing, B. C. Heezen, and R. J. Menzies, Biological and geological observations on the first photographs of the Arctic Ocean deep-sea floor, Limnology and Oceanography, 5(2), 154-161, 1960.
- Hunkins, K. L., Seismic studies of the Arctic Ocean floor, in Geology of the Arctic, Vol. I, edited by G. O. Raasch, pp. 645-665, University of Toronto Press, Toronto, Ontario, 1961.
- Hunkins, K. L., T. Herron, H. Kutschale, and G. Peter, Geophysical studies of the Chukchi Cap, Arctic Ocean, Jour. Geophys. Res., 67(1), 235-247, 1962.

- Hunkins, K. L., Submarine structure of the Arctic Ocean from earthquake surface waves. in Proc. of the Arctic Basin Symp., Oct. 1962, pp. 3-8, Arctic Institute of North America, Washington, D. C., 1963.
- Hunkins, K. L., The arctic continental shelf north of Alaska, in Continental Margins and Island Arcs, edited by W. H. Poole, pp. 197-205, Geol. Survey of Canada Paper 66-15, 1966.
- Hunkins, K. L., and H. W. Kutschale, Quaternary sedimentation in the Arctic Ocean, in Progress in Oceanography, Vol. 4, edited by Mary Sears, pp. 89-94, Pergamon Press, New York, 1967.
- Hunkins, K. L., Geomorphic provinces of the Arctic Ocean, in Arctic Drifting Stations, edited by J. E. Sater, pp. 365-376, Arctic Institute of North America, Montreal, Quebec, 1968.
- Hunkins, K. L., E. M. Thorndike, and Guy Mathieu, Nepheloid layers and bottom currents in the Arctic Ocean, Jour. Geophys. Res., 74(28), 6995-7008, 1969a.
- Hunkins, K. L., H. W. Kutschale, and J. K. Hall, Studies in marine geophysics and underwater sound from drifting ice stations, Lamont-Doherty Geological Observatory Final Report, Contract Nonr 266(82), 102 p., 1969b.
- Hunkins, K. L., Guy Mathieu, S. R. Teeter, and A. Gill, The floor of the Arctic Ocean in photographs, Arctic, in press, 1970.
- International Geophysical Year, The floor of the Arctic Ocean, National Academy of Sciences, IGY Bulletin, No. 22, 1-4, 1959.
- International Geophysical Year, Arctic Basin seismic studies from IGY drifting station Alpha, National Academy of Sciences, IGY Bulletin, No. 46, 1-5, 1961.
- Irving E., and L. G. Parry, The magnetism of some Permian rocks from New South Wales, Geophysical Journal, 7, 395-411, 1963.
- Jeletzky, J. A., Eastern slope, Richardson Mountains: Cretaceous and Tertiary structural history and regional significance, in Geology of the Arctic, Vol. I, edited by G. O. Raasch, pp. 532-583, University of Toronto Press, Toronto, Ontario, 1961.
- Johnson, G. L., and E. D. Schneider, Depositional ridges in the North Atlantic, Earth Planet. Sci. Lett., 6, 416-422, 1969.
- Karas'k, A. M., Magnetic anomalies of the Hakkel' Ridge and origin of the Eurasian subbasin of the Arctic Ocean. Geophysical Methods of Prospecting in the Arctic, No. 5, 8-19, Leningrad, 1968.
- Kez., M. J., D. L. Barrett, G. N. Ewing, B. D. Loncarevic, and K. S. Manchester, The continental margin of eastern Canada: Nova Scotia to Nares Straits.

- Kent, P. E., and W. A. C. Russell, Evaporite piercement structures in the northern Richardson Mountains, in Geology of the Arctic, Vol. I, edited by G. O. Raasch, pp. 584-595. University of Toronto Press, Toronto, Ontario, 1961.
- Kerr, J. Wm., Nares submarine rift valley and the relative rotation of Greenland, Bull. Can. Petrol. Geol. 15(4), 483-520, 1967.
- King, E. R., I Zeitz, and L. R. Alldredge, Genesis of the Arctic Ocean Basin, Science, 144, 1551-1557, 1964.
- King, E. R., I Zeitz, and L. R. Alldredge, Magnetic data on the structure of the central Arctic region, Bull. Geol. Soc. Amer., 77(6), 619-646, 1966.
- Koch, Lauge, Precambrian and Early Paleozoic structural elements and sedimentation: north and east Greenland, in Geology of the Arctic, Vol. I, edited by G. O. Raasch, pp. 148-154, University of Toronto Press, Toronto, Ontario, 1961.
- Ku, T. L., and W. S. Broecker, Rates of sedimentation in the Arctic Ocean, in Progress in Oceanography, Vol. 4, edited by M. Sears, pp. 95-104, Pergamon Press, New York, 1967.
- Kutschale, H. W., Arctic Ocean geophysical studies: The southern half of the Siberia Basin, Geophysics, 31(4), 683-710, 1966.
- Lachenbruch, A. H., and B. Vaughn Marshall, Heat flow through the Arctic Ocean floor: The Canada Basin - Alpha Rise boundary, Jour. Geophys. Res. 71(4), 1223-1248, 1966.
- Le Pichon, X., R. D. Hyndman, and Guy Pautot, A geophysical study of the opening of the Labrador Sea, Jour. Geophys. Res., in preparation, 1970.
- Matthews, D. J., Tables of the velocity of sound in pure and sea water, Brit. Admir. Hydrogr. Dept. Rept. 282, 1939.
- Milne, A. R., A seismic refraction measurement in the Beaufort Sea, Bull. Seismol. Soc. Amer. 56(3), 775-779, 1966.
- Nafe, J. E., and C. L. Drake, Physical properties of marine sediments, in The Sea, Vol. 3, edited by M. N. Hill, pp. 794-815. Interscience, London, 1963.
- National Geographic Society, The World Map, National Geographic Society, Washington, D. C., 1966.
- Nautical Almanac Offices of the United Kingdom and the United States of America, Explanatory Supplement to the Astronomical Ephemeris and the American Ephemeris and Nautical Almanac, H. M. Stationary Office, London, 505 p., 1961.
- Oliver, J., M. Ewing, and F. Press, Crustal structure of the arctic regions from the Lg phase, Bull. Geol. Soc. Amer., v.66, 1063-1074, 1955.

- Ostenson, N. A., Geophysical investigations of the Arctic Ocean basin, Univ. of Wisc. Geophys. Polar Res. Center Res. Rept. 62-4, 124 p., 1962.
- Ostenson, N. A., Geomagnetism and gravity of the Arctic Basin, in Proc. of the Arctic Basin Symp., Oct. 1962, pp. 9-40, Arctic Institute of North America, Washington, D. C., 1963.
- Ostenson, N. A. and R. J. Wold, Aeromagnetic survey of the Arctic Ocean: Techniques and interpretations, Jour. of Marine Geophys. Res., in press, 1970.
- Packard, M, and R. Varian, Proton gyromagnetic ratio, Phys. Rev., 93, p. 941, 1954.
- Pitman, W. C., and M. Talwani, in preparation, 1970.
- Rassokho, A. I., L. I. Senchura, R. M. Demenitskaya, A. M. Karasik, Yu. G. Kiselev, and N. K. Tomoshenko, The Mid-Arctic Range as a unit of the Arctic Ocean mountain system, Doklady. Akad. Nauk SSSR, 172(3), 659-662, 1967.
- Smith, D. D., Development of surface morphology on Fletcher's Ice Island, T-3, Air Force Cambridge Res. Center, Scientific Rept. No. 4, Contract AF19(604)-2159, 70 p., 1960.
- Smithsonian Astrophysical Observatory Star Catalog, Positions and proper motions of 258,997 stars for the epoch and equinox 1950.0, in four parts, Smithsonian Institution, Washington, D. C., 1966.
- Somov, M. M., Observational data of the scientific-research drifting station of 1950-1951, v. I-III, Morskoi Transport 1954-1955, (Translated by the Amer. Met. Soc., ASTIA Doc. 117-133), 1955.
- Steuerwald, B. A., D. L. Clark, and J. A. Andrew, Magnetic stratigraphy and faunal patterns in Arctic Ocean sediments, Earth Planet. Sci. Lett., v. 5, 79-85, 1968.
- Sykes, L. R., The seismicity of the Arctic, Bull. Seismol. Soc. Amer., 55(2), 501-518, 1965.
- Tailleur, I., Speculations on North Slope geology, Part I, The Oil and Gas Journal, September 22, 1969, 215-226, 1969a.
- Tailleur, I., Rifting speculation on the geology of Alaska's North Slope, Part II, The Oil and Gas Journal, September 29, 1969, 128-130, 1969b.
- Talwani, M., J. L. Worzel, and Mark Landisman, Rapid gravity computations for two-dimensional bodies with application to the Mendocino submarine fracture zone. Jour. Geophys. Res., 64(1), 49-59, 1959.
- Talwani, M., X. Le Pichon, and M. Ewing, Crustal structure of the mid-ocean ridges, 2. Computed model from gravity and seismic refraction data, Jour. Geophys. Res., 70(2), 341-352, 1965.

- Talwani, M., J. Dorman, J. L. Worzel, and G. M. Bryan, Navigation at sea by satellite, Jour. Geophys. Res., 71(24), 5891-5902, 1966.
- Thorndike, E., and M. Ewing, Photographic nephelometers for the deep-sea, in Deep-Sea Photography, edited by J. B. Hersey, pp. 113-116, Johns Hopkins Press, Baltimore, 1967.
- Thorsteinsson, R., Lower Paleozoic stratigraphy of the Canadian Arctic Archipelago, in Geology of the Arctic, Vol. I, edited by G. O. Raasch, p. 380, University of Toronto Press, Toronto 1961.
- Thorsteinsson, R., and E. T. Tozer, Structural history of the Canadian Arctic Archipelago since Precambrian time, in Geology of the Arctic, Vol. I, edited by G. O. Raasch, pp. 339-360, University of Toronto Press, Toronto, Ontario, 1961.
- Threshnikov, A. F., L. L. Balakshin, N. A. Belov, R. M. Dementitskaya, V. D. Dibner, A. M. Karasik, A. O. Shpeiker, and N. D. Shurgayeva, A geographic nomenclature for the chief topographic features, the bottom of the Arctic Basin, Problems of the Arctic and Antarctic, p. 27, 1967.
- Vine, F. J., and D. H. Matthews, Magnetic anomalies over ocean ridges, Nature, 199(4897), 947-949, 1963.
- Vogt, P. R., and N. A. Ostenso, Magnetic and gravity profiles across the Alpha Cordillera and their relation to Arctic seafloor-spreading. Jour. Geophys. Res., 75(26), 4925-4937, 1970.
- Walker, J. C. G., Geomagnetic observations on Fletcher's Ice Island, T-3, Arctic Ocean, Lamont Geol. Obs. Sci. Rept. No. 5 Contract AF19(604) 7442, 6 p., 1962.
- Wenk, Eduard, Tertiary of Greenland, in Geology of the Arctic, Vol. I, edited by G. O. Raasch, pp. 278-284, University of Toronto Press, Toronto, Ontario, 1961.
- Wilson, J. Tuzo, Continental Drift, Scientific American, 208(4), 86-100, 1963.
- Wilson, J. Tuzo, Did the Atlantic close and then reopen? Nature, v. 211, 676-681, 1966.
- Woolard, E. W., Theory of the rotation of the earth about its center of mass, Astronomical Papers prep. for the use of the Amer. Ephem. and Naut. Almanac, v. XV, Part I, 1953.
- Woollett, R. S., Theory of the piezoelectric flexural disk transducer with applications to underwater sound, U. S. Navy Underwater Sound Laboratory Res. Rept. No. 490, 1960.
- Worzel, J. L., and G. Lynn Searbet, Gravity interpretations from standard oceanic and continental crustal sections. Geol. Soc. Amer. Spec. Pap. 62, 87-100, 1955.

## APPENDIX

Five of the data reduction programs used in this investigation were considered to be of sufficiently broad interest to be presented here. The programs are written in Fortran for an IBM 1130 digital computer with 16K word core storage, card reader/punch, and a disk storage system. With small changes the programs should be compatible with other computers. Program listings, without control cards, are given below. Examples of data input and output are included.

Celestial Navigation Programs: EDOC, LUNE, and CELPS

Over 2400 celestial fixes were used in the preparation of the T-3 drift track from 1962 through 1970. Each fix, consisting of three or more lines of position, required checking, and often recomputation. Because the observational methods afforded more precision than that available by reduction using the Nautical Almanac, and in order to achieve some measure of uniformity in the work of numerous navigators, the fixes were recalculated by computer.

Three steps are entailed in determining a fix. The first involves reducing the observations, the second requires the calculation of the celestial coordinates of the bodies observed, and the third consists of finding that geographic position which satisfies the observations. The programs are written so that the first and third steps are lumped together, and the second step is performed first.

Celestial coordinates are computed by two programs, one for the sun and stars, the second for the moon. The planets are not programmed as their motions are considerably more complex than the other bodies. However a provision was made so that planet data could be used with somewhat diminished accuracy. Program EDOC (Ephemeris Data on Cards) computes the solar or stellar Greenwich Hour Angle, declination, horizontal parallax, and semi-diameter, while LUNE (lunar Ephemeris) does the same for the moon. The coordinates for the sun in the hour angle system are determined by trigonometrically transforming the solar ecliptic latitude and

longitude, computed from the Newcomb theory. Brown's theory is used in a similar fashion for the moon. In these theories, the latitude, longitude, and radius vector are described by generating functions with numerous additional terms stemming from the perturbations of the planets. The formulae employed are given by Woolard (1953). In practice the maximum errors in the computed coordinates should be less than 3" of arc (0.05 nautical miles). Star coordinates are determined by updating the right ascension system coordinates of navigational stars at epoch 1950.0, as determined from the Smithsonian Astrophysical Observatory Star Catalog (1966). The method of updating is given in the Explanatory Supplement to the American Ephemeris and Nautical Almanac of the Almanac Office (1961).

A punch card is prepared for each observation, giving Greenwich date and time of observation, a code number for the body observed, the altitude and relative azimuth of the body, the air temperature and barometric pressure, the approximate position, and the body name. The observation cards, each followed by a blank card, are fed into the computer, the proper coordinates are computed by EDOC or LUNE, and the results are punched on the blank. The observation cards with their coordinate data are then grouped into fixes (up to six observations per fix), terminated by another blank, and processed by a third program called CELPS (Celestial Positions).

Program CELPS computes the following:

- a) The correction for atmospheric refraction to be applied to the observed altitude, determined from the Pulkova formulation,
- b) The latitude and longitude of the intersection of every two lines of position,
- c) The latitude and longitude of the center of the circle inscribed into each triangle determined by three lines of position, along with the radius of that circle in nautical miles,
- d) The perpendicular distance from each line of position to the center of the smallest inscribed circle, in nautical miles,

e) The latitude and longitude determined by a least squares solution of all lines of position,

f) The azimuth of the zero-line of the theodolite horizontal circle referenced to true north, for each line, calculated from the center position of the smallest inscribed circle, and

g) The average time of all intersections and triangles determined from the original times of the observations comprising them, and the duration of the fix in hours.

The results are printed out (Figure 38), and the position associated with the smallest circle of error - assumed to be the best position - is punched onto the final blank card as data to be used in subsequent programs. Data from planets, or any other body for that matter, can be used by obtaining the hour angle and declination from the Nautical Almanac or American Ephemeris and entering these numbers on a blank card following that particular observation card. This method can also be used for visible earth satellites if their coordinates are known. If only one observation is available the assumed position is used to compute the theodolite zero-line azimuth.

Several merits and limitations of the CELPS program should be noted. Two generating functions for the water vapor pressure as a function of temperature are used in the refraction formulae, permitting corrections over a very broad range of temperatures (-75° to +40°C). The program is written for the northern hemisphere; slight alterations might be required for observations south of the equator. Finally, the instrumental height above sealevel  $H$ , is set at 5 meters, but should be changed if observation altitudes are appreciably different.

Six subroutines are used by these programs. Given the sine and cosine of an angle, QUAD gives the angle in the range 0 to  $2\pi$ . List element UPR is the units per radian, equal to 57.2957795131 if the result ANGLE is desired in degrees. JULDT converts the civil calendar date and Greenwich Mean Time to various forms of Julian time. TJ is days after 0000Z January 0, 1900, a convenient form for handling

data collected over a broad time span, TJA is referenced to the beginning of the Julian calendar, and TJC is the fraction of the current Julian century, used in the astronomical generating functions. Subroutine TIME converts any of the aforementioned times back to civil date and Greenwich Mean Time. INLOP determines the intersection of the lines of position and the center and radius of the inscribed circles, while XYC and PFKY are discussed in the next section.

Together these programs offer a convenient way to obtain position and azimuth information without the necessity of mastering celestial navigation, at least beyond the point of obtaining correct sights on identifiable bodies.

#### Wind Drift Program: WDP

An ice island, unattached buoy, or any other drifting body moves in response to the winds and currents, which are themselves often wind produced. If position fixes are obtained infrequently, then frequent wind observations can help define the track of the body in the intervening periods. Such techniques have proved of great value in determining the drift of manned ice stations, and should prove useful in the future for the unmanned drifting scientific stations to be located and interrogated by earth satellite.

Nansen observed from the drift of the FRAM that the ice drift was approximately  $1/50$  the wind speed in a direction  $28-30^\circ$  to the right of the wind (in the northern hemisphere). A computer program is presented that is based upon a similar assumption, except that the deviation angle and speed factor is calculated, and used with the observed winds to compute intermediate positions.

Program WDP (Wind Derived Positions) reads in a maximum of 2000 positions, followed by up to 5000 wind observations. Proceeding from fix to fix, it uses average winds between wind observations over the interval between fixes to compute not only the deviation angle and speed factor required, but also the ocean currents

required if the ice responds to the wind according to Nansen's average values of  $30^\circ$  and 0.02. Printing these results, the program then calculates, for the time of each wind observation, the positions resulting from both the purely wind derived drift solution, and the wind plus current solution. A card is punched at each calculation point giving the time and most probable position in a standard format compatible with the other reduction programs. The wind and current solution is used in place of the purely wind derived solution whenever the calculated wind speed factor exceeds 0.035 or falls below 0.0075, which is an indication that currents or the effects of winds acting at a distance are acting during periods of calm, or that the ice is restrained and cannot respond.

In addition to the most probable position, the program punches out the wind drift and current parameters and interval duration on the fix card ending each interval, making this information available for plotting theoretical currents etc. . Three new subroutines are called by this program. AWDP is an auxiliary subroutine of no special interest. XYC computes the cartesian coordinates of any point with latitude SLA and longitude SLO on a north polar stereographic projection, such that the ordinate is zero along the meridian  $(UMAX + UMIN)/2$ . The coordinates are expressed in nautical miles, and angles in radians. PFXY converts these coordinates back to degrees and minutes of latitude and longitude.

In all programs negative latitudes and longitudes represent the southern and western hemispheres, respectively.

#### Gravity Tie Program: GRVT

Program GRVT (Gravity Tie) was written to perform the rather laborious task of correcting gravity ties for earth tides, and to compute gravity meter base values and drift corrections. This program is tailored to the Lacoste and Romberg geodetic (Model G) meter, a widely used instrument, but can be altered to work for other gravity meters.

The following data are entered into the computer: an identification card listing the tie site, the latitude, longitude, height above sealevel, and the gravity value at the site, the date and individual readings and observation times in GMT. The program uses abbreviated lunar and solar ephemeris generators to calculate the altitude and distance to the moon and sun for each observation, in order to compute the magnitude of the earth-tide effect. The corrected readings are averaged, and the screw calibration (entered into the program via a DATA statement) used to calculate the gravity corresponding to a zero reading. This gravity is called the base value for the meter.

After a tie, gravity may be measured by adding the observed meter reading, converted to milligals by the screw curve, to the base value. Any drift between ties will be reflected in changes in the computed base value. If several ties are entered, the program computes the drift rate in milligals per hour and per day, and lists all the tie dates, base values, interval durations, and meter drift rates.













GRV DATA ENTRY - SAMPLE DATA DECK AND PUNCHED ANSWERS

BARROW 71-19.6N -156-40.6W 2.00 MMSL 982699.60 MGALS  
 LACOSTE AND ROMBERG G-27 GRAVITY METER CALIBRATION TIE WITH MARL BARRON  
 03 04 1967 0235 6030.689  
 0615 6030.651  
 1232 6030.757  
 1645 6030.760

BARROW 71-19.6N -156-40.6W 2.00 MMSL 982699.60 MGALS  
 LACOSTE AND ROMBERG G-27 GRAVITY METER CALIBRATION TIE WITH MARL BARRON  
 30 04 1967 1045 6030.985  
 1820 6030.92  
 1920 6030.92

BARROW 71-19.6N -156-40.6W 2.00 MMSL 982699.60 MGALS  
 LACOSTE AND ROMBERG G-27 GRAVITY METER CALIBRATION TIE WITH MARL BARRON  
 18 05 1967 0710 6031.115  
 2406 6031.115  
 2222 6031.110

BARROW 71-19.6N -156-40.6W 2.00 MMSL 982699.60 MGALS  
 LACOSTE AND ROMBERG G-27 GRAVITY METER CALIBRATION TIE WITH MARL BARRON  
 11 09 1967 0300 6031.225  
 0815 6031.31  
 1720 6031.23

2430584.899 026350.693 -0.0081990  
 2430582.194 026350.469 -0.0091915  
 2430580.142 026350.701 -0.0018037  
 2430575.855 026350.115

PRINTER OUTPUT

3 4 1967 JULIAN DAY 24564  
 TIME COUNT CORR COUNT TIDE(MG)  
 236 6030.689  
 615 6030.651 -0.027  
 1232 6030.757 -0.059  
 1645 6030.760 -0.087

RESULTS OF TIE  
 AVERAGE TIME GMT DAY NO AV COUNT 0000 COUNTS - BASE VALUE  
 3 4 1967 032 24564.397 6030.672 076350.693 MGALS

LACOSTE AND ROMBERG G-27 GRAVITY METER CALIBRATION TIE WITH MARL BARRON  
 LAT 71-19.6 LONG -156-40.6 2.00 METERS ABOVE MSL 982699.600 MGALS

30 4 1967 JULIAN DAY 24591  
 TIME COUNT CORR COUNT TIDE(MG)  
 1045 6030.985  
 1820 6030.92 -0.066  
 1920 6030.950 -0.076

RESULTS OF TIE  
 AVERAGE TIME GMT DAY NO AV COUNT 0000 COUNTS - BASE VALUE  
 30 4 1967 1608 24591.872 6030.884 976350.469 MGALS

LACOSTE AND ROMBERG G-27 GRAVITY METER CALIBRATION TIE WITH MARL BARRON  
 LAT 71-19.6 LONG -156-40.6 2.00 METERS ABOVE MSL 982699.600 MGALS

18 5 1967 JULIAN DAY 24609  
 TIME COUNT CORR COUNT TIDE(MG)  
 710 6031.100 -0.056  
 1806 6031.130 -0.072  
 2222 6031.100 -0.066

RESULTS OF TIE  
 AVERAGE TIME GMT DAY NO AV COUNT 0000 COUNTS - BASE VALUE  
 18 5 1967 1553 24609.661 6031.044 976356.301 MGALS

LACOSTE AND ROMBERG G-27 GRAVITY METER CALIBRATION TIE WITH MARL BARRON  
 LAT 71-19.6 LONG -156-40.6 2.00 METERS ABOVE MSL 982699.600 MGALS

11 9 1967 JULIAN DAY 24725  
 TIME COUNT CORR COUNT TIDE(MG)  
 0 6031.250 -0.060  
 815 6031.310 -0.077  
 1720 6031.230 0.010

RESULTS OF TIE  
 AVERAGE TIME GMT DAY NO AV COUNT 0000 COUNTS - BASE VALUE  
 11 9 1967 832 24725.355 6031.220 976350.115 MGALS

COMPUTED DRIFTS

DAY	MON	YEAR	HOUR	JULIAN DATE	BASE VALUE	DAYS	DRIFT MG/DAY	DRIFT %/ME
3	4	1967	032	24564.397	076350.693	21.2	-0.0081990	-0.000118
30	4	1967	1608	24591.872	076350.469	17.4	-0.0091915	-0.000123
18	5	1967	1553	24609.661	076356.301	115.6	-0.0018037	-0.000026
11	9	1967	832	24725.355	076350.115			





## DOCUMENT CONTROL DATA - R &amp; D

Security Classification of title, body of abstract and indexing annotation must be entered when the overall report is classified

1. ORIGINATING ACTIVITY (Corporate author)		2a. REPORT SECURITY CLASSIFICATION	
Lamont-Doherty Geological Observatory of Columbia University		Unclassified	
3. REPORT TITLE		2b. GROUP	
Arctic Ocean Geophysical Studies: The Alpha Cordillera and Mendelejev Ridge.		Arctic	
4. DESCRIPTIVE NOTES (Type of report and inclusive dates)			
Technical Report			
5. AUTHOR(S) (First name, middle initial, last name)			
John K. Hall			
6. REPORT DATE	7a. TOTAL NO. OF PAGES	7b. NO. OF REFS	
November 1970	125	104	
8a. CONTRACT OR GRANT NO	9a. ORIGINATOR'S REPORT NUMBER(S)		
N00014-67-A-0108-0016	2		
b. PROJECT NO	9b. OTHER REPORT NO(S) (Any other numbers that may be assigned this report)		
NR 307-320/1-6-69 (415)			
c.			
d.			
11. DISTRIBUTION STATEMENT			
Reproduction of this document in whole or in part is permitted for any purpose of the U. S. Government.			
11. SUPPLEMENTARY NOTES		12. SPONSORING MILITARY ACTIVITY	
		Office of Naval Research Washington, D. C.	
13. ABSTRACT			
<p>The geophysical findings from Fletcher's Ice Island (T-3) for the period mid-1962 to mid-1970 are presented. During this time the ice station traversed the Chukchi Rise, portions of the Alpha Cordillera and Mendelejev Ridge, and the Chukchi, Mendelejev, and Canada Plains. The findings, together with pertinent observations from older investigations, support the suggestion of earlier investigators that the Alpha Cordillera is an inactive center of seafloor spreading. Several fractures were observed to cut the Mendelejev Ridge and Alpha Cordillera, and many other closely spaced fractures are suggested by topographic, magnetic, and gravity trends. These fractures appear to parallel the 142° West meridian. Seismic reflection profiles show a buried topography similar to that of the Mid-Atlantic Ridge. Offsets in the apparent axial rift suggest that the fractures are the traces of transform faults. The angular relationship between the Mendelejev Ridge and the Alpha Cordillera appears to result from a southerly displacement of the cordillera crest along numerous en echelon transform faults. Magnetic anomalies are consistent with the seafloor spreading hypothesis. A crustal gravity model based upon a continuous 600 km long gravity and bathymetric profile and one reversed refraction measurement from Station Alpha shows the observed gravity to be consistent with a section of East Pacific Rise type with a 5 km thick oceanic layer overlying 27 km of anomalous (<math>\rho = 3.15</math>) mantle.</p>			

Continued overleaf.

DD FORM 1473  
NOV 65

